Master's thesis

NTNU
Norwegian University of Science and Technology
Faculty of Engineering
Department of Energy and Process Engineering

Susanne Vestgren

Development of local energy recovery and distribution

Master's thesis in Mechanical Engineering
Supervisor: Armin Hafner
June 2020

NTNU
Norwegian University of
Science and Technology

Susanne Vestgren

Development of local energy recovery and distribution

Master's thesis in Mechanical Engineering
Supervisor: Armin Hafner
June 2020

Norwegian University of Science and Technology
Faculty of Engineering
Department of Energy and Process Engineering

NTNU

Kunnskap for en bedre verden

Abstract

+CityxChange is a smart city project that focuses on finding solutions for cities to utilize their resources optimally by implementing new technologies [+CityxChange, 2019]. Parts of the project takes place at Sluppen in Trondheim, and the goal is for Sluppen to become a Positive Energy District. In this context this means a district with annual net zero energy import and net zero carbon dioxide (CO_2) emissions, working towards an annual local surplus production of renewable energy [+CityxChange, 2019]. To reach this goal thermal energy must be recovered from the existing processes in the district, and Sluppenvegen 10 and 17A have been chosen for this purpose. In these buildings the waste heat originates from a chilling facility and computer cooling, respectively.

This master's thesis focuses on heat recovery from Sluppenvegen 10. To utilize the recovered heat, three alternatives for heat delivery have been identified. Alternative 1 is delivering the heat to the district heating grid by using a high temperature heat pump (HTHP), this will require a large temperature lift and a cascade heat pump using e.g. propane in the low temperature cycle (LTC) and butane in the high temperature cycle (HTC). Alternative 2 is delivering hot water to the buildings at Sluppen, for instance the brewery or the fitness center. For this purpose, a heat pump water heater (HPWH) utilizing CO_2 or propane can be used. Lastly, alternative 3 is delivering heat to space heating, which probably will achieve a high performance due to a small temperature lift.

The chosen heat delivery alternative, for this master's thesis, is heating of hot water. To recover the waste heat from the chilling facility a CO_2 circuit extracting the heat from the glycol stream upstream of the chillers have been proposed. Initially three models were developed, two CO_2 models, one including an internal heat exchanger (IHX) and one without, and a propane model. The theoretical models were developed using the Dynamic Modeling Laboratory (Dymola) 2017 (Dassault Systems, Vélizy-Villacoublay) and TIL library for modeling thermal systems TIL 3.5.0 (TLK-Thermo GmbH, Braunschweig, Germany).

The CO_2 model without an IHX was tested at four high pressures, three water outlet temperatures and three CO_2 outlet temperatures from the gas cooler. These simulations resulted in the following conclusions regarding performance:

- The discharge temperature increases and the coefficient of performance (COP)

decreases as the high pressure is increased.

- When increasing the outlet water temperature the COP is reduced.
- With a lower CO_2 outlet temperature from the gas cooler the COP is increased.

The results from the CO_2 model were also compared to simulations with the IHX model at three high pressures, where the CO_2 model without an IHX showed the highest COP in all three cases. However, an important difference between the models is the superheat in the suction line, which is only achieved for the IHX model. The propane model was simulated with three different water outlet temperatures and compared to the CO_2 model, where the propane model had a higher COP in all the three cases. Using the propane model a COP of 3.65 was achieved when heating water from 10 °C to 60 °C. A simplified economic analysis was also conducted with results from the CO_2 model. The two scenarios presented in the analysis both resulted in profitable investments.

Sammendrag

+CityxChange er et prosjekt med et mål om å forbedre ressursutnyttelsen i byene på best mulig måte ved å installere ny teknologi [+CityxChange, 2019]. En del av prosjektet foregår på Sluppen i Trondheim, og målet er at Sluppen skal bli en plussenergibydel. I denne sammenhengen betyr det en bydel med netto null årlig energiimport og netto null karbondioksidutslipp, hvor det jobbes mot et årlig overskudd av lokalprodusert fornybar energi [+CityxChange, 2019]. For å nå dette målet må det gjenvinnes termisk energi fra de prosessene som allerede foregår i bydelen. Sluppenvegen 10 og 17A har blitt valgt til dette formålet, og overskuddsvarmen her stammer henholdsvis fra et kjølelager og datakjøling.

Denne masteroppgaven fokuserer på varmegjenvinning fra Sluppenvegen 10. For å utnytte varmen som gjenvinnes er det foreslått tre mulige varmedistribusjonsmetoder. Alternativ 1 er å levere varmen til fjernvarmenettet ved å bruke en høytemperatur varmepumpe. Dette er et alternativ som krever et høyt temperaturløft, og en mulig varmepumpeløsning kan være en kaskadevarmepumpe som bruker propan i lavtemperaturtrinnet og butan i høytemperaturtrinnet. Alternativ 2 er å levere varmt vann til bygninger på Sluppen som har et varmtvannsbehov, for eksempel et bryggeri eller et treningssenter. For å varme vannet kan det brukes en varmepumpe med CO_2 eller propan som arbeidsmedium. Siste alternativ er å levere varme til romoppvarming, noe som mest sannsynlig vil resultere i høy ytelse på grunn av lavt temperaturløft. Dette alternativet forutsetter at det er en eller flere bygninger på Sluppen med et vannbårent varmesystem og et varmebehov.

Det valgte alternativet for denne masteroppgaven er oppvarming av vann. For å gjenvinne varmen fra kjøleanlegget er det foreslått en CO_2-sløyfe som henter varmen direkte fra glykolen i kjøleanlegget oppstrøms av kjølemaskinene. Tre teoretiske varmepumpemodeller har blitt utviklet, to CO_2-modeller, én med og én uten internvarmeveksler, og en propanmodell. Modellene ble utviklet ved hjelp av Dynamic Modeling Laboratory (Dymola) 2017 (Dassault Systems, Vélizy-Villacoublay) og TIL biblioteket for modellering av termiske systemer TIL 3.5.0 (TLK-Thermo GmbH, Braunschweig, Tyskland).

CO_2-modellen uten internvarmeveksler ble testet med fire forskjellige høytrykk, tre utløpstemperaturer på vannet og tre utløpstemperaturer på CO_2 ut av gasskjøleren. Disse simuleringene resulterte i følgene slutninger:

- Trykkgasstemperaturen øker samtidig som effektfaktoren (COP) synker når høytrykket økes.
- Økt utløpstemperatur på vannet medfører lavere COP.
- Med en lavere utløpstemperatur på CO_2 ut av gasskjøleren øker modellens COP.

Resultatene fra CO_2-modellen ble sammenliknet med resultatene fra modellen med en internvarmeveksler ved tre forskjellige høytrykk, og modellen uten internvarmeveksler viste en høyere COP i alle de tre tilfellene. Dette utfallet må tas med en klype salt, ettersom det viste seg at det kun var modellen med internvarmeveksler som hadde overopphetet gass i sugegassledningen, noe som kan påvirke resultatet. Propanmodellen ble testet med tre forskjellige utløpstemperaturer på vannet, og resultatene ble sammenliknet med tilsvarene resultater fra CO_2-modellen. Propanmodellen viste høyere COP ved alle de tre temperaturene. Ved å bruke propanmodellen oppnådde man en COP på 3.65 når vann ble varmet fra 10 °C til 60 °C. Det har i tillegg blitt utført en forenklet økonomisk analyse på anskaffelsen av en CO_2-varmepumpe, hvor resultatene fra simuleringene har blitt brukt. Det er presentert to forskjellige scenarier, hvor begge konkluderte med at varmepumpen er en lønnsom investering.

Preface

This master's thesis was carried out during the spring semester of 2020 and was submitted to the Department of Energy and Process Engineering at the Norwegian University of Science and Technology (NTNU). The master's thesis was submitted as the last part of the study program Mechanical Engineering, and it comprises of 30ECTS.

I would like to thank my supervisor Prof. Armin Hafner for guidance and discussion helping me get a better understanding of the working principles of a heat pump, as well as limitations in real life applications. I would also like to thank him for including me in the project +CityxChange and bringing me to meetings to keep up with the progression in the project, which has been a great motivation. I would also like to thank Åmund Utne and Morten Fossum in Statkraft Varme for helping me during the prework of this master's thesis, and teaching me about the district heating grid as well as giving me insight to how things are done in real life projects.

Trondheim, June 10, 2020

Susanne Lykkedrang Vestgren

Contents

List of Figures

List of Tables

Nomenclature

Abbreviations

CFC	=	Chlorofluorocarbon
CO_2	=	Carbon dioxide
COP	=	Coefficient of Performance
DHW	=	Domestic hot water
Dymola	=	Dynamic Modeling Laboratory
e.g.	=	exempli gratia (for instance)
etc.	=	et cetera (and so on)
GHG	=	Greenhouse gases
GWP	=	Global warming potential
HCFC	=	Hydrochlorofluorocarbon
HCFO	=	Hydrochlorofluoroolefins
HFC	=	Hydrofluorcarbon
HFO	=	Hydrofluoroolefins
HPWH	=	Heat pump water heater
HTC	=	High temperature cycle
HTHP	=	High temperature heat pump
i.e.	=	id est (that is)
IHX	=	Internal heat exchanger
IRR	=	Internal rate of return
LFL	=	Lower flammability level
LTC	=	Low temperature cycle
NPV	=	Net present value
NTNU	=	Norwegian University of Science and Technology
OPD	=	Ozone depletion potential
PBP	=	Payback period
PED	=	Positive Energy District
SH	=	Space Heating
VCC	=	Vapor compression cycle

Variables and Parameters

A	=	Area [m^2]
C	=	Net cash flow
C_p	=	Specific heat capacity [kJ/kgK]
f	=	Frequency [s^{-1}]
h	=	Enthalpy [kJ/kg]
I_0	=	Investment cost
k	=	Proportional gain [-]
$\dot{m}$	=	Mass flow rate [kg/s]
N	=	Total number of time periods
n	=	Given time period
p	=	Pressure [bar]
$\dot{Q}$	=	Heat transfer rate [kW]
r	=	Discount rate
s	=	Specific entropy [kJ/kgK]
T	=	Temperature [°C]
Ti	=	Time constant [s]
U	=	Overall heat transfer coefficient [W/m^2K]
v	=	Specific volume [m^3/kg]
$\dot{V}$	=	Volume flow [m^3/h]
$\dot{W}$	=	Work [kW]
η_{is}	=	Isentropic efficiency of the compressor [-]
ΔT	=	Temperature difference [K]
λ	=	Volumetric efficiency of the compressor [-]

Subscripts

0	=	Evaporator conditions
c	=	Condenser conditions
comb	=	Combined
comp	=	Compressor
crit	=	Critical
f	=	Fluid
is	=	Isentropic
LMTD	=	Logarithmic mean temperature difference
real	=	Actual conditions
R	=	Refrigerant
s	=	Stroke
sat	=	Saturated

Chapter 1

Introduction

Nowadays climate change is gaining importance, and due to extensive carbon dioxide (CO_2) emissions and the greenhouse effect, global policy focuses on actions to reduce the harmful impact on the environment. +CityxChange is a smart city project, which focuses on finding solutions for cities to optimally utilize their resources by implementing new technologies. The energy situation is becoming more complex, with key elements as renewable energy sources, energy storage and smart grids. +CityxChange aims at creating greener energy positive cities. To achieve this, the energy must be utilized smarter in the future, by only buying the energy needed and sell any surplus. To enable this change, new politics and trade agreements, in addition to new business models are necessary. New positive energy blocks will be developed for +CityxChange, and the solutions will be tested in multiple European cities. By doing this, it will be possible to utilize locally produced energy in a way that is optimal for citizens, businesses and the society in the future. [+CityxChange, 2019]

Trondheim is one of the lighthouse cities in the project, and it has been initiated three smaller projects in the region. This thesis will focus on the part of the project located at Sluppen, primarily on the thermal energy aspect. The goal for +CityxChange Sluppen is to achieve a Positive Energy District (PED). In this context, PED is seen as a district with annual net zero energy import and net zero CO_2 emissions, working towards an annual local surplus production of renewable energy [+CityxChange, 2019]. To reach this goal, thermal energy must be recovered from existing processes in the district. For this purpose Sluppenvegen 10 and 17A have been chosen. Processes at these addresses have heat as a byproduct, and the

heat is rejected to the atmosphere. Instead of this, the heat should be reused, for instance by using heat pump technology to increase the quality of the heat, i.e. making it more useful. Then more alternatives for heat delivery becomes evident. An aspect making heat recovery more attractive is the possibility of both energy and cost savings.

In this master's thesis heat recovery from Sluppenvegen 10 will be the focus, and alternative heat distribution cases for heat delivery will be investigated. The waste heat will be upgraded by using heat pump technology. The heat pumps must be innovative, cost efficient and reliable. The focus will be given to configurations applying natural working fluids, due to the long-term perspective of the project owners and the goal to utilize this technology in several installations in the future.

The master's thesis will include a review of relevant literature about heat pumps, high temperature heat pumps, working fluids, heat pump water heaters, space heating, combined space and hot water heating systems, as well as cascade systems, district heating and economic analysis. Today's situation at Sluppen will be presented, as well as different alternatives for heat delivery from Sluppenvegen 10. Furthermore, models for one of the heat delivery alternatives will be developed, and there will be performed simulations with these models at relevant operating conditions. The results obtained from these simulations will be analyzed in terms of validity, system performance, energy demand and simplified costs. Lastly, there will be a discussion, conclusion and proposals for further work. In addition, a draft version of a scientific paper based on the main findings of the thesis will be included. This master's thesis is a continuation of the specialization project conducted during the fall semester of 2019.

Chapter 2

Theoretical framework

This chapter aims at providing the reader with relevant information about heat pump configurations and available technology, as well as potential working fluids. Heat pumps for different purposes are presented, among them domestic hot water and space heating. The chapter will also present some of the challenges faced by heat pumps today as well as giving short introduction to district heating. Finally, the three most common methods for economic analysis of an investment will be presented.

2.1 Heat pumps

A heat pump is an energy system that transfers heat from a heat source to a heat sink by use of external work. There are several different heat pump configurations which can be used for various purposes. Among them the vapor compression cycle (VCC), which is often referred to as the typical heat pump. The VCC has a working fluid circulating in a closed cycle where the main components are the compressor, the expansion valve, the condenser, and the evaporator, as shown in figure 2.1. The VCC is shown in a pressure-enthalpy (log p-h) diagram and in a temperature-entropy (T-s) diagram in figure 2.2.

The working principle of the VCC is:

- **1-2:** A mechanical compressor sucks low pressure gas out of the evaporator, increasing the pressure and the temperature. The compressor is used to control the pressure difference between the evaporator and the condenser to

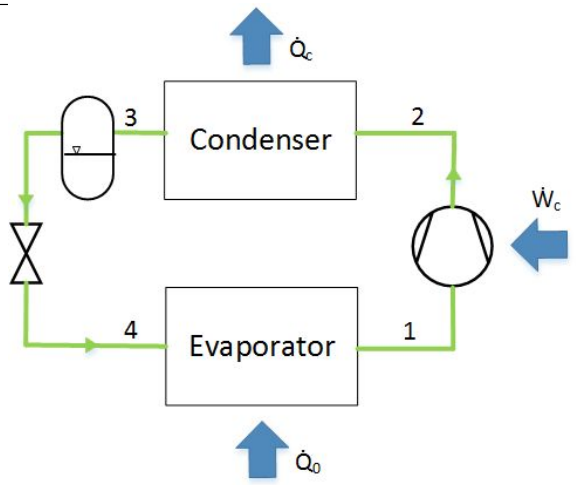

Figure 2.1: Simple vapor compression cycle configuration. The blue arrows describe the energy transfer.

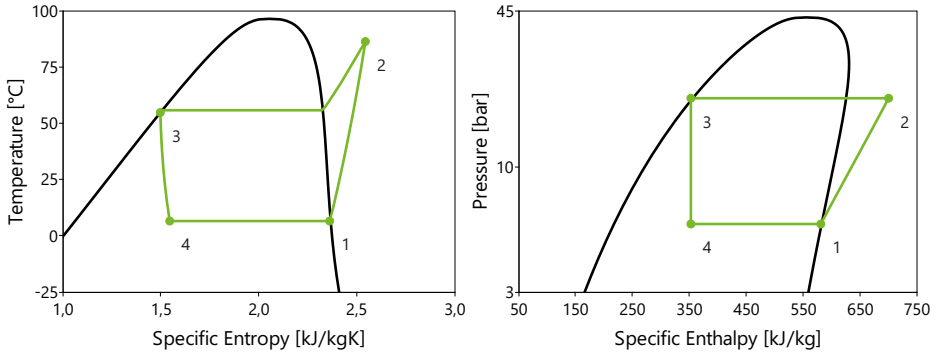

Figure 2.2: Log p-h diagram and T-s diagram for a typical simple vapor compression cycle.

maintain the proper phase change temperatures to interact with the heat source and heat sink. The compressor is driven by mechanical work, which can be supplied by e.g. an electric motor or a diesel engine. Ideal compression is isentropic, which implies that the process is both adiabatic and reversible, i.e. no friction loss or heat transfer out of the system, and is described by:

$$\dot{W}_{is} = \dot{m}_R \cdot (h_2 - h_1) \tag{2.1}$$

Where $\dot{m}_R$ is the working fluid mass flow and $\dot{W}_{is}$ is the isentropic compressor work. Real life applications of compression will not be isentropic, and an isentropic efficiency should therefore be defined. The real compression work can then be expressed as a function of the isentropic efficiency as follows:

$$\dot{W}_{real} = \frac{\dot{W}_{is}}{\eta_{is}} \tag{2.2}$$

Where η_{is} is the isentropic efficiency.

- **2-3:** The compressor discharges the gas into the condenser, where heat is rejected to a heat sink through condensation of the working fluid. The delivered heat is more useful and at a higher temperature than the heat source. The delivered amount of heat is the sum of the heat absorbed in the evaporator and the work input to the compressor, or in other words, the working fluid mass times the enthalpy difference over the condenser, described by:

$$\dot{Q}_c = \dot{Q}_0 + \dot{W}_{comp} = \dot{m}_R \cdot (h_2 - h_3) \tag{2.3}$$

Where $\dot{Q}_0$ is the heat absorbed in the evaporator and $\dot{W}_{comp}$ is the work performed by the compressor on the working fluid.

- **3-4:** The high pressure liquid at the end of the condenser is expanded, by use of an expansion valve, to the low pressure of the evaporator. The expansion is assumed to be an isenthalpic process, i.e.:

$$h_3 = h_4 \tag{2.4}$$

- **4-1:** Heat is transferred from the heat source to the working fluid in the evaporator through evaporation of the working fluid, which is assumed to be an isotherm process, i.e. the temperature is constant. The amount of heat transferred in the evaporator is equal to the working fluid mass flow times the enthalpy difference over the evaporator:

$$\dot{Q}_0 = \dot{m}_R \cdot (h_1 - h_4) \tag{2.5}$$

To express the performance of such a system it is common to use the coefficient of performance (COP). The COP is a dimensionless ratio of useful thermal energy over power input to the system, thus the amount of work added to the cycle influences the COP. The COP is defined as in equation (2.6).

$$COP = \frac{\dot{Q}_c}{\dot{W}_{comp}} \tag{2.6}$$

The simple VCC also contains a liquid receiver, placed at the outlet of the condenser and upstream the expansion valve. The liquid receiver stores high pressure liquid leaving the condenser, and it can collect fluid when load fluctuations occur. It is sized to contain the whole working fluid charge when the heat pump is not in operation. [Grassi, 2018]

The compressor must be able to operate at loads differing from its design point. The simplest control method is on/off, but this is also very energy consuming. In addition, the amount of starts and stops for the compressor should be limited to avoid excess stresses on the compressor and the electric motor. Techniques that make it possible to operate the compressor at part load have therefore been developed. For piston compressors this can be done by deactivating some of the cylinders, by bypassing some of the fluid from suction to discharge of the cylinder through signal submission to the solenoid valve. This way, there will be a stepwise reduction in activated cylinders and capacity. Another method is changing the rotational speed of the driving motor. Electric heat pumps often use an inverter to change the feeding frequencies. This will give a more continuous operation and result in increased COP. [Grassi, 2018]

In conjunction with heat pumps there are some terms that are important to understand. In this paragraph some of the terms used later in this master's thesis are explained using figure 2.3. The evaporation and the condensation process happen in the two-phase region, which is enclosed under the dome in figure 2.3. The compression happens in the vapor region, where also the desuperheating process happens. Desuperheating means cooling of the discharge gas at constant temperature to the saturated gas line. In figure 2.3 the critical point is marked, which is the point where the boiling point curve meets the dew point curve. It is only below this point that a liquid and its gas can coexist. In conjunction with heat pumps, the critical temperature and critical pressure is often mentioned, which is the temperature and the pressure at the critical point. In a heat pump system, subcooling means cooling of the liquid out of the condenser at a constant pressure below the saturation temperature in the liquid region. Subcooling happens in the liquid region.

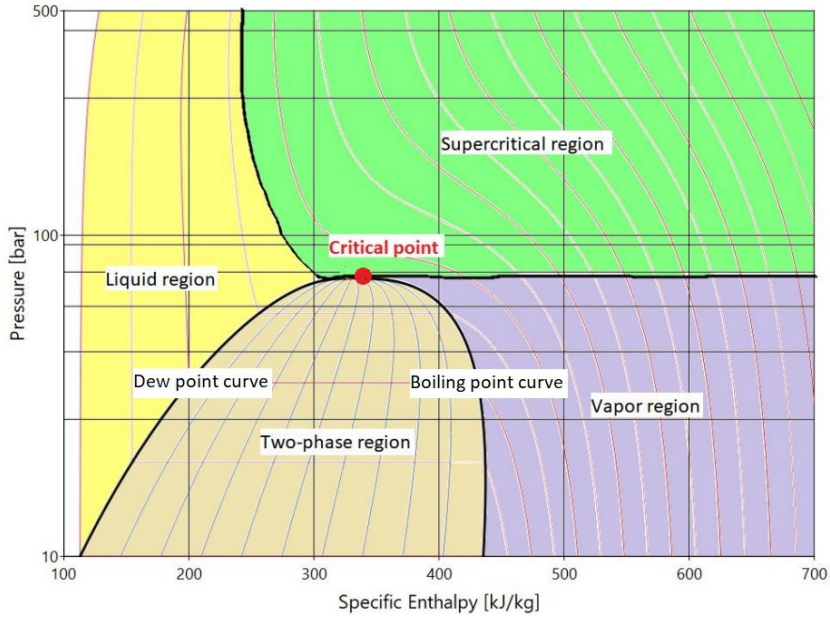

Figure 2.3: Sketch of the different regions for a working fluid which is mentioned in conjunction with heat pumps. The curved vertical light red lines on the figure represent constant temperature.

2.2 High temperature heat pumps

A high temperature heat pump (HTHP) is a normal heat pump, but applied in high temperature operations, which means the components must be modified to withstand the high temperatures. Theoretical analysis of HTHP cycles show that most of the irreversible losses occur in the compressors and heat exchangers. In general, more research is needed on high temperature components to reduce these losses. There have been a lot of development in heat pump technology for low temperature heat delivery, but not so much for temperature applications above 80°C. Several studies have been conducted on the development of effective heat exchangers, but studies on compressors are also necessary [Bamigbetan et al., 2017]. Important parameters for heat exchangers are the heat transfer coefficient, heat transfer area, and pressure drop. For compressors, challenges that must be solved are compressor cooling, lubrication, and material compatibility. [Bamigbetan et al., 2017]

HTHPs are often used in connection with the industrial sector, mainly for recovery of waste heat. However, the definition of a HTHP is not clear. Some define it as

a heat pump with heat sink temperatures above 100 °C, while others define it as having heat sink temperatures up to 150 °C for heat recovery and upgrading in industry, but also for heating, cooling and air conditioning in non-residential buildings [Arpagaus et al., 2018]. In this thesis it is defined as a heat pump delivering heat above 80 °C.

There are multiple heat pumps in the marked able to deliver heat at temperatures of at least 90 °C, but only a few can supply temperatures up to 120 °C. The highest temperature a heat pump can deliver depends on the working fluid, the design, and the compressor type. In all heat pumps the oil in the compressor must be selected to fit the working fluid, however in high temperature applications the thermal stability of the oil must also be evaluated, as the high discharge temperatures can cause problems [Arpagaus et al., 2018]. There are many other challenges dealing with high temperatures. One of them are the high risk of condensation during compression, which can cause damage to the compressor. To avoid this, high superheat in the suction line is necessary [Moisi and Rieberer, 2017]. Superheat means heating of the gas above the saturation temperature in the vapor region. The minimum required superheat depends on the working fluid, condensation and evaporation temperatures and the isentropic efficiency of the compressor. The amount of superheat necessary range between 5-35 K. For instance, using butane a superheat of 14 K is minimum to avoid entering the two-phase region, when evaporation happens at 40 °C and condensation at 125 °C, assuming an isentropic efficiency of 1 [Arpagaus et al., 2018]. This means that the superheat most likely needs to be even higher due to compressor losses, however, an isentropic efficiency of 1 is unlikely. High superheat in the suction line gives lower evaporation temperatures, which will decrease the heat pump efficiency. Thus, to avoid this, one can use an internal heat exchanger, suction gas cooled compressors or other external heat sources. [Moisi and Rieberer, 2017]

To get the required superheat the use of an internal heat exchanger (IHX) is possible. The IHX heats the gas coming out of the evaporator and subcools the liquid from the condenser at the same time [Arpagaus et al., 2018]. Figure 2.4 shows a simple VCC with an internal heat exchanger, and figure 2.5 shows a corresponding log p-h diagram. The internal heat exchanger will reduce the expansion losses, but also increase superheat losses and compressor work. Therefore, the internal heat exchanger will be a beneficial component for the system only if the effect of increased specific refrigeration capacity is larger than the effect of the increased specific volume of the gas in the suction line. Using an IHX also have other disadvantages, among them increased discharge gas temperature, high oil temperature

and reduced cooling potential for the electric motor if the compressor is hermetic or semi-hermetic. Subcooling will, as mentioned, reduce the expansion losses, as the expansion starts at a lower temperature, which results in a smaller entropy difference. From figure 2.5 one can see that the subcooling results in a larger specific refrigeration capacity. When increasing the specific refrigeration capacity, the mass flow rate can be reduced, which will influence the power consumption of the compressor. Subcooling is also used to avoid flash gas that can harm the expansion valve. [Eikevik, 2018]

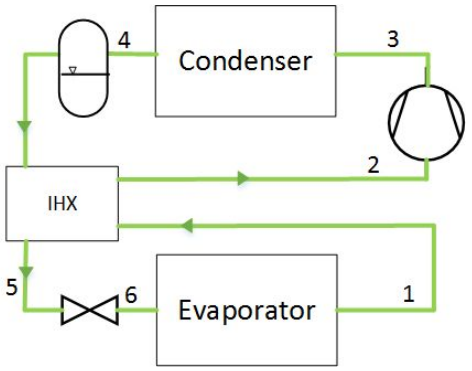

Figure 2.4: Simple vapor compression cycle with internal heat exchanger. The numbers correspond to the numbered points in figure 2.5.

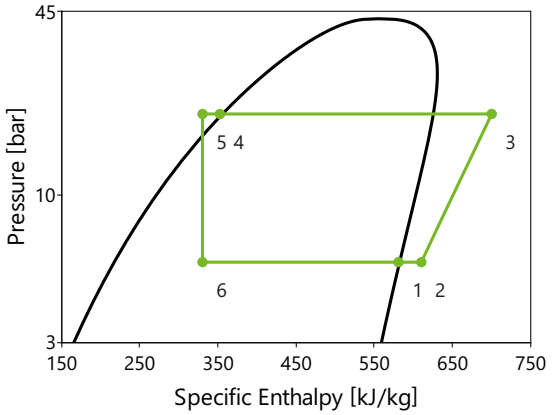

Figure 2.5: Log p-h diagram showing the effect of the internal heat exchanger. The superheating process is shown between point 1 and 2, and the subcooling between point 4 and 5.

In HTHPs the condensing temperature will be high, and increasing the condensing temperature has many consequences. Among them, decreased cycle efficiency, if assuming constant evaporation temperature. With a higher temperature lift, the pressure ratio will increase, which can decrease the isentropic efficiency and result in increased specific compressor work [Moisi and Rieberer, 2017]. The enthalpy of condensation decreases with increasing temperature and becomes smaller the closer to the critical temperature the condensation happens, as can be seen from the narrowing of the two-phase region with increasing temperature in figure 2.5. The critical temperature determines the maximum condensing temperature for subcritical operation. To ensure subcritical operation, i.e. operation only below the critical point, a minimum temperature difference of 10-15 K between condensing temperature and critical temperature is recommended [Arpagaus et al., 2018]. However, there are also heat pumps operating in the transcritical area, which will be addressed later in this thesis. To compensate for the lost enthalpy of condensation closer to the critical point, more subcooling of the liquid can be applied. However, the degree of subcooling depends on the heat sink temperature lift. If this lift is small, large subcooling can lead to increased condensation temperature, which should be avoided to achieve a high efficiency for the heat pump. Increasing the condensing temperature will increase the condensing pressure, which for some working fluids can lead to issues with too high pressures [Moisi and Rieberer, 2017].

Compressors used in HTHPs experience very high temperatures because both the condensing and the discharge temperatures are high. Therefore, a reliable lubricant is important to ensure a long lifetime. Generally, compressors that do not need lubrication would be ideal. In addition, in vapor compression heat pumps, the electric motor must be modified for high temperature applications. High temperatures in the evaporator will lead to high mass flow rates and high torques, which means that the motor must be larger than for standard applications. In the prototype cascade heat pump built by Bamigbetan et al. [2019b], the electric motor had 25 % larger capacity for effective load and stress management. Additionally, for hermetic and semi-hermetic compressors, cooling of the motor and oil can be difficult at high temperatures. Due to all of this, the best compressor technology for high temperature applications might be turbo compressors. However, these compressors must be developed for the specified working fluid and operating conditions, which is very costly [Ayou et al., 2019]. Risk of failure due to wear, mechanical faults, overheating, etc., will be larger if the compressor is operated outside its normal operating range, thus, this should be avoided. [Bamigbetan

et al., 2019b]

2.3 Working fluids

Selection of the working fluid is a key element in the design process of a heat pump and has a large impact on the overall performance. When selecting the working fluid multiple factors are important to assess. Some of these factors are the working fluids' thermal properties, toxicity, flammability, environmental impact, price, and availability. When assessing the environmental impact, one can look at the global warming potential (GWP) and the ozone depletion potential (ODP). The GWP is a measure of the effect a gas has on the global warming, relative to carbon dioxide (whose GWP is one), and the ODP is defined as the amount of ozone destroyed by a compound relative to the same mass of R-11 (whose ODP is one). As different working fluids have different properties it is important to select one with suitable properties for the application. It is beneficial with high heat of evaporation as less working fluid will need to be circulated to achieve the desired cooling/heating capacity. The amount of circulating working fluid will directly affect the diameter of the pipes, the capacity of the compressor and the size of the heat exchangers and the other components. All of this will impact the cost and design of the heat pump system.

There are many different working fluids that can be utilized in heat pumps and refrigeration systems. The working fluid must be stable, and not corrode the material in the components of the heat pump, which must be considered both in selection of the working fluid and materials for the components. Some working fluids are synthetic, e.g. chlorofluorocarbons (CFCs), hydrochlorofluorocarbons (HCFCs), hydrofluorcarbons (HFCs) and hydrofluoroolefins (HFOs), and some are natural, e.g. ammonia and hydrocarbons.

The Montreal Protocol of 1987 aimed at reducing the production and use of chemicals that contribute to depletion of the ozone layer. At first, only a reduction of these substances was planned but it was eventually amended to a complete phase out of the substances with an ODP unequal to zero, e.g. the CFCs and HCFCs [Encyclopædia Britannica, 2019]. The Kyoto Protocol of 1997 contains specific numbers and deadlines for reductions in emissions of greenhouse gases (GHGs) for industrial countries. As HFCs have high GWP they are considered as GHGs, even though they have zero ODP, which means they are concerned by the Kyoto Protocol [FN-sambandet, 2019]. In 2016 the Kigali Amendment was introduced,

as an extension to the Montreal Protocol. The Kigiali amendment aims at a phase down of HFCs by reducing the production and consumption [UNIDO].

Many of the working fluids affected by these measures are, or have been, common working fluids. Therefore it is necessary to find good replacements with have low GWP and zero ODP. Synthetic replacements have been developed, e.g. the HFOs and the hydrochlorofluoroolefins (HCFOs), and they have approximately zero ODP and low GWP because they are rapidly degraded in the atmosphere. However, their decomposition products are highly toxic in combination with water, and if released to the atmosphere they can be distributed everywhere, which is unfavorable and harmful [Hafner, 2017]. Thus, these gases may have additional unforeseen consequences to the environment.

Natural working fluids are also potential replacements for CFSs, HCFCs and HFCs, and they are substances occurring naturally in the atmosphere. In the context of heat pumps the natural fives are usually mentioned, which include CO_2, ammonia, hydrocarbons, water, and air. They have zero ODP and low GWP which results in minimum impact on the environment. The advantages and disadvantages of selected natural working fluids will be mentioned later in this chapter.

With respect to HTHPs, the thermodynamic properties of many common natural working fluids make them unfit for use. Nevertheless, some hydrocarbons, ammonia, water, and CO_2 are excellent choices for HTHPs. In table 2.1 typical properties for a selection of natural working fluids applicable in HTHPs are listed. Recent research shows that some of these substances have equally good, or better, performance than the synthetic working fluids [Bamigbetan et al., 2018]. However, for some of the natural working fluids, e.g. ammonia, existing compressor technology is limiting for the maximum heat sink temperature [Bamigbetan et al., 2019a]. Meaning the development of new and improved compressor technology is essential for high temperature applications.

Suitable working fluids for HTHPs have high critical temperature to achieve a high COP, assuming subcritical operation. Theoretical studies have shown that the maximum COP occurs when operating at a condensing temperature approximately 20 K below the critical temperature of the working fluid [Mota-Babiloni et al., 2018]. The critical temperature determines the highest temperature a working fluid can deliver in subcritical operation, and the heat sink temperature is also important to consider when selecting working fluid. The working fluid should also have a low boiling point temperature to limit the volumetric flow rate to keep the size of the compressor relatively small [Bamigbetan et al., 2017].

Table 2.1: Typical properties for natural working fluids applicable in high temperature applications [Bamigbetan et al., 2017].

Working fluid	ODP	GWP 100yr	Normal boiling point (°C)	Critical temp. (°C)	Critical pressure (bar)
Propane (R290)	0	3.3	-42.1	96.7	42.48
Butane (R600)	0	4.0	0.0	152.0	37.96
Isobutane (R600a)	0	3.0	-11.7	134.7	36.40
Pentane (R601)	0	4.0	36.1	196.6	33.58
Isopentane (R601a)	0	4.0	27.7	187.8	33.78
Ammonia (R717)	0	0.0	-33.3	132.4	112.80
Water (R718)	0	0.2	100.0	373.9	220.60
CO_2 (R744)	0	1.0	-78.0	31.0	73.80

2.3.1 Hydrocarbons

Hydrocarbons are becoming more common to use as working fluids due to their environmental profile, with low GWP and zero ODP. The main advantage of hydrocarbons, compared to other working fluids, is that they are in many respects similar to the halogenated hydrocarbons which the industry is already accustomed to. Hence, limiting redesign of systems and components when changing the working fluid to a hydrocarbon. Hydrocarbons are also expected to have performance as good as the CFCs, HCFCs and HFCs. [Palm, 2008b]

Hydrocarbons have many application areas. In Europe, isobutane is the most frequently used working fluid, as it is dominating in household refrigerators. Propane and propene are common for many heat pump manufactures and are also used in air conditioners and in commercial refrigeration systems. In addition, isopentane, pentane and butane are considered for use, but they are not yet used commercially. [Palm, 2008b]

Hydrocarbons are flammable and explosive, which is one of the biggest challenges when using them in heat pump technology and imposes strong regulations for its use. Safety requirements regarding heat pumps and refrigeration systems in Norway are given in the standard NS-EN 378 Kuldeanlegg og Varmepumper - Sikkerhets- og miljøkrav, part 1, 2, 3 and 4.

Limits for the working fluid charge for heat pumps and refrigeration systems depends on the unit location, the toxicity, and the lower flammability level (LFL) of the working fluid. If the equipment is placed in a machine room (which fulfill the

Table 2.2: Safety limits for selected natural working fluids for heat pump applications. Values obtained from [Standard Norge, 2016].

Working fluid	Safety class	Practical limit [kg/m^3]	LFL [kg/m^3]	Auto ignition temp. [°C]
Propane (R290)	A3	0.008	0.038	470
Butane (R600)	A3	0.008	0.038	365
Isobutane (R600a)	A3	0.011	0.043	460
Pentane (R601)	A3	0.008	0.035	260
Isopentane (R601a)	A3	0.008	0.038	420
Ammonia (R717)	B2L	0.00035	0.116	630
CO_2 (R744)	A1	0.1	-	-

requirements to be classified as a machine room) or outdoors, the limits for the working fluid charge is 5 kg. [Standard Norge, 2016]

The practical limit is equivalent to approximately 20 % of LFL and gives sufficient safety margin to avoid accumulation of local concentrations exceeding the LFL. The practical limit represents the highest concentration that does not create a risk of ignition of the working fluid. The highest temperature of the working fluid throughout the heat pumping process must be at least 100 K lower than the auto ignition temperature. The gas phase of many hydrocarbons is heavier than air (e.g. isobutane and propane), and a leakage will make an explosive concentration close to the floor. Therefore, the placement of detectors and ventilation components are of importance. There should be at least one sensor in each machine room and/or in the lowest placed room, when using working fluids heavier than air. [Standard Norge, 2016]

All the hydrocarbons in table 2.2 belongs to safety class A3, which represents working fluids with high flammability and low toxicity. Detectors for this class should activate an alarm at a level of about 25 % of LFL. When the alarm goes off, emergency ventilation must start, and the heat pump system must be shut down. [Standard Norge, 2016]
Reduced charge through indirect systems and compact heat exchangers, sensors, alarms and forced ventilation, as well as outdoor placing of the heat pump unit are all measures applied to reduce the safety risks during normal operation when using hydrocarbons as working fluids.

Hydrocarbons are suitable for HTHPs due to their thermodynamic properties. Some of the hydrocarbons that can match the performance of the synthetic work-

ing fluids are propane, butane, and isobutane [Bamigbetan et al., 2017]. As mentioned, the highest delivered temperature depends on the critical temperature, and from table 2.1 it can be seen that propane has a low critical temperature of 96.7 °C, which means propane will not be able to deliver temperatures much higher than 80 °C. Butane on the other hand has a critical temperature of 152 °C, and will be a better option for temperature delivery above 100 °C. For immediate implementation of a HTHP, the study by Bamigbetan et al. [2018] showed that butane is the most suitable natural working fluid right now, this is based on existing compressor technology where simple modifications can be made.

2.3.2 Ammonia

Ammonia can be used for both heating and cooling applications. From table 2.1 it can be seen that ammonia has an ODP and GWP of zero. The table also shows that ammonia has both high critical temperature and pressure. Due to the high discharge pressure, ammonia is rarely used in industrial heat pumps with heat sink temperature above 90 °C [Arpagaus et al., 2018]. Ammonia has high phase transition energy, which makes it able to absorb and reject large amounts of heat. This will result in high COP and can give low working fluid charge per kW installed power. [Småland and Øverland, 2020]

Ammonia reacts with copper in the presence of water, i.e. it will corrode copper and copper alloys. Thus, other materials must be used in ammonia heat pumps, and these kinds of components have been developed over the years [Bamigbetan et al., 2017]. Copper is most common for refrigeration systems and it is also the cheapest pipe material. The best alternative for ammonia is steel pipes with welded joints, which is a more expensive option. Other disadvantages of ammonia are high discharge temperatures and low miscibility with oil, which leads to limitations of compression ratios and the need of a mechanical oil return system. [Småland and Øverland, 2020]

Ammonia is toxic and belongs to safety class B2L. Due to the toxicity it should not be used in direct applications where leakage is considered a high risk. An option will be to introduce a secondary circuit. However, this will reduce the possible outlet temperature for the heat sink [Bamigbetan et al., 2017]. Another solution for ammonia heat pumps can be to place the heat pump unit in a pressurized cabinet to control potential leakages [Småland and Øverland, 2020].

Ammonia has a sharp, irritating odor, which is easily detected at small concentrations. In case of leakage, ammonia vapor will rise because it is lighter than

air, which means it can get quickly diluted and removed by the ventilation [Eikevik, 2018]. In practice, toxicity and panic will be the biggest safety issues when using ammonia in heat pumps. The distinct smell of ammonia, which can cause panic, will also alert about a leakage at a very early stage. Regulations do not consider ammonia as flammable in many contexts, this is because ammonia is not easily ignited, and very large gas concentrations are needed for ignition [Norsk Kjøleteknisk Forening, 2018].

Ammonia is widely used in heat pumps, especially for large capacity requirements. It has rarely been used in small scale systems after the 1930s when the CFCs became common, due to the fear for the safety. Therefore there is limited commercially available technology, which makes it less applicable [Palm, 2008a]. There have been made several attempts the last decade to make low capacity heat pumps, but unfortunately many have failed due to lack of components [Zajacs et al., 2017]. When using ammonia in relatively small heat pumps it is possible to reduce the amount of working fluid, so called low charge system, by utilizing compact heat exchangers. In the 9 kW heat pump designed by Palm [2008a], plate heat exchangers were used and resulted in a charge of 120 g ammonia.

As mentioned, ammonia has high discharge pressure which sets limitations for the condensation temperature, thus making it unsuitable for HTHPs. However, ammonia has a significantly higher discharge temperature than saturation temperature at a given discharge pressure. This opens the possibility of utilizing the heat in the superheat region, which can contribute to the heating capacity of the heat pump. This means that it may not be necessary to keep the condensation temperature significantly higher than the heat sink target outlet temperature [Bamigbetan et al., 2017]. For instance, Palm [2008a] designed a small ammonia heat pump for space heating and hot water production, where the heat sink was 40 °C for space heating and the hot water were heated to 60 °C by the superheat in a separate desuperheater.

2.3.3 CO_2

CO_2 is a working fluid with a low critical temperature of 31 °C and a high critical pressure of 73.8 bar, as seen from table 2.1. This means that if using CO_2 in subcritical operation it is only possible to achieve a temperature of maximum 28 °C. However, CO_2 is often used in transcritical operation, which means the condensation is replaced with heat rejection at a gliding temperature in the supercritical region. This causes the condenser to be replaced by a gas cooler.

The high critical pressure gives high energy density and volumetric heat capacity, which results in smaller compressor volumes, meaning the dimensions of CO_2 pipes, valves, etc. can be smaller. However, the pipes must be thicker, compared to applications with other working fluids, in order to withstand the high pressures. In addition, the high pressures give lower pressure ratios, which means less work for the compressor. This can lead to a better efficiency for the process. CO_2 has a slightly lower COP in subcritical operation compared to other working fluids. This is because the condensation happens close to the critical point leading to large throttling losses. This will also be the case for a transcritical cycle if the temperature of the CO_2 at the gas cooler outlet is high. [Eikevik, 2018]

Advantages of CO_2 is that it is non-toxic or non-flammable (safety class A1), inexpensive, readily available and has an ODP of zero and by definition a GWP of one, as seen in table 2.1. However, as it is a fluid without a distinct smell it is important to control that a high concentration of CO_2 does not build up along the floor as it can be harmful to humans. High concentrations of CO_2 can lead to suffocation, but before the concentration reach this level symptoms as increased heart rate, dizziness and breathing difficulties can be experienced [Småland and Øverland, 2020].

Disadvantages of heat pumps utilizing CO_2 is that they cannot be used in applications where the heat source reaches a higher temperature than the critical temperature (31 °C), because it leads to high evaporation temperatures or no evaporation at all. This excludes several areas of application, where other working fluids must be utilized instead. Another disadvantage is problems due to the high discharge pressure. [Pitarch et al., 2017]

Due to the fact that heat pumps utilizing CO_2 can operate in transcritical mode, delivery temperature above 80 °C is achievable. Nevertheless, heat sink outlet temperatures above 100 °C is still a challenge for CO_2 because the available technology cannot handle the high pressures [Bamigbetan et al., 2017].

2.4 Heat pump water heaters

Most water heaters are electric or oil fired, and a disadvantage with these is the very low system efficiency. However, they are quite simple, which makes maintenance easier. By using a heat pump water heater (HPWH) instead it is a potential for high electricity savings, due to the high efficiency of heat pumps [Nawaz et al., 2017]. Possible working fluids for HPWH can be hydrocarbons, for instance

propane and CO_2.

For domestic hot water (DHW) a temperature of 60-85 °C is needed. Minimum storage temperature is 55-60 °C due to prevention of growth of the legionella bacteria, which can cause illness. In DHW, cold city water will be used as heat sink, where the temperature can be assumed to be about 10 °C.

According to Ju et al. [2008] there is presently no perfect pure working fluid that meets all the requirements to replace conventional working fluids in HPWH. However, by mixing multiple working fluids one can achieve a mixture where the undesired properties are eliminated. In the study by Ju et al. [2008] the zeotropic blend of CO_2 and propane is proposed as a potential replacement for R22. In this blend the flammability of the propane is reduced. There are also other advantages with this blend, as reduced operating pressure compared to pure CO_2 systems, and good system efficiency by taking advantage of the temperature glide. When compared to R22 this blend achieved a higher COP.

Some heat pumps are equipped with a desuperheater, which can utilize the high discharge temperature of the gas from the compressor for heating of DHW. Another possibility, which is more energy efficient, is to use the condenser for preheating of DHW, and the desuperheater for reheating. [Stene, 2004]

2.4.1 CO_2 HPWH

As mentioned before, CO_2 has a low critical temperature of 31 °C, and maximum condensing temperature will therefore be 28 °C. Thus, if delivering higher temperatures the heat pump must be operated transcritical. The pressure during transcritical heat rejection will be approximately constant. Heat rejection at a temperature glide is suitable for hot water heating when the temperature difference for the heat sink is large, given counter flow in the gas cooler, as the temperature of the CO_2 can be matched to the temperature of the water, see figure 2.6. By matching the heat sink temperature to the temperature of the working fluid in the gas cooler the exergy destruction in the gas cooler is minimized [Bamigbetan et al., 2017]. An advantage of using CO_2 for DHW is that no auxiliary heating methods are necessary, as water temperatures up to 90 °C can be produced without any problems [Nekså et al., 1998]. A typical system configuration for a CO_2 heat pump for DHW is shown in figure 2.7.

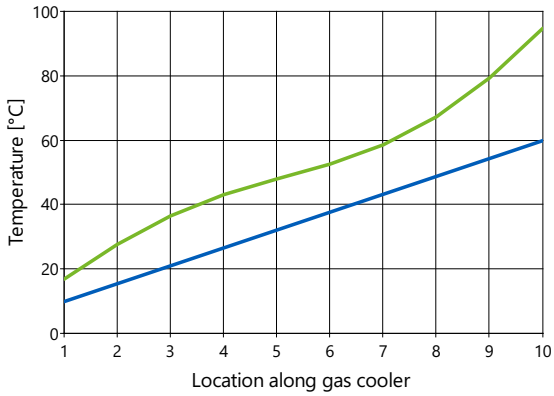

Figure 2.6: The diagram shows the excellent temperature match that can be achieved using a transcritical CO_2 cycle. The water is heated from 10 °C to 60 °C, and is represented by the blue line. The green line represents the temperature of the CO_2.

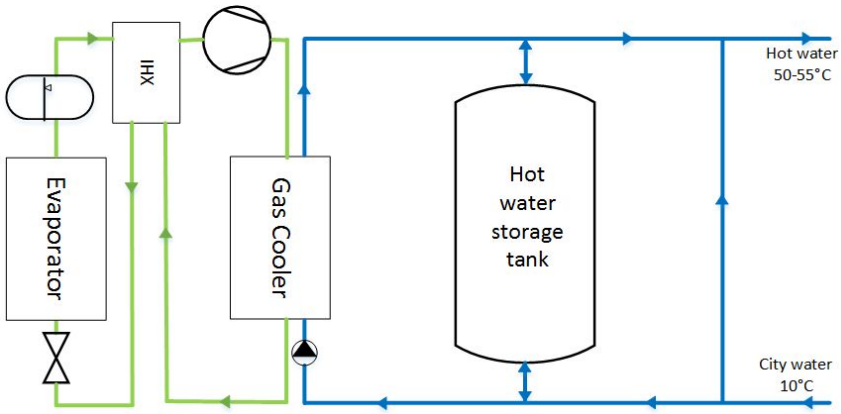

Figure 2.7: Principle sketch of a CO_2 heat pump water heater. The green lines represent the CO_2 in the heat pump, while the blue lines represent water.

Nekså et al. [1998] tested a 50 kW CO_2 heat pump for heating of water. The COP of the heat pump was in the range 3.0 - 4.3 when the water was heated from 9 °C to 60 °C with evaporation temperatures ranging from -20 °C to 0 °C.

Compression in a CO_2 system (point 1-2 on figure 2.8) have a very low pressure ratio. Typically the high pressure will be about 90 bar and the low pressure 35 bar, which gives a pressure ratio of 2.6. CO_2 systems also have less significant

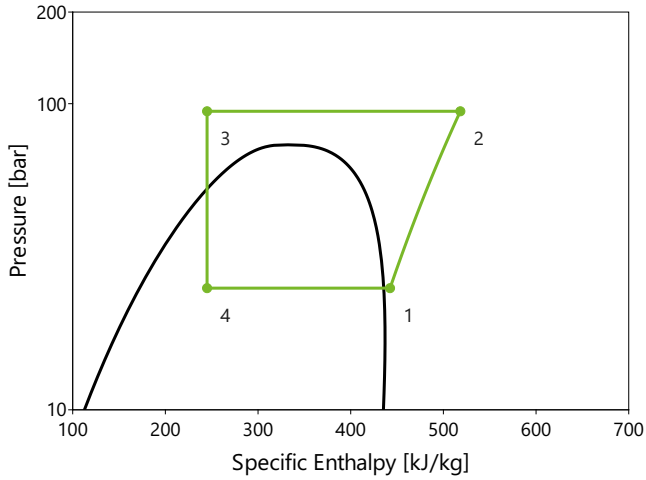

Figure 2.8: Log p-h diagram for a typical CO_2 heat pump water heater. The depicted cycle has an evaporation temperature of -12 °C and heats water from 10 °C to 60 °C.

pressure losses compared to other working fluids due to the high pressures. [Nekså et al., 1998]

For transcritical CO_2 cycles the design of the gas cooler is critical as it affects the heat rejection pressure, water outlet temperature and working fluid outlet temperature, which will impact the total performance [Nawaz et al., 2018]. In the gas cooler it is a pinch point, which is not possible to avoid. The pinch point is defined as the location where the heat transfer fluids have minimum temperature difference. It is located at one of the ends of the gas cooler or somewhere inside the gas cooler. It is preferable to avoid a pinch point inside the gas cooler. [Chen, 2019]

2.5 Heat pumps for space heating

Heat pumps for space heating (SH) is not foreign, and can be connected to many different heat sources, e.g. solar heat, geothermal heat, waste heat. SH systems have variable temperature inlet/outlet of the distribution system depending on type of distribution system and the outdoor temperature. One can do as Hesaraki et al. [2015] and classify the temperature levels for the heating system, where 55 °C is medium temperature, 45 °C low and 35 °C very low. For a conventional radiator the temperature will be about 45 °C. Hydronic heating systems for space heating normally have the heat emitting elements connected in parallel and operated with the same inlet temperature [Stene, 2007].

More buildings are becoming more energy efficient due to better insulation, less infiltration and more efficient heating and ventilation systems. This means that heat losses from the buildings are becoming smaller, and that may be the reason why the heating systems in buildings can operate at lower temperatures. If the temperatures in the heating systems are lower there will be less heat losses from the distribution system, which opens for using heat with lower quality, e.g. renewables and waste heat. Lower temperature in the heating system will require a smaller temperature lift if using a heat pump, which will increase the efficiency of the heat pump. Another important aspect is that in the future the temperature in the district heating grid most likely will be lowered, and the systems will not receive as high temperatures as today. [Hesaraki et al., 2015]

For space heating it is possible to use heat pumps with multiple configurations and working fluids, among them propane. Piscopiello et al. [2016] tested a water to water heat pump with propane for SH. In SH mode, when delivering water at 45 °C, the COP was 3.3 when delivering an amount of heat of approximately 45 kW.

2.6 Combined space and hot water heating

There are heat pumps for only space heating or hot water heating, but multiple studies have also looked at the possibility of combining SH and hot water heating in a single heat pump unit. For this purpose, a CO_2 heat pump can be used. Then the gas cooling process can be divided into three sub-processes: preheating of hot water, low-temperature space heating and reheating of hot water, see figure 2.9. All the heat rejection processes can be gathered in a single counter flow gas cooler

[Stene, 2005]. In a setup like this, problems can arise if the heat demand is lower than the available heat. Then the return temperature to the gas cooler may be too high due to low hot water consumption and therefore an equalization of the temperature in the hot water tank may happen. A solution can be to insert an electrical heat element or a bypass on the first gas cooler so that the lukewarm water from the tank either is heated to 60 °C or used for space heating.

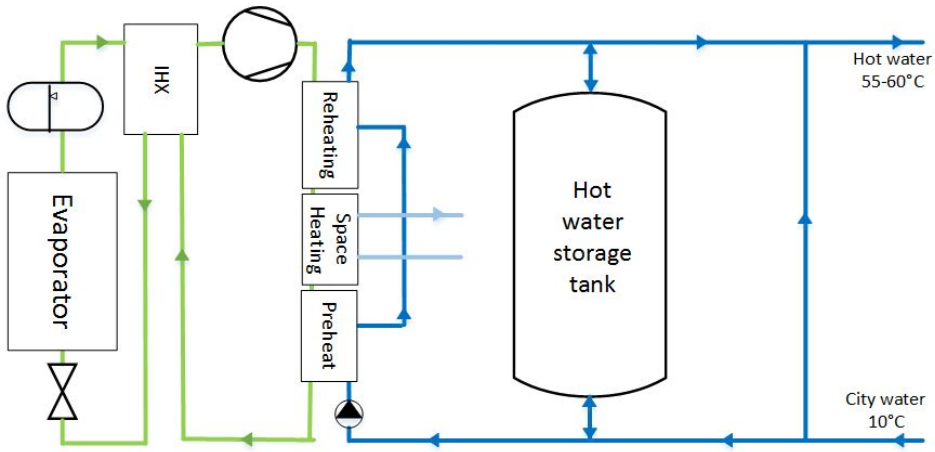

Figure 2.9: Principle sketch of a combined system for space heating and hot water heating. The green lines represent the working fluid and the dark blue lines the hot water system, while the light blue lines represent the water in the space heating system.

To achieve a high COP the heat must be rejected over a large temperature range, which results in a low CO_2 outlet temperature from the gas cooler. The heat pump system shown in figure 2.9 can be operated in three different modes, space heating only, hot water heating (DHW) only and simultaneous space heating and hot water heating (combined mode). When operating in the SH mode there will be no water circulating in the DHW circuit. The study by Stene [2005] showed that the COP in the SH modes was considerably lower than the DHW and combined mode. This is a result of the bad temperature fit between the CO_2 and the water and that the CO_2 outlet temperature is limited by the return temperature from the space heating system. The COP of the DHW mode and the combined mode was relatively similar, but the COP of the SH mode was about 20-30 % lower.

Piscopiello et al. [2016] tested a propane heat pump for simultaneous SH and DHW. The test showed a negligible difference in COP and amount of rejected heat for the simultaneous production as for only SH and gave a COP of 3.3 and

rejected heat of 45 kW.

2.7 Cascade systems

A cascade system is several heat pump cycles connected in series. The cycles are connected by common heat exchangers, for instance, for a two-stage system the condenser in the low temperature cycle (LTC) will be the evaporator in the high temperature cycle (HTC). Using a cascade system allows for a higher temperature range and lift, because different working fluids can be used for the different stages, taking advantage of their distinct properties. By using a cascade system, reasonable pressure ratios can also be obtained. Another advantage when using more than one working fluid, is the possibility of also using different lubrication oils. However, choosing the best combination of working fluids is critical in the design process of cascade systems. In addition, selecting the intermediate pressure as well as the degree of subcooling and superheating is important for the energy performance of the cascade heat pump. To further improve the energy performance an internal heat exchanger can be implemented. The performance of a cascade system also depends on the operating conditions and additional components. Moreover, cascade heat pumps can result in higher energy performance than other configurations. [Mota-Babiloni et al., 2018]

The intermediate pressure in a cascade or multistage system is important as it determines the compressor's pressure ratio, volumetric efficiency, and isentropic efficiency, which will influence the total performance of the system [Kim et al., 2013]. To find the intermediate pressure, several methods are presented in literature. Some state the optimal temperature to be the geometric mean of evaporation and condensation temperatures (for two-stage), while others claim it depends on the working fluid. [Mota-Babiloni et al., 2018]
In many studies the optimized intermediate temperature is determined numerically. However, there is no general explanation to the methods applied, which only makes them valid for the specific study and hard to adopt to other studies. [Kim et al., 2013]

In the laboratory at NTNU, Bamigbetan et al. [2019a] built a high temperature cascade heat pump prototype, able to deliver heat at a temperature of 115 °C. Its capacity was 20 kW, and it used propane in the LTC and butane in the HTC. Both the heat source and the heat sink were water streams. The heat pump utilized heat at 30 °C as the heat source. The butane compressor was modified for high

temperature operations, while a commercially available propane compressor was used. The average value for the combined COP was 3.1, with a temperature lift of 98-101 K. The combined COP was calculated using equation (2.7). [Bamigbetan et al., 2019a]

$$COP_{comb} = \frac{\dot{Q}_{c,HTC} + \dot{Q}_{0,LTC}}{\dot{W}_{comp,HTC} + \dot{W}_{comp,LTC}} \tag{2.7}$$

Where $\dot{Q}_{c,HTC}$ is heat rejected at the condenser, $\dot{Q}_{0,LTC}$ is heat absorbed at the evaporator, $\dot{W}_{comp,HTC}$ is the HTC compressor power and $\dot{W}_{comp,LTC}$ is the LTC compressor power.

The COP of a cascade heat pump is defined as in equation (2.8).

$$COP = \frac{\dot{Q}_{c,HTC}}{\dot{W}_{comp,HTC} + \dot{W}_{comp,LTC}} \tag{2.8}$$

2.8 District heating

The district heating grid transports hot water to consumers, while the colder water is transported back to the energy central in a closed circuit, making it possible with heat production several kilometers away from the consumer. District heating takes advantage of local energy sources as biofuel, municipal waste and industrial processes, resources that would not be utilized otherwise. This can reduce the emissions of greenhouse gases, depending on the environmental friendliness of the energy sources the district heating replaces. District heating can reduce the peak loads on the electricity grid caused by electric heating and eliminate the need for electric heating in buildings/areas connected to the district heating grid. Thus, reducing the total electric energy consumption. The heat from district heating can be used for various heating purposes, e.g. space heating and heating of water. Usually the price of district heating matches the electricity price but will result in a lower cost due to avoidance of additional fees. [Statkraft Varme AS, 2019a]

The district heating system in Trondheim is different from many other cities, because the base heat load comes from burning of municipal waste. Only the municipal waste that cannot be used for any other purposes will be burned. Approximately the same amount of waste is produced throughout the year, which

means there will also be burning of waste during the summer as no economically feasible solution for storage of the waste is available. Due to a low heating demand during the summer, there may be excess heat. In many other cities, the amount of produced heat will be adjusted to the demand, with lower production during the summer. For the coldest periods, the district heating in Trondheim have auxiliary methods, like burners using fossil fuel, to be able to meet the demand. Generally, one tries to use bio-fuels instead of fossil fuel.[Statkraft Varme AS, 2019a]
The district heating in Trondheim covers 30 % of the heat demand in the city, and 83.7 % of the heat originates from heat recovery from the waste burning process. [Statkraft Varme AS, 2019b]

The district heating grid in Trondheim normally has a maximum temperature of 110 °C in the feed line, but it can get as high as 120 °C, which gives a temperature range of 80-120 °C. The return line should hold a temperature about 50 K lower, and should always be below 60 °C. The pressure in the district heating grid have seasonal and local variations and will be in the range 0.5 - 2.0 MPa. [Statkraft Varme AS, 2017]

2.9 Economic analysis

Installation of a heat pump is considered as a significant investment, and before purchasing a heat pump a simplified economic analysis should be performed. In this section three different methods for calculating the profitability of an investment will be briefly presented. Often these three methods are used in combination. It will always be uncertainty related to the results as the methods tries to predict the future.

One of the methods is called the payback period (PBP) method, which is the simplest method. It calculates how many years it takes to earn back the investment cost. The PBP is defined in equation (2.9). There are obvious weaknesses with this method. First of all the method does not consider the time value of the cash flows. In addition the method only tells how fast an investment is refunded and not anything about the profitability after the payback period. [Hagaland Finans]

$$PBP = \frac{investment\ cost}{anticipated\ yearly\ revenue} \tag{2.9}$$

Another method is the net present value (NPV) method. This is the recommended method as it is considered the most accurate. The method takes the time value of

the cash flows into account, by considering when the payments happen so the cash flows can be adjusted correctly. A positive NPV suggest a profitable investment, while a negative NPV indicates a non-profitable investment. In an ideal world all investments with a positive NPV should be conducted. However, in the real world where there is not unlimited capital one needs to choose the investments that is most likely to give the highest return, thus, the one with highest NPV. The NPV is calculated by using equation (2.10). [Hagaland Finans]

$$NPV = -I_0 + \sum_{n=1}^{N} \frac{C_n}{(1+r)^n} \tag{2.10}$$

Where I_0 is the investment cost, C_n is the net cash flow during a time period n, r is the discount rate, n is the given time period and N is the total number of time periods.

The discount rate must be determined and can affect the outcome greatly. The discount rate represents the risk and uncertainty related to the investment and is the required rate of return for the investment. A rule of thumb is that the investment at least needs to give the same return as it would get in the bank, and in addition it should be compensated for the risk of an investment. Thus, the higher the risk the higher the discount rate. [Hagaland Finans]

The third method is the internal rate of return (IRR) method. The internal rate of return is a target of return and shows the return that will be achieved on the capital invested at any given time in the project, given in percent. This is a method that makes it easier to compare the investment to other alternatives where the return is given in percent. IRR is used to determine which discount rate that makes the present value equal to the initial investment cost, i.e. the discount rate that satisfies equation (2.11). [Hagaland Finans]

$$I_0 = \sum_{n=1}^{N} \frac{C_n}{(1+r)^n} \tag{2.11}$$

Chapter 3

+CityxChange - Case Sluppen

This chapter aims at thoroughly presenting the available information about facilities in the two buildings at Sluppen selected for the thermal energy part of +CityxChange, namely Sluppenvegen 10 and 17A. Possible heat sources will be described, and suggested solutions for heat recovery will be presented.

The two selected buildings both accommodate processes where waste heat is generated. At Sluppenvegen 17A it comes from computer cooling and in Sluppenvegen 10 from cold stores. Most of the waste heat from these two systems is released to the surroundings through air-cooled condensers. Instead of rejecting this heat to the ambient, it can be utilized. By using a heat pump, the heat can be recovered, and it is possible to upgrade the quality of it by increasing the temperature. Higher quality heat is more useful, thus it is more applicable for use in heating systems. To be future oriented and take the environmental impact into account, only natural working fluids will be considered in the heat pump configurations for the Sluppen area.

3.1 Sluppenvegen 17A

Sluppenvegen 17A is a six-story building that was built in 2011. It is mainly used as office space, but the basement contains storage, machine rooms etc. The waste heat originates from computer cooling, and the existing cooling system is placed in a machine room in the basement of the building. A sketch of the current system is shown in figure 3.1. Some of the waste heat is recovered internally to the buildings' hydronic heating system, and the rest is rejected to the atmosphere through air-cooled condensers placed on the roof of the building. The water stream on the warm side of the existing chillers usually holds a temperature of approximately 32 °C. This temperature is high enough for the heating system of the building during the summer and parts of the spring and autumn. However, during the winter the hydronic heating system holds a higher temperature than during summer. Therefore, the temperature of the waste heat is often too low for any of the heat to be recovered, and all the heat will be rejected to the ambient. Hence, not utilizing the waste heat during the winter. Sluppenvegen 17A is connected to the district heating grid and uses heat from the grid when the heat recovery is not enough to cover the building's heat demand.

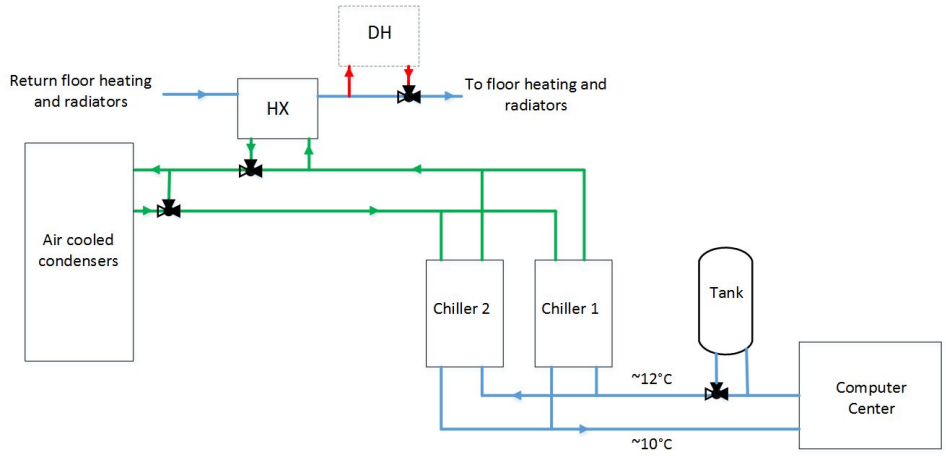

Figure 3.1: Drawing of existing system for Sluppenvegen 17A. Some of the waste heat is recovered internally, while the rest is rejected to the surroundings through the air-cooled condensers. The building is connected to the district heating grid.

Today, two chillers with a cooling capacity of 264 kW each are installed, which is oversized for normal use. Each of the chillers have four compressors, but never uses more than three simultaneously. It is alternating operation on the chillers,

only one operate at a time, while the other one serves as back-up. Measurements done on the hot side of the chillers show a daily average of 89 kW heat rejected from the system. We have the following relations:

$$COP_0 = \frac{\dot{Q}_0}{\dot{W}_{comp}} \tag{3.1}$$

$$\dot{Q}_0 = \dot{Q}_c - \dot{W}_{comp} \tag{3.2}$$

Where $\dot{Q}_0$ is the cooling capacity and COP_0 is the cooling coefficient of performance. By combining equation (3.1) and (3.2), the following expression for the cooling capacity is obtained:

$$\dot{Q}_0 = \frac{\dot{Q}_c}{1 + \frac{1}{COP_0}} \tag{3.3}$$

When assuming a cooling COP of 2.5, the cooling power results in 63.5 kW. Thus, if installing a heat pump on the cold side it should be sized for approximately 60 kW cooling capacity. The return water line from the data center holds a temperature of 12 °C and the feed line 10 °C, as can be seen from figure 3.1.

A possible way of integrating the new heat pump in the existing system can be to remove the existing accumulator tank (see figure 3.1 for placement of the tank) and then connect the heat pump to where the tank is placed today. The accumulator tank is rarely in use, and is not necessary in the existing system, therefore, removing it will not affect the process noticeably. By connecting the heat pump in this place, the existing system will function as a back-up, and can maintain the process cooling if for some reason the heat pump stops running. Maintaining the main process is very important in a project like this, as there may be large consequences of disturbing the main process.

For Sluppenvegen 17A it is decided that the heat recovered by the inserted heat pump should be fed into the district heating grid. To increase the temperature to a level that matches the district heating grid in Trondheim, a high temperature heat pump must be utilized. Ideally, the heat pump will deliver heat to the feed line, above 100 °C. The heat pump can have different designs, but the main principle has been decided to be a cascade system using hydrocarbons as working fluid. The most likely option will be a configuration similar to the one depicted in figure

3.2, with the process as depicted in the T-s diagram in figure 3.3. In the project thesis written during the fall semester of 2019 this configuration was modeled with propane in the LTC and butane in the HTC. Simulations were run and they resulted in a COP of 2.32, when assuming a heat sink inlet temperature of 98 °C.

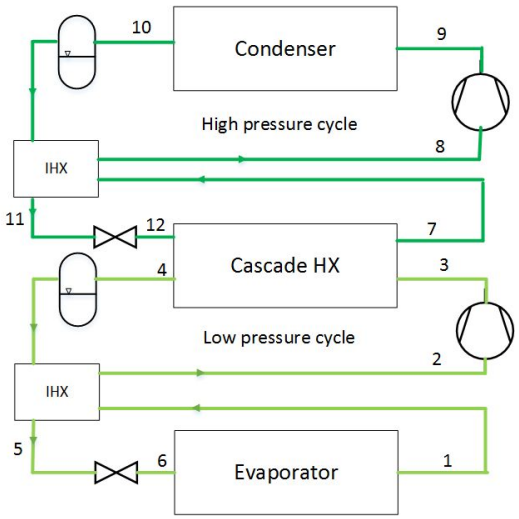

Figure 3.2: 2-stage cascade heat pump system for high temperature application.

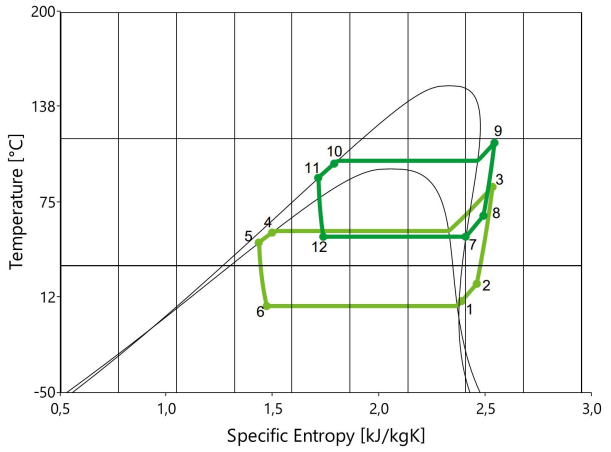

Figure 3.3: T-s diagram for cascade system with configuration as shown in figure 3.2 with propane in the LTC and butane in the HTC. Evaporation and condensing temperature for the LTC is 7 °C and 56 °C, while for the HTC 53 °C and 103 °C, respectively.

3.2 Sluppenvegen 10

Sluppenvegen 10 is a building that consist mainly of a chilled warehouse for storage of fruits, vegetables and flowers. The oldest part was built in 1969, but the floor area has almost been doubled since then. Today, four refrigeration units are in operation. The biggest one, called chiller 3 in figure 3.4, has a cooling capacity of 346 kW and it is able to cover the area covered by chiller 4 as well. The size of the other machines is presumably about 120 kW each.

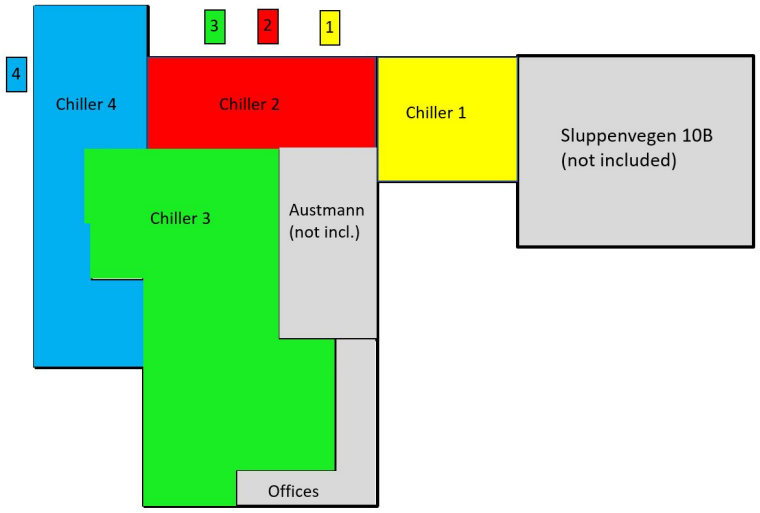

Figure 3.4: Overview of the area covered by the different chillers at Sluppenvegen 10. The gray areas are not a part of the refrigerated warehouse.

The operation strategy for the chillers is unknown, and there are few measurements on the chillers. In figure 3.5, the floor plan with the temperature levels for the different rooms in the building is shown. The products arriving at the chilling facility are already cooled to the desired temperature, so there is no additional heat load from cooling of the products. The refrigerated warehouse only contains chilling rooms, no freezing, and the temperature levels for the different rooms are shown in figure 3.5. From the figure it is clear that most of the rooms are either 2 - 4 °C or 10 - 12 °C. However, some rooms have higher temperatures as well, and during the winter these zones sometimes need heating.

In Sluppenvegen 10 there have been conducted measurements of the chillers' electricity consumption. The measurements from 2019 is depicted in figure 3.6. In the graph the outdoor temperature is also included to show a potential correlation.

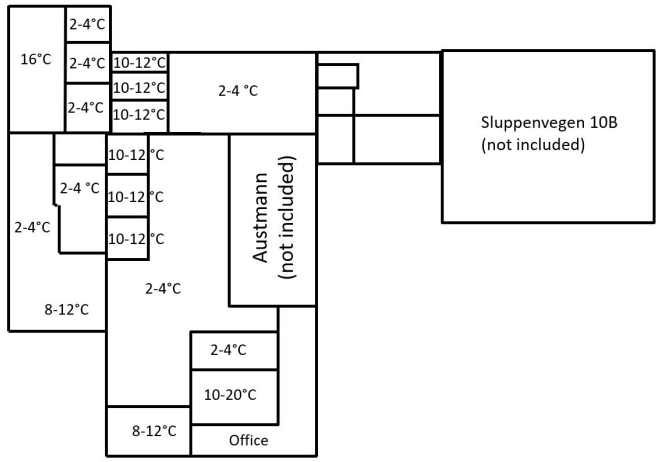

Figure 3.5: Floor plan of Sluppenvegen 10 with temperature levels for the chilled rooms. The drawing is based on a floor plan drawing of the sprinkler system, and does not show all the partition walls.

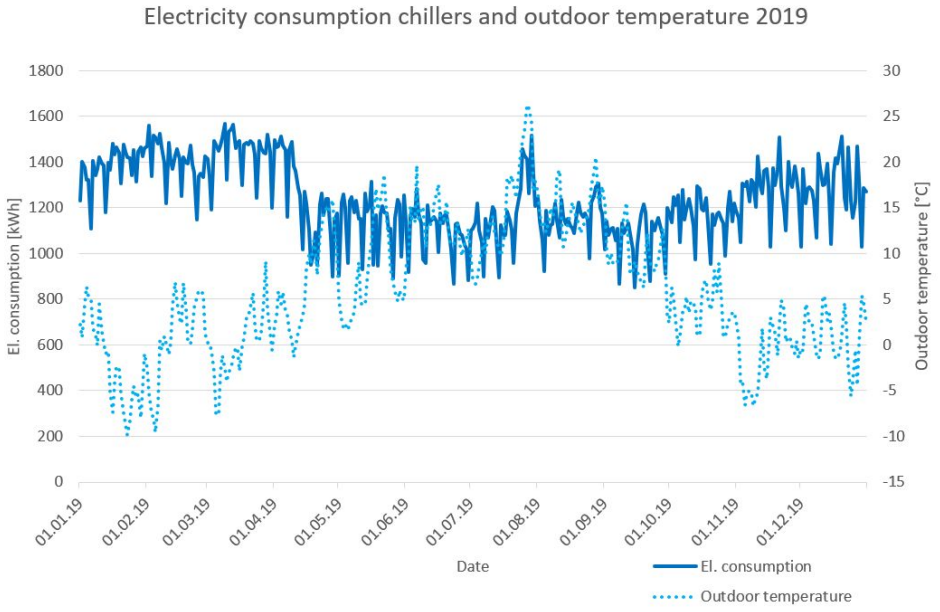

Figure 3.6: Electricity consumption for the chillers at Sluppenvegen 10 compared to the outdoor temperature for 2019.

However, there is no clear correlation between the electricity consumption and the outdoor temperature. From the graph it can be seen that it is only small variations in the energy consumption, with a slight reduction at higher outdoor temperatures during summer. This is not as expected, but a reason can be the need for heating in certain zones during periods of cold weather. Another explanation can be that the performance of the chillers is lower at part load, which leads to increased electricity consumption per kW delivered cooling. If assuming a COP of 2 for the chillers one can estimate the possible amount of heat delivered from the chillers, that can be used for other purposes. The graph in figure 3.7 shows the assumed heat delivered. During 2019 the average heat delivery was 103 kW. To calculate the amount of heat, the number of operating hours is of importance. If assuming 8 700 operating hours yearly, the amount of heat that was rejected from the chillers at Sluppenvegen 10 in 2019 was 896 100 kWh.

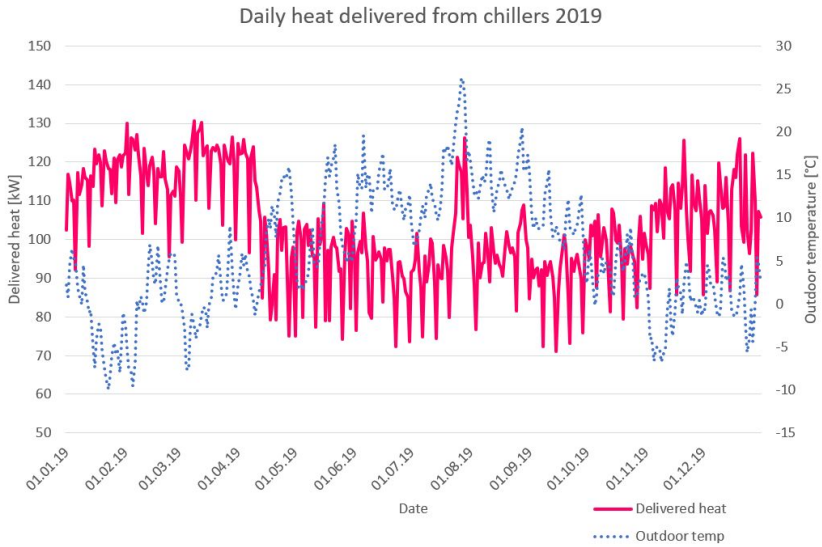

Figure 3.7: Possible heat delivery from the chillers at Sluppenvegen 10, when assuming a COP of 2. The outdoor temperature is included to see a potential correlation between the heat delivery and the outdoor temperature.

When designing the heat pump for heat recovery it is important to decide the capacity of the unit. The capacity is decided based on the sizes of the existing chillers and the electricity consumption. To ensure a large number of operating hours at full load, the heat pump will have a smaller capacity than the energy consumption indicates that it should have to utilize all the waste heat. The main

process, in this case chilling, does not depend on the heat pump and will not be affected if the heat pump cannot recover all the heat. In that case, the remaining heat will be rejected through the air-cooled condensers, as is today's situation. A heat pump of 60 kW cooling capacity has been identified as the best solution, as the +CityxChange project should test different solutions to verify whether they can be implemented other places, making many operating hours for proper testing important.

A proposed solution for the heat recovery at Sluppenvegen 10 is an external CO_2 circuit that absorbs heat from the existing system, upstream of the chillers, see figure 3.8. The CO_2 extracts heat directly from the glycol circuit in the refrigeration facility through heat exchangers. Afterwards, the CO_2 rejects heat to the heat pump working fluid by evaporation in the evaporator. The necessity of having an external circuit arose because the heat pump must be placed somewhere outside of the building. By using CO_2 instead of for instance glycol, the pipes can have a much smaller diameter. This will make it cheaper to lay the pipes in the ground, as you could dig smaller holes for the pipes.

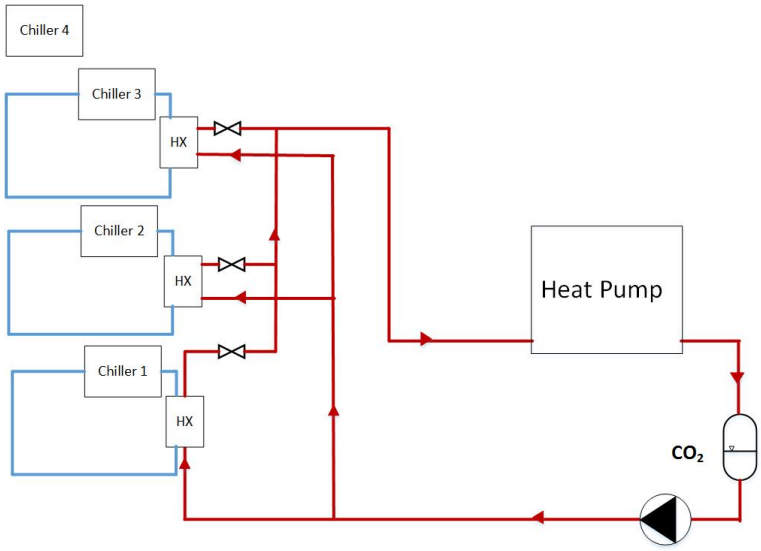

Figure 3.8: Proposed solution for heat recovery at Sluppenvegen 10. The CO_2circuit will absorb the heat from the glycol circuit upstream the chillers and transfer it to the heat pump working fluid. Chiller number 4 is not included as there have been plans of replacing it. The red lines represent the CO_2 and the blue lines the glycol.

The CO_2 circuit is not known to have been tested anywhere else, and can be considered as an innovative solution. As innovative solutions are important for the +CityxChange project, the CO_2 circuit represents the innovation and the project can tolerate a less innovative heat pump configuration. The heat pump unit can have different designs depending on the purpose of the heat delivery, and there are multiple possible customers for the heat recovered at Sluppen, which will be presented in the following sections.

3.2.1 Alternative 1 - District heating

The first possibility that is to be considered is delivering the heat to the district heating grid using a high temperature heat pump. Delivery to the district heating grid requires a high temperature lift for the heat pump, as the condensing temperature should be about 103 °C, resulting in a temperature lift of 115 K. For this purpose, a cascade heat pump system with configuration as shown in figure 3.2 can be used. By using this configuration one can utilize hydrocarbons as working fluids. An example can be to use propane in the LTC and butane in the HTC. With these working fluids and evaporation and condensing temperature for the LTC of -12 °C and 46 °C, and for the HTC 43 °C and 103 °C, respectively, one can achieve a COP of 1.96. This number originates from simulations conducted in the project thesis conducted during the fall semester of 2019.

Heat delivery to the district heating grid is the chosen solution for the heat pump system to be installed at Sluppenvegen 17A. In retrospect this have been considered as a relatively bad solution for Trondheim as the district heating grid has a large surplus of heat during the summer, and Statkraft would not be willing to pay for the heat if they were not a partner in the project. Therefore, another heat delivery solution is desirable for Sluppenvegen 10.

3.2.2 Alternative 2 - HPWH

Another alternative for the heat delivery can be to deliver the heat to a water heater for DHW. There are buildings close by that have a hot water demand, for instance a fitness center and a brewery.

In determining whether this is a good solution, one needs to evaluate the hot water demand for the possible customers. It is uncertain how much heat that can be recovered from Sluppenvegen 10, and whether this will be enough to cover the entire hot water demand for the potential customers. However, it would at least be possible to cover parts of the demand or the heat could be used for preheating of hot

water. For the fitness center it can be assumed that the necessary temperature of the hot water is about the same as for normal domestic hot water (DHW). However, for the brewery more information is needed in order to perform a proper evaluation.

3.2.3 Alternative 3 - Heating of water for space heating

The third alternative will be to deliver heat to the heating systems of the surrounding buildings. For this it would be necessary to identify buildings with a hydronic heating system and a heat demand. For instance, NTNU rents a building used for conducting exams. For this purpose, a temperature of 40 - 50 °C should be sufficient, and the necessary technology is likely to be commercially available. However, it has not been verified whether this building has a hydronic heating system or not. For space heating it is possible to test the performance of different working fluids, e.g. ammonia and propane. As this solution gives a smaller temperature lift for the heat pump compared to the other alternatives, a relatively high COP is likely to be achievable.

Chapter 4

Methodology

This chapter aims at thoroughly describing the development of the heat pump models that was used to generate the results in this master's thesis. This includes the calculations that formed the basis for the input values and explanation of the choices, simplifications and assumptions that were made, as well as challenges arising in the process.

The theoretical heat pump models were developed using the Dynamic Modeling Laboratory (Dymola) 2017 (Dassault Systems, Vélizy-Villacoublay) and TIL library for modeling thermal systems TIL 3.5.0 (TLK-Thermo GmbH, Braunschweig, Germany).

The rest of this master's thesis will only focus on Sluppenvegen 10. The heat delivery method for Sluppenvegen 10 selected for this master's thesis was heating of hot water. This was considered as the most exciting heat delivery case and was believed to have good prospects.

4.1 CO_2 HPWH

Firstly a simplified model of a heat pump that can be used for heating of hot water was developed. The model was a transcritical CO_2 heat pump, as this type of heat pump has shown excellent results for hot water heating due to the temperature match between the CO_2 and the water in the gas cooler.

The initial model consisted of a heat pump with an evaporator, a liquid receiver, a compressor, a gas cooler and an expansion valve, as seen in the upper part of

figure 4.1. The evaporator absorbs heat from a CO_2-circuit, which is connected to a heat exchanger that extracts heat from the glycol circuit in a chilled store. In the model it has been used propylene glycol 40 % instead of ethylene glycol 40 % as the latter was not an option in the TIL library, and this will be addressed in the discussion in chapter 6. The glycol circuit for the chilling store was designed with a temperature of -6 °C to maintain the desired temperature in the store. With a temperature difference of 3 K in the heat exchangers, this means that the inlet temperature of the CO_2 in the first heat exchanger, called heat exchanger in figure 4.1, must be -9 °C. Thus giving an evaporation temperature of -12 °C for the heat pump, and a constant low pressure of 25.03 bar. This formed the basis for the enthalpy calculations in the development of the initial model. Initially the heat pump was designed to heat water from 10 °C to 60 °C. The heat sink outlet temperature determined the high pressure of the cycle. This was initially set to 95 bar, but multiple pressures was tested later.

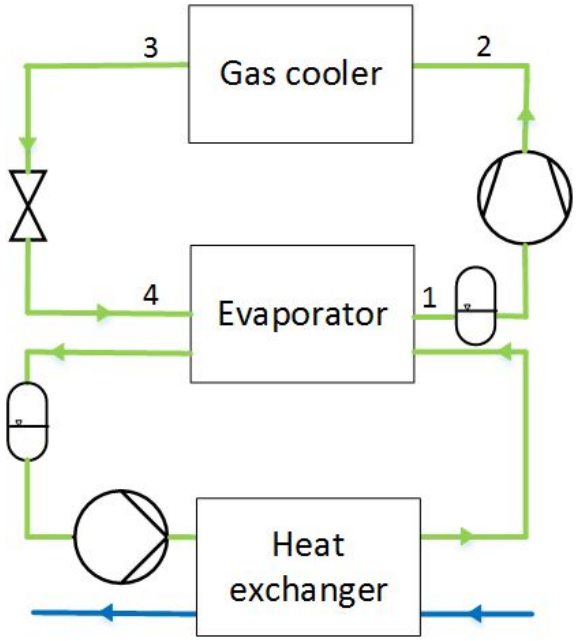

Figure 4.1: Heat pump configuration used in the initial model. The upper part is a simple CO_2 heat pump, which is connected to a CO_2 circuit that extracts heat from the glycol circuit in the cooling system of a cold store. The green lines represent CO_2 and the blue lines represent glycol.

In performing the enthalpy calculations, a superheat of 5 K out of the evaporator

was decided. To achieve high performance for the heat pump, the temperature of the CO_2 at the outlet of the gas cooler must be low, and as a starting point this temperature was set to 15 °C. When calculating the enthalpy in this point the following approximation was used:

$$h(T,p) \approx h_f(T) + v_f(T) \cdot (p - p_{sat}(T)) \tag{4.1}$$

Where h_f is the enthalpy of the saturated liquid, v_f is the specific volume of the saturated liquid and p_{sat} is the saturated pressure.

Table 4.1 shows the initial values used in the development of the model in Dymola. The values have been calculated by using the Refrigerant calculator in CoolPack version 1.5. Most of the properties for the working fluids used in this master's thesis have also been obtained using this program.

Table 4.1: Values used for the initial simulation with a model configuration as shown in figure 4.1.

Point	T [°C]	p [bar]	h [kJ/kg]	s [kJ/kgK]
1	-7.0	25.03	442.42	1.93425
2s	97.0	95.00	503.17	1.93425
2	114.3	95.00	529.21	-
3	15.0	95.00	245.00	-
4	-12.0	25.03	245.00	-

In the model the heat source was modeled as a glycol stream. Only one heat exchanger was used for extracting the heat from the heat source, even though in reality there should be three heat exchangers as there are three chillers. This was a simplification made to avoid a high degree of complexity and was not considered to have a large impact on the end result as this one heat exchanger exchanges the same amount of heat as the three smaller heat exchangers. The mass flow in the glycol stream was calculated by:

$$\dot{m} = \frac{\dot{Q}_0}{\Delta h} = \frac{\dot{Q}_0}{C_p \cdot \Delta T} \tag{4.2}$$

Where Δh is the enthalpy difference in the heat exchanger, which is defined as the specific heat capacity at constant pressure times the temperature difference. In this equation the specific heat capacity is assumed to be constant, which is only valid with small temperature differences. Using $C_{p,glycol}$=3.747 kJ/kgK, the mass

flow becomes, ṁ=4.003 kg/s. The pressure was set to 1.1 bar.

As the heat pump must be placed somewhere else than inside the chilled store it was, as earlier mentioned, used a CO_2 circuit to extract the heat from the chilling system at Sluppenvegen 10. This circuit extracts the heat at temperatures in the range from -2 °to -5 °C, and the glycol outlet temperature from the heat exchanger should be -6 °C. Using a temperature difference of 3 K in the heat exchanger this results in a CO_2 inlet temperature of -9 °C to the heat exchanger (assuming counter current flow). To account for deviations from the calculations in the model, the pressure in the CO_2 circuit was set equal to the liquid saturation pressure of CO_2 at a temperature of -7 °C, 28.84 bar, respectively. The mass flow was calculated using equation (4.2), with $C_{p,CO_2} = 1.465$ kJ/kgK and a temperature difference of 2 K, resulting in a mass flow of 20.48 kg/s.

The heat sink was modeled as a water stream. The pressure was set to 1.1 bar and the mass flow was calculated by using equation (4.2). The specific heat of water was assumed to be constant even though the water has a large temperature difference between the inlet and the outlet of the gas cooler. However, tables giving specific heat capacity of water at different temperatures showed a negligible difference from 10 °C to 100 °C. Using a heat capacity of 4.2 kJ/kgK and a temperature difference of 50 K the mass flow was set to 0.411 kg/s for the heat sink.

All the heat exchangers used in the model were plate heat exchangers with counter current flow, and the size of these were necessary input variables. When calculating the heat transfer area of the heat exchangers equation (4.3) was used, however this equation only gives the total heat transfer area, meaning the geometry must be determined based on this.

$$\dot{Q} = U \cdot A \cdot \Delta T_{LMTD} \tag{4.3}$$

Where $\dot{Q}$ is the heat transferred, U is the overall heat transfer coefficient, A is the heat transfer area of the heat exchanger and ΔT_{LMTD} is the mean logarithmic temperature difference. To calculate the logarithmic mean temperature difference for the heat exchangers equation (4.4) was used.

$$\Delta T_{LMTD} = \frac{\Delta T_A - \Delta T_B}{ln(\frac{\Delta T_A}{\Delta T_B})} \tag{4.4}$$

Where ΔT_A is the temperature difference between the hot and cold fluids at one end of the heat exchanger, while ΔT_B is the difference at the other end. E.g. ΔT_A

is hot fluid inlet minus cold fluid outlet and ΔT_B is hot fluid outlet minus cold fluid inlet.

To determine the overall heat transfer coefficients, different literature have been used to find a relevant range and then the values have been assumed based on this range. The selected U-values are listed in table 4.2. It was assumed that the overall heat transfer coefficients were constant throughout the entire heat exchangers, which may not be the case, but this will be addressed in the discussion in chapter 6. Table 4.2 gives the mean logarithmic temperature difference and theoretical heat exchanger area for the heat exchangers in the model.

The heat exchangers were developed separately before they were combined in the final model. By using the calculated theoretical area of the heat exchangers the heat transfer was too small, thus, the actual size of the heat exchangers was decided by gradually increasing the size until the desired heat transfer rate was reached. The heat exchanger areas used in the model are listed to the right in table 4.2 and are larger than the theoretical areas. This might give some errors in the results and will be included in the discussion in chapter 6.

Table 4.2: Key parameters for the heat exchangers.

HX	$\dot{Q}$ [kW]	U [W/m^{2}K]	ΔT_{LMTD} [K]	A [m^2]	A_{real}[m^2]
Heat exchanger	60.00	1200	3.915	12.77	47.60
Evaporator	60.00	500	3.476	34.52	74.36
Gas cooler	86.38	1860	20.670	2.25	16.00

After developing a static model, the need for controllers became evident. Different processes require different combinations of control parameters. If a process allows for deviations from the set-point a P-regulator can be used. If deviations are not allowed, a PI-regulator is a better option [Nasjonal Digital Læringsarena (ndla)]. Firstly, the expansion valve was regulated to maintain the desired high pressure. In addition the compressor was regulated to maintain a constant evaporation pressure. To determine the regulating parameters the Ziegler Nichols method was used. This method is based on finding the critical fluctuation point, which is found by using a P-regulator. The set points for the process was determined and the proportional gain of the controller was gradually increased until the system started oscillating, the proportional gain in this point is called the critical gain. Identifying the critical fluctuation point was done by trial and error. The proportional gain of the controller, k, is defined as: $k = 0.45 \cdot k_{crit}$ and the time constant of the

integrator block, $Ti = 0.85 \cdot T_{crit}$ [Nasjonal Digital Læringsarena (ndla)]. Where k_{crit} is the proportional gain where the system starts oscillating and T_{crit} is the inverse of the frequency at this k, i.e. $1/f_{crit}$.

The performance of a heat pump depends on the operating load. Usually the performance is best at design load and then decreases with decreasing load. Therefore it was desirable to use varying efficiencies for the compressor in the model. By using the BITZER software a possible compressor for the heat pump was found, and the model was 4GTE-20K. The application area for this compressor is depicted in figure 4.2, where the red dots represent the ideal operation point based upon the cooling capacity and the evaporation temperature. The high pressure is lower than the required pressure to deliver hot water at 60 °C. However, from the figure it is clear that the compressor would still be inside the application area even if operating with a high pressure of 100 bar.

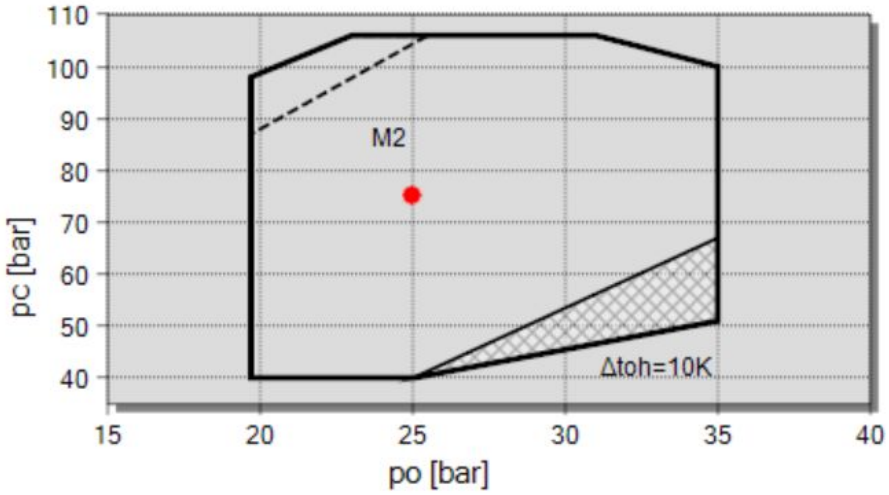

Figure 4.2: Application area for BITZER compressor 4GTE-20K. The red dot shows the optimal operation point based on cooling capacity and evaporation temperature. However, the outlet temperature of the heat sink is not taken into account when deciding the high pressure. The y-axis, p_c, represents the high pressure and the x-axis, p_0, represent the evaporation pressure.

From the BITZER software a polynomial for the compressor power was obtained. The polynomial uses the high pressure and the evaporation temperature to calculate the compressor work. By using equation (2.2) the polynomial was rewritten to an expression for the isentropic efficiency. It was made attempts to include this

expression in the Dymola model. However, these attempts failed, and there may be several explanations. For instance that Dymola uses the isentropic efficiency to calculate the temperature and pressure, thus cannot use these parameters as input for calculating the isentropic efficiency. Another reason may be that components from the TIL Library is not compatible with all functions from Dymola, thus cannot implement this polynomial. Therefore, the efficiencies used in the models were set as constant with values given in table 4.3. In the table the stroke volume, compressor work, and cooling and heating loads are given. In figure 4.3 a screenshot of the Dymola model is depicted.

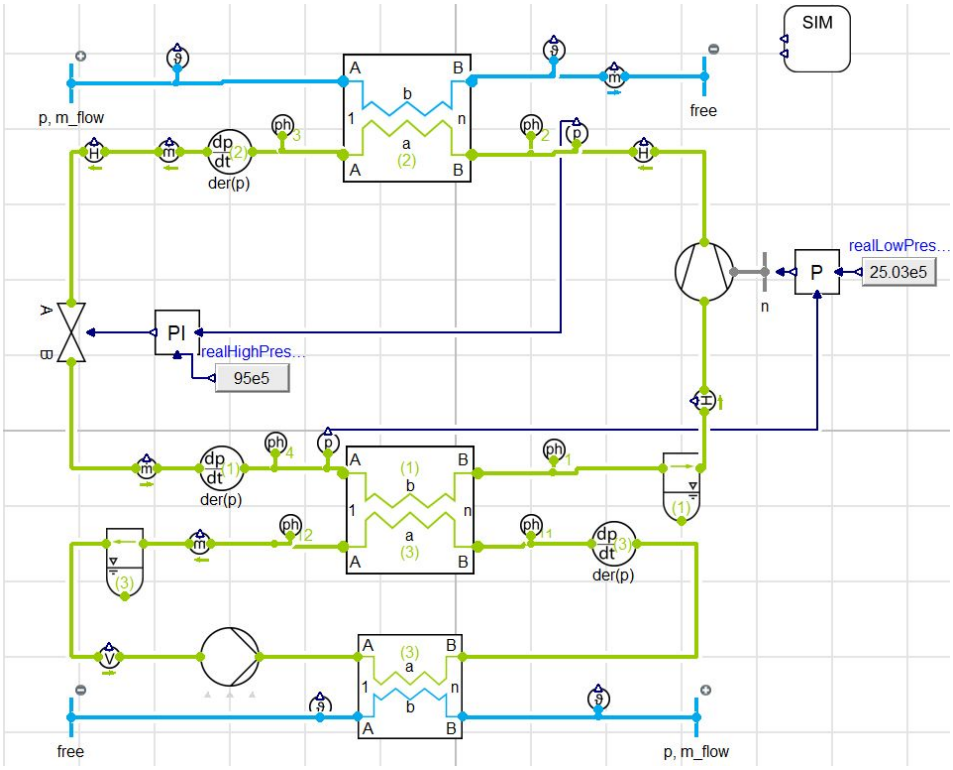

Figure 4.3: An illustration of the model from Dymola. The green lines represent CO_2 while the blue lines represent liquid, which in the bottom is glycol and in the top water.

Table 4.3: Cooling load, compressor work, heating load and COP of the cycle, as well as isentropic and volumetric efficiency and stroke volume for the compressor.

$\dot{Q}_0$ [kW]	$\dot{W}_{comp}$ [kW]	$\dot{Q}_c$ [kW]	COP	η_{is}	λ	$\dot{V}_s$ [m^3/h]
60.00	26.38	86.38	3.27	0.7	0.8	21.41

4.1.1 CO_2 HPWH with internal heat exchanger

The model was modified by inserting an internal heat exchanger, resulting in a heat pump configuration as shown in figure 4.4. The IHX was designed to give a 5 K superheat out of the evaporator, and thus give a subcooling equal to this amount of energy, calculated by the energy balance of the IHX:

$$h_5 = h_1 - h_2 + h_4 \tag{4.5}$$

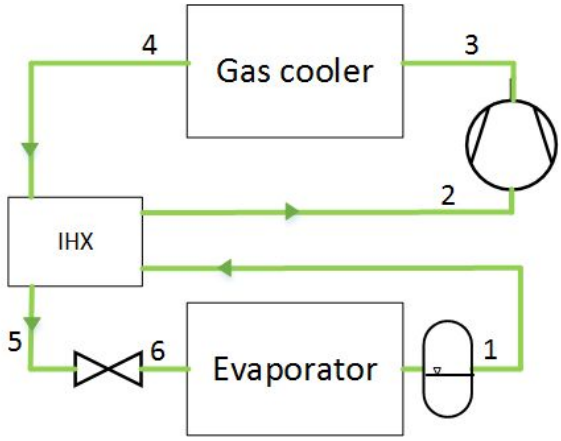

Figure 4.4: CO_2 heat pump configuration with internal heat exchanger.

The size of the IHX was calculated by equation (4.3), and key parameters for the IHX are given in table 4.4. Dymola was not able to run simulations with an IHX of the theoretical size, as this was too small. It was therefore decided to use the smallest heat exchanger area that the software would allow. The most important input values for the cycle including an IHX are given in table 4.5 and 4.6.

Table 4.4: Key parameters for the internal heat exchanger.

HX	$\dot{Q}$ [kW]	U [W/m^{2}K]	ΔT_{LMTD} [K]	A [m^2]	A_{real}[m^2]
IHX	2.06	500	23	0.18	1.57

Table 4.5: Values used in the initial simulations with a model configuration as shown in figure 4.4.

Point	T [°C]	p [bar]	h [kJ/kg]	s [kJ/kgK]
1	-12.0	25.03	435.66	-
2	-7.0	25.03	442.42	1.93425
3s	97.0	95.00	503.17	1.93425
3	115.3	95.00	529.21	-
4	15.0	95.00	245.00	-
5	-	95.00	238.24	-
6	-12.0	25.03	238.24	-

Table 4.6: Cooling load, compressor work, heating load and COP of the cycle with an IHX, as well as isentropic and volumetric efficiency and stroke volume for the compressor.

$\dot{Q}_0$ [kW]	$\dot{W}_{comp}$ [kW]	$\dot{Q}_c$ [kW]	COP	η_{is}	λ	$\dot{V}_s$ [m^3/h]
60.00	26.38	86.38	3.27	0.7	0.8	21.41

4.2 Propane HPWH

A propane HPWH was also developed for comparison to the CO_2 model. Modeling of the CO_2 circuit and the heat source for the propane HPWH were obtained from the previously made CO_2 model. Firstly the evaporator and the condenser were modeled to get the correct heat transfer and to determine the size of these heat exchangers. The theoretical sizes were calculated by using equation (4.3), with the values displayed in table 4.7. The condensing temperature of the propane cycle was found by trial and error, by investigating which temperature that gave high enough water outlet temperature. The temperature of the inlet water was set to 10 °C and the desired outlet temperature to 60 °C. The most important input parameters for the cycle are given in table 4.8. Based on these input variables the heat transfer rates and the compressor work were calculated, they are given in table 4.9. In the same table, input parameters for the compressor are given.

Table 4.7: Key parameters for the heat exchangers in a propane HPWH.

HX	$\dot{Q}$ [kW]	U [W/m^{2}K]	ΔT_{LMTD} [K]	A [m^2]	A_{real}[m^2]
Heat exchanger	60.00	1200	3.915	12.8	47.6
Evaporator	60.00	500	0.833	144.0	148.5
Condenser	83.39	1000	11.784	7.1	19.6

Table 4.8: Values used in the initial simulations of a propane HPWH.

Point	T [°C]	p [bar]	h [kJ/kg]	s [kJ/kgK]
1	-7.0	3.20	572.05	2.42763
2s	74.4	21.18	664.02	2.42763
2	90.2	21.18	703.44	-
3	13.0	21.18	235.27	-
4	-12.0	3.20	235.27	-

Table 4.9: Cooling load, compressor work, heating load and COP of the propane cycle, as well as isentropic and volumetric efficiency and stroke volume of the compressor.

$\dot{Q}_0$ [kW]	$\dot{W}_{comp}$ [kW]	$\dot{Q}_c$ [kW]	COP	η_{is}	λ	$\dot{V}_s$ [m^3/h]
60.00	23.39	83.39	3.57	0.7	0.8	116.15

The rest of the development process was very similar to what is described in section 4.1.

4.3 Economic analysis

To determine whether a heat pump for hot water heating is an economical choice for heat recovery from Sluppenvegen 10 it is important to investigate whether the heat pump can be profitable or not. To make the heat pump a desirable solution the economic analysis should result in a profitable investment.

For the economic analysis of the project a spreadsheet in Excel was developed, which is attached in Appendix I. As there are multiple uncertainties around many of the values regarding economy, as investment cost, electricity price, operation cost etc., it is possible to easily change the parameters in the spreadsheet. Formulas for the NPV, PPB and IRR were set up in the spreadsheet and will be updated automatically if changing the input parameters.

In the economic analysis the number of operating hours is an important input parameter. The heat pump was designed to have continuous operation, and has a smaller cooling capacity than the average heat rejected from the existing chillers. The heat pump is likely to need some maintenance, but this was assumed to be only a few hours. Therefore an assumption of 8 700 operating hours were used, meaning it operates 99.3 % of the year.

The yearly cost of the chillers for the cooling store was given by the building owner to be approximately 250 000 NOK. Exactly what this estimate includes is uncertain, but it was assumed that this sum includes maintenance and electricity cost.

The spreadsheet was used to calculate the profitability of two different scenarios which are presented in the results.

Chapter 5

Results

This chapter will present the most relevant results from simulations using the models described in chapter 4. The models have been tested under different operating conditions, and the results will be presented using figures and tables. The main findings from these figures and tables will be highlighted.

In the figures that depicts the temperature profile in the gas cooler or the condenser from the models, the x-axis represents the total length of the heat exchanger divided into 100 equidistant nodes. This means that node number 1 is one end of the heat exchanger and node number 100 is the other end. For the other heat exchangers in the model the x-axis represents the same but is only divided into 10 nodes.

The results are obtained by running the simulations for 3 600 seconds to ensure steady-state, and the number of intervals is set to 500. The evaporation temperature is constantly set to -12 °C.

5.1 CO_2 HPWH

The initial simulations were as earlier mentioned run with a high pressure of 95 bar. The log p-h and the T-s diagrams for the process are shown in figure 5.1. As can be seen from the figure the discharge temperature is 109.7 °C, and the temperature of the CO_2 at the gas cooler outlet is 12.9 °C. From the diagrams it is also clear that the desired superheat is not achieved, and the suction line contains saturated gas.

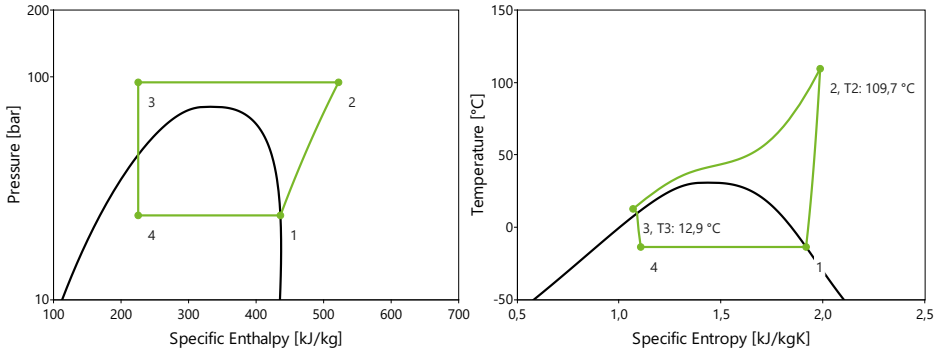

Figure 5.1: Log p-h and T-s diagram of simulations with initial values for the CO_2 model. The high pressure is set to 95 bar.

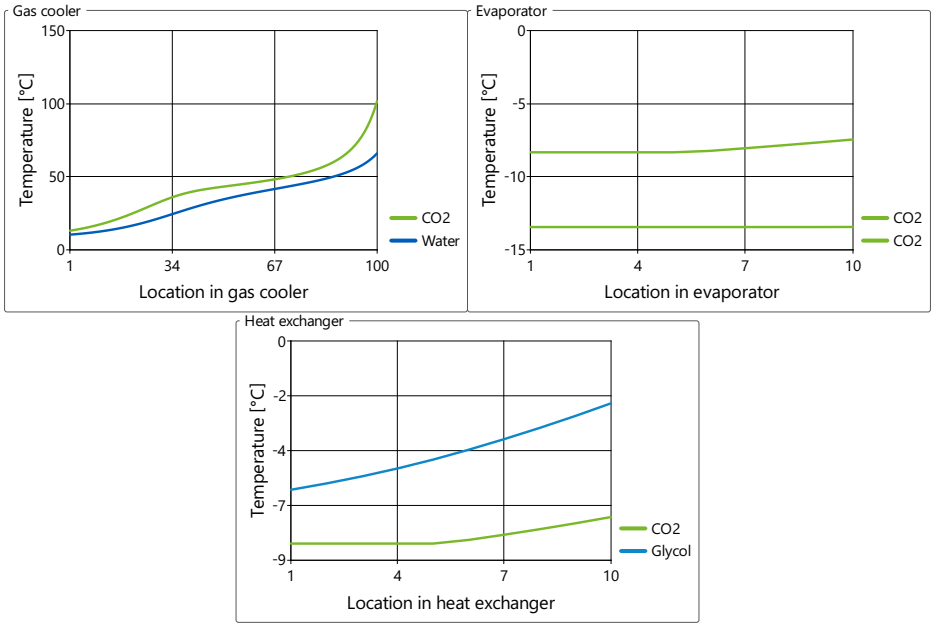

Figure 5.2: Temperature profile in the three heat exchangers used in the CO_2 model.

Figure 5.2 shows the temperature profile in the heat exchangers with the initial model. In the evaporator the highest temperature represents the CO_2 in the CO_2 circuit, while the lower temperature is the CO_2 in the heat pump. From the temperature profile in the evaporator it is clear that the evaporation temperature

is slightly lower than the set point of -12 °C. It can also be seen that there is no superheating in the evaporator, as indicated by the diagrams in figure 5.1. From the temperature profile in the heat exchanger it can be seen that the CO_2 in the CO_2 circuit is evaporated by the glycol. In addition it can be seen that the glycol outlet temperature is approximately -6 °C.

5.1.1 Effect of changing the high pressure

The model was run with different high pressures, where the only additional modification to the model was changing the displacement volume to ensure that the desired pressures were reached. The four high pressures tested were 85 bar, 90 bar, 95 bar and 100 bar.

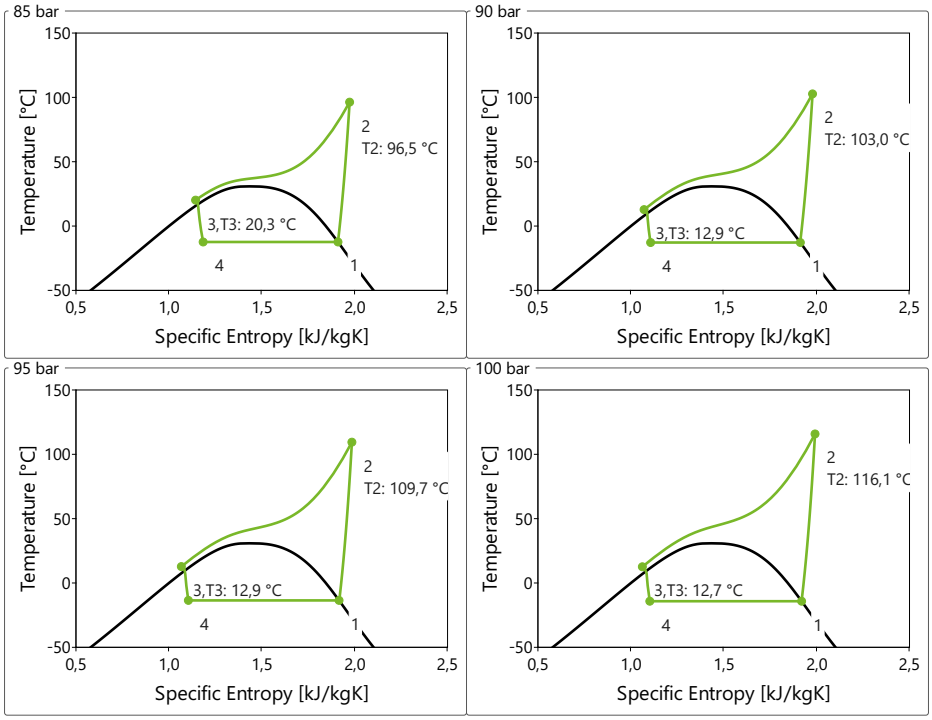

Figure 5.3: The T-s diagram for the cycle at four different high pressures, namely 85 bar, 90 bar, 95 bar and 100 bar. In the T-s diagrams the discharge temperature and the CO_2 temperature out of the gas cooler are given.

In figure 5.3 the T-s diagram for each of the four high pressures tested is depicted. From the figure it is clear that a superheat of 5 K out of the evaporator is not

achieved in any of the cases. Another thing to notice is that the discharge temperature increases with increasing pressure, and for the simulation done at 100 bar the discharge temperature reaches 116.1 °C. Another observation is that the temperature at the outlet of the gas cooler, point 3, is approximately equal for 90 bar, 95 bar and 100 bar (≈ 13 °C), while for 85 bar this temperature is significantly higher (20 °C).

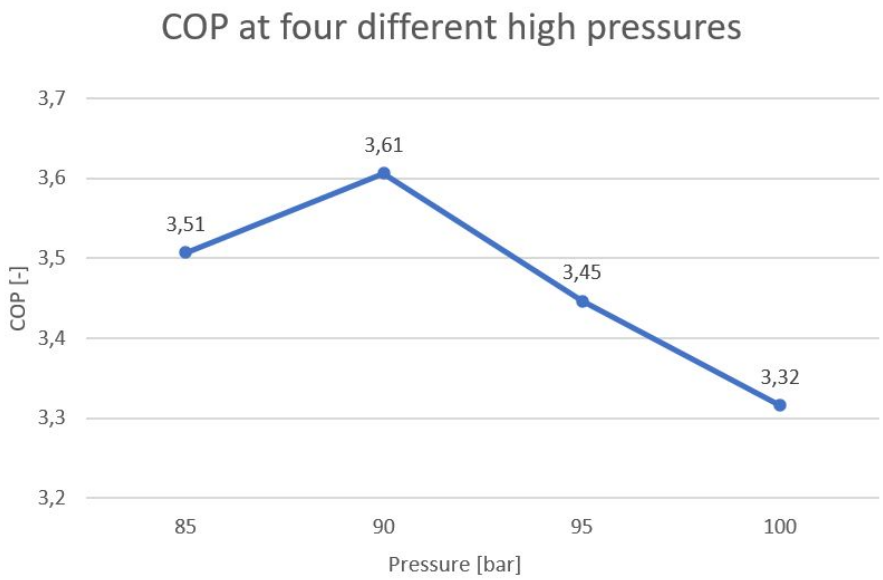

Figure 5.4: COP for the cycle at four different high pressures, namely 85 bar, 90 bar, 95 bar and 100 bar.

Figure 5.4 displays the COP for each of the different high pressures tested. The figure shows an increase in COP from 85 bar to 90 bar, this increase is of 2.8 %. Nevertheless, at the three highest pressures it is a clear trend of a decrease in COP as the pressure is increased. From 90 bar to 95 bar it is a reduction of 4.4 % in performance, and from 95 bar to 100 bar the reduction is of 3.8 %.

As the only additional modification when changing the high pressure was changing the displacement volume of the compressor, there is no guarantee that the water outlet temperature is constantly 60 °C. Figure 5.5 shows the water temperature through the gas cooler for each of the four different high pressures. The figure shows that the inlet water temperature is constantly at 10 °C for the four high pressures, moreover it shows that the outlet water temperature is not equal for

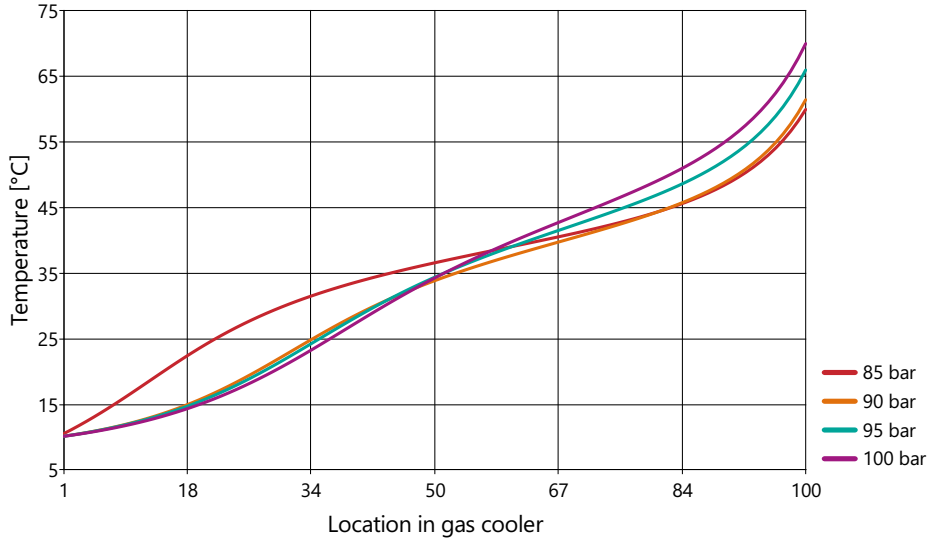

Figure 5.5: Water temperature in gas cooler at four different high pressures, 85 bar, 90 bar, 95 bar and 100 bar, respectively.

the four cases. For the simulation with a high pressure of 85 bar the outlet temperature is 60 °C, and for 90 bar it is a slight increase in temperature. However, for 95 bar and 100 bar the temperature is significantly higher, and at 100 bar the outlet water temperature reaches 70 °C. A clear trend of increasing water outlet temperature with increased high pressure can be seen from the figure. The figure also shows a non-linear temperature distribution for the water, something that was not expected.

5.1.2 Optimal high pressure

The optimal pressure can be determined by localizing the pinch point for the gas cooler. It is desirable with a pinch point at the working fluid outlet of the gas cooler, and the optimal high pressure will be the lowest pressure where this is the case.

In figure 5.6 the pinch points at different pressures are identified, marked with red circles. From the figure it can be seen that for simulations run at a high pressure of 85 bar the pinch point is located inside the gas cooler, close to the middle. The three other high pressures tested in the simulations were 90 bar, 95 bar and 100 bar, and they all resulted in pinch points at the CO_2 outlet of the gas cooler. As

it is most favorable with low pressures in a system, this means that the optimal pressure for this model is somewhere between 85 and 90 bar.

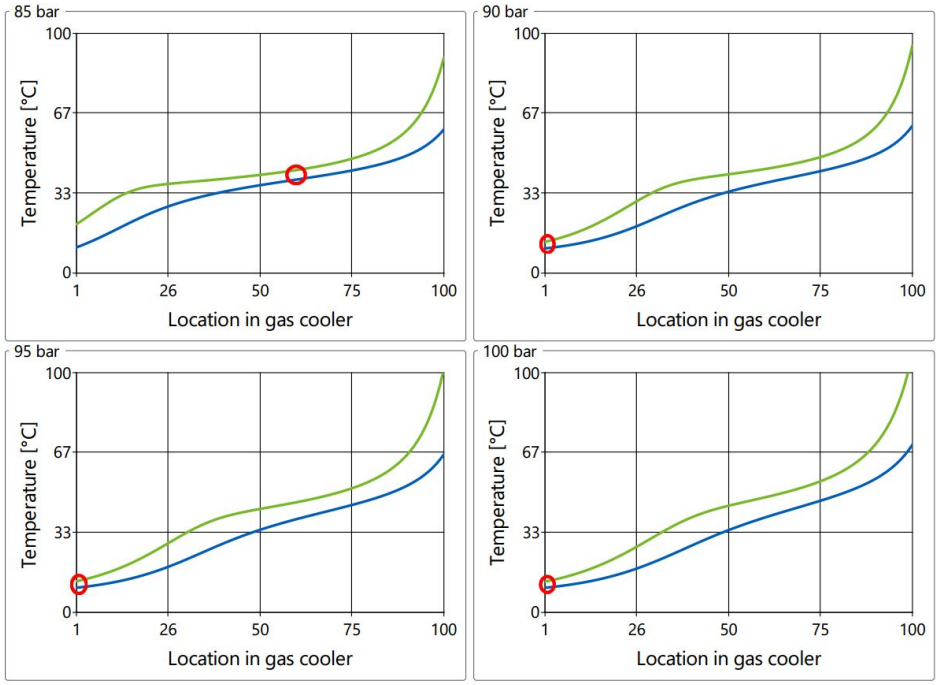

Figure 5.6: The figure identifies the pinch points at four different high pressures, which is marked by red circles. The blue lines represent the water in the gas coolers, while the green lines represent the CO_2.

5.1.3 Changed heat sink outlet temperature

The HPWH was initially designed to deliver 60 °C, but simulations with higher heat sink outlet temperatures were also conducted. The high pressure for these simulations was 95 bar. As the previously results have shown a varying heat sink outlet temperature, the results in this section were obtained by running another set of simulations. The heat sink outlet temperatures in these results are 60 °C, 70 °C and 78 °C. A heat sink outlet temperature of 78 °C was used as the model with a high pressure of 95 bar could not deliver higher temperature. In addition, in the simulation with 78 °C water outlet temperature, the gas cooler has a larger heat transfer area than the two other water outlet temperatures.

In figure 5.7 the T-s diagrams for the simulations run at 60 °C, 70 °C and 78 °C are

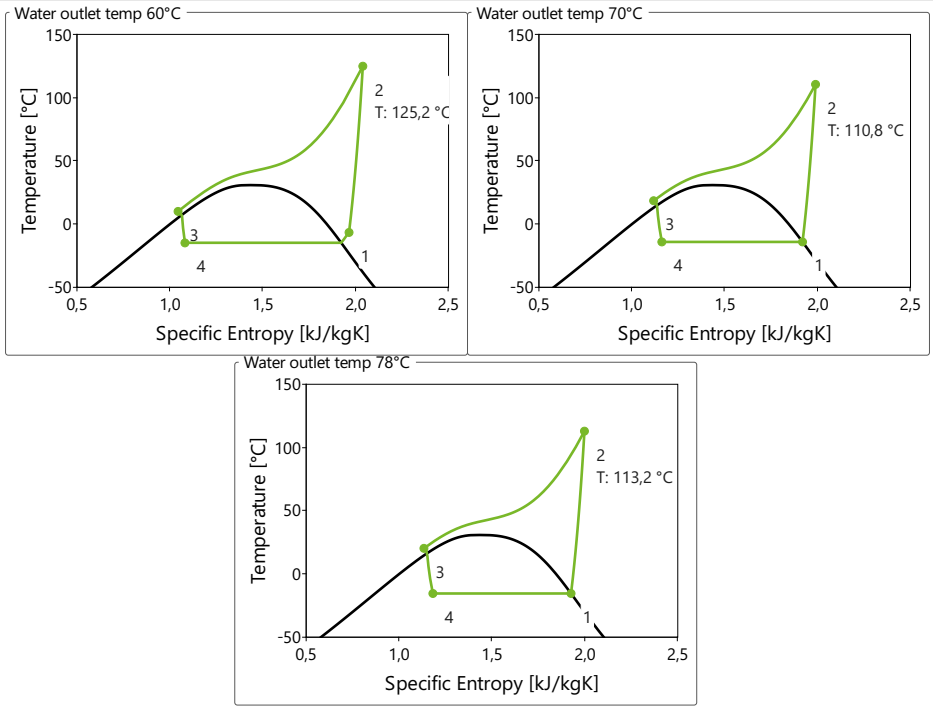

Figure 5.7: T-s diagrams for three different heat sink outlet temperatures, namely 60 °C, 70 °C and 78 °C.

shown. From the figure it can be seen that the discharge temperature is highest (125.2 °C) when the water outlet temperature is 60 °C, this is also the only T-s diagram where 5 K superheat out of the evaporator is achieved. For 70 °C and 78 °C it seems like the suction line contains saturated vapor.

The COP of the model with the three different heat sink outlet temperatures are shown in figure 5.8. From the figure it can be seen that the COP changes with varied heat sink outlet temperature, and it is a clear trend that the COP decreases when the outlet water temperature increases. In table 5.1 the cooling, heating and compressor power is given. From this table it can be seen that more heat is transferred in the evaporator when the heat sink temperature increases. For both 60 °C and 70 °C the size of the heat exchangers is equal, but for 78 °C the gas cooler is slightly larger. Moreover, the displacement volume for the three heat sink outlet temperatures is different. The table also shows that with increased water temperature more compressor work is used.

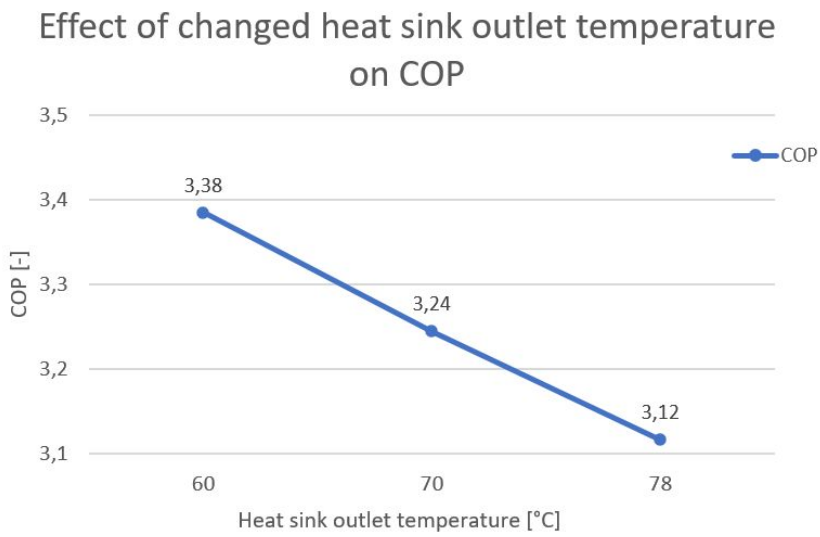

Figure 5.8: COP of the model with three different water outlet temperatures, 60 °C, 70 °C and 78 °C.

Table 5.1: Cooling, heating and compressor power for the model with three different heat sink outlet temperatures. The results were obtained from models with different compressor displacement volumes, and for the highest temperature the gas cooler area is slightly larger.

Water temp [°C]	Cooling power [kW]	Compressor power [kW]	Heating power [kW]
60	53.9	22.6	76.5
70	62.9	28.0	90.9
78	69.9	33.1	103.0

5.1.4 Changed CO_2 outlet temperature from gas cooler

To evaluate how the performance is affected by the CO_2 outlet temperature from the gas cooler, the model was run with three different CO_2 outlet temperatures. These temperatures were 15 °C, 20 °C and 25 °C. The only change in the models for these simulations was using regulation of the compressor to achieve the correct CO_2 outlet temperature from the gas cooler instead of controlling the low pressure.

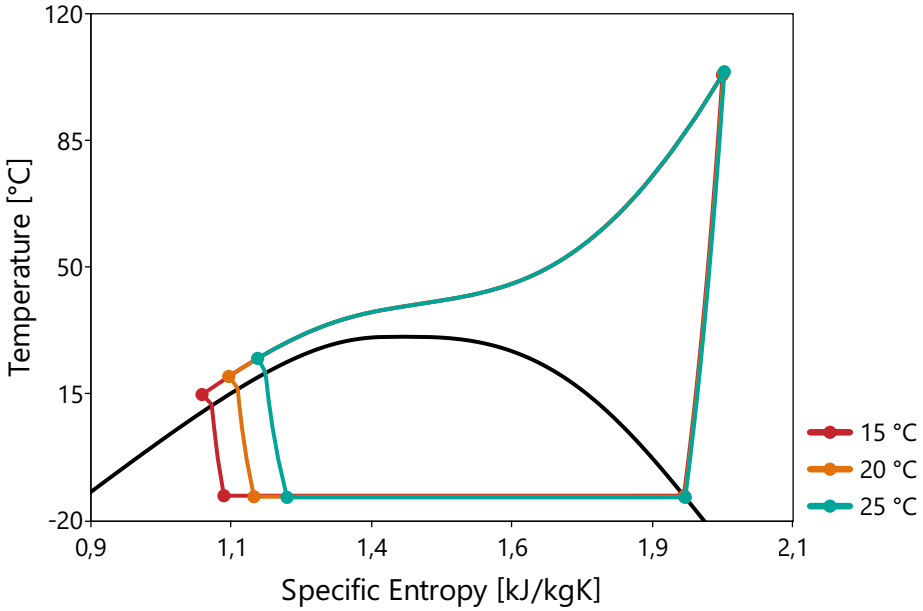

Figure 5.9: T-s diagram showing the CO_2 cycle for three different CO_2 temperatures out of the gas cooler. The three different temperatures are 15 °C, 20 °C and 25 °C.

Figure 5.9 shows the cycle with three different CO_2 outlet temperatures from the gas cooler. From the figure it can be seen that it is only the outlet temperature from the gas cooler, and thus the location of the evaporator inlet that change. The compression process is the same for all the three temperatures.

Figure 5.10 shows the water temperature in the gas cooler. From the figure it can be seen that the outlet water temperature increases slightly with increased CO_2 outlet temperature. However, the difference is only about 5 K between the simulations with outlet temperature 15 °C and 25 °C.

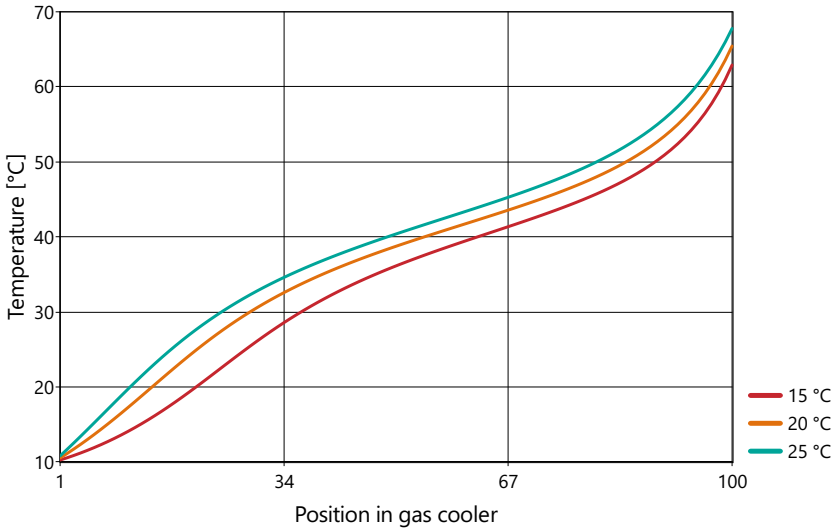

Figure 5.10: Temperature profile from the gas cooler showing the water temperatures when simulations were run with three different CO_2 outlet temperatures from the gas cooler, 15 °C, 20 °C and 25 °C, respectively.

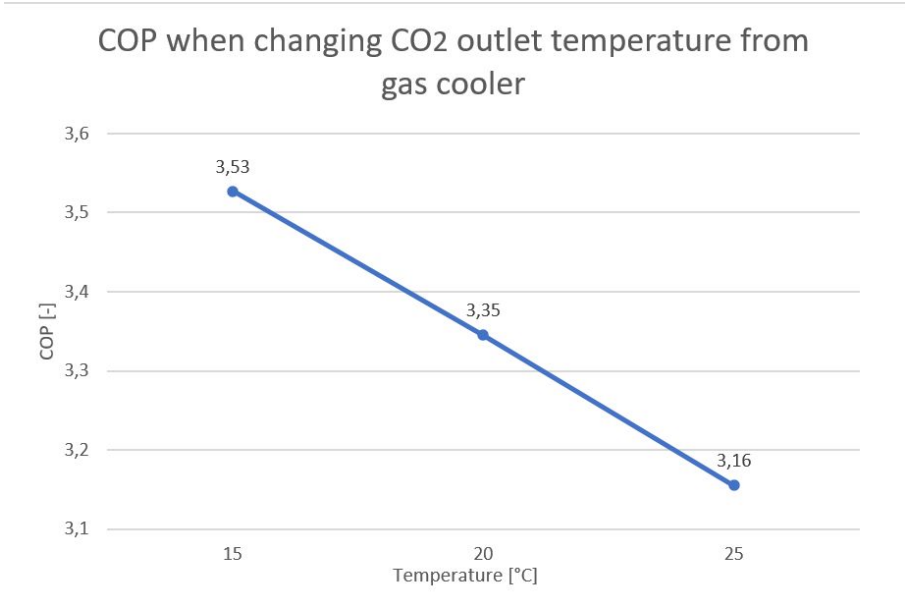

Figure 5.11: The COP of the cycle when the CO_2 outlet temperature from the gas cooler is set to three different temperatures, namely 15 °C, 20 °C and 25 °C.

The goal of running simulations with different CO_2 outlet temperatures from the gas cooler was to investigate how this would affect the COP of the heat pump model. In figure 5.11 the COP for the three simulations are given. From the figure it can be seen that the COP decreases when the CO_2 outlet temperature increases. The decrease is significant with a reduction of 5.1 % between 15 °C and 20 °C and a reduction of 5.7 % between 20 °C and 25 °C.

5.1.5 Internal heat exchanger

The model was modified by including an IHX, and the log p-h and the T-s diagrams from the initial simulation are shown in figure 5.12. The figure shows a discharge temperature of 129 °C and a liquid temperature of 10.6 °C before the expansion valve, which is only 0.6 K higher than the inlet water temperature. For comparison, the model without an IHX holds a temperature of 12.9 °C in the same point, which indicates that with an IHX it is possible with a lower temperature and this can reduce expansion losses.

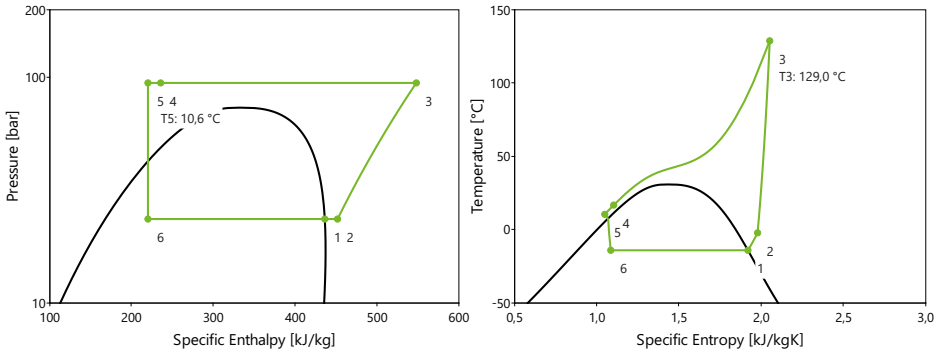

Figure 5.12: Log p-h and T-s diagram of simulations with initial values for the CO_2 model with an internal heat exchanger. The high pressure is set to 95 bar.

Simulations with the IHX model were run at three different high pressures, 90 bar, 95 bar and 100 bar. The T-s diagrams resulting from these simulations are depicted in figure 5.13. This figure shows the same trend as the results without an IHX, i.e. that increased high pressure gives increased discharge temperature. Thus, the maximum discharge temperature was obtained in the simulation performed with a high pressure of 100 bar, which had a discharge temperature of 134.7 °C.

Inserting an IHX to the model changes it in many ways, and it was therefore decided to identify the optimal pressure for the IHX model as well. When running

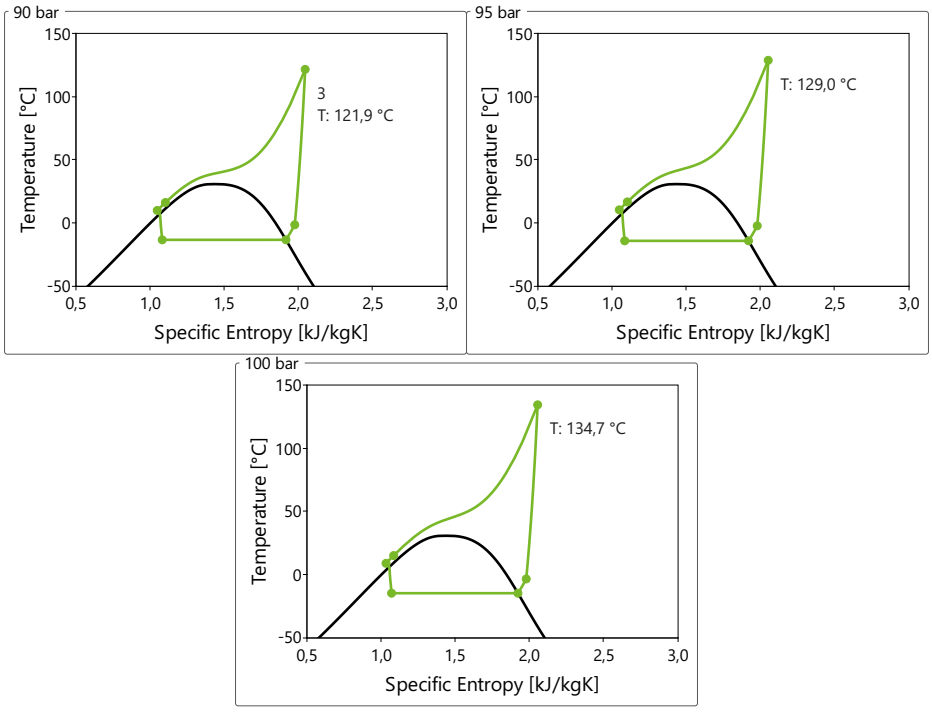

Figure 5.13: T-s diagram of simulations with three different high pressures, 90 bar, 95 bar and 100 bar. The discharge temperature of each of the high pressures are given.

simulations with the IHX model the pinch point appears at different locations than when using the model without an IHX. The pinch point for the IHX model was identified at three different pressures, 90 bar, 95 bar and 100 bar, and is marked with red circles in figure 5.14. The pinch point is located close to the middle of the gas cooler when simulations with high pressures 90 bar or 95 bar were run, while it is located at the CO_2 outlet for simulations with a high pressure of 100 bar. This means that the optimal pressure for the CO_2 model with an IHX is in the range 95 - 100 bar.

Figure 5.15 shows the effect the IHX has on the performance of the heat pump compared to the model without an IHX. The two models were tested at three different pressures, which all show the same trend, namely a reduction in COP when the model includes an IHX. However, there is a small reduction in the difference of performance between the two models as the pressure is increased.

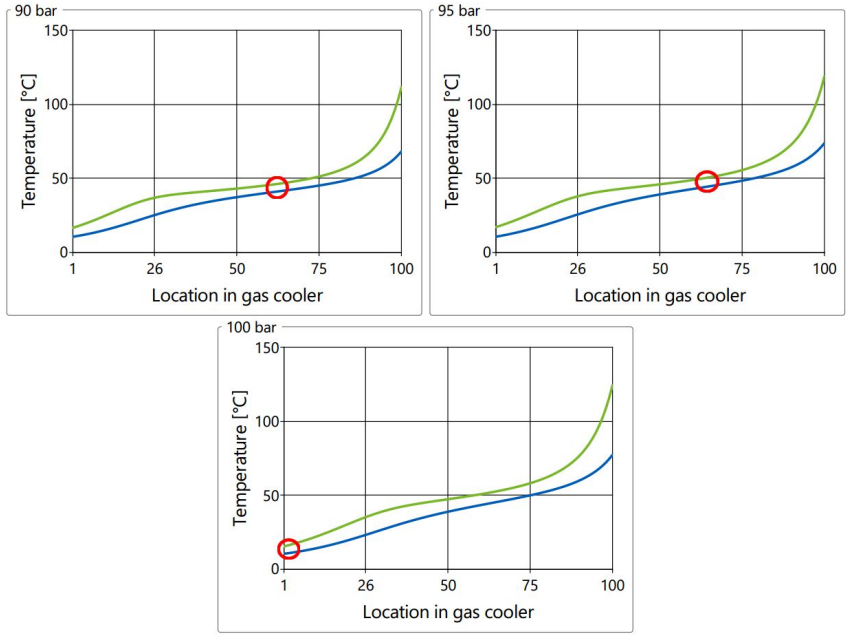

Figure 5.14: The figure identifies the pinch point at three different high pressures when running the model with an IHX. The pinch points are marked by red circles. The blue lines represent the water in the gas cooler, while the green lines represent the CO_2.

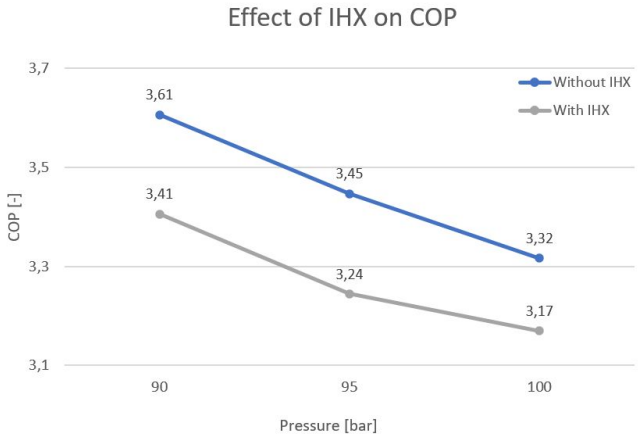

Figure 5.15: The figure shows the effect an IHX has on the COP of a CO_2 heat pump. The COP is compared at three different high pressures, 90 bar, 95 bar and 100 bar, respectively.

Figure 5.16 shows the temperature of the water through the gas cooler. The inlet water temperature is constantly at 10 °C but the outlet temperature has some variations, however all the outlet temperatures are equal to or above 60 °C. From the figure it is clear that the outlet water temperature increases with increasing pressure. It is also clear that the model containing an IHX delivers higher temperature than the one without. Looking at both figure 5.15 and 5.16 it can be seen that the higher outlet water temperature is connected to a lower COP value, as expected due to a larger temperature lift for the heat pump.

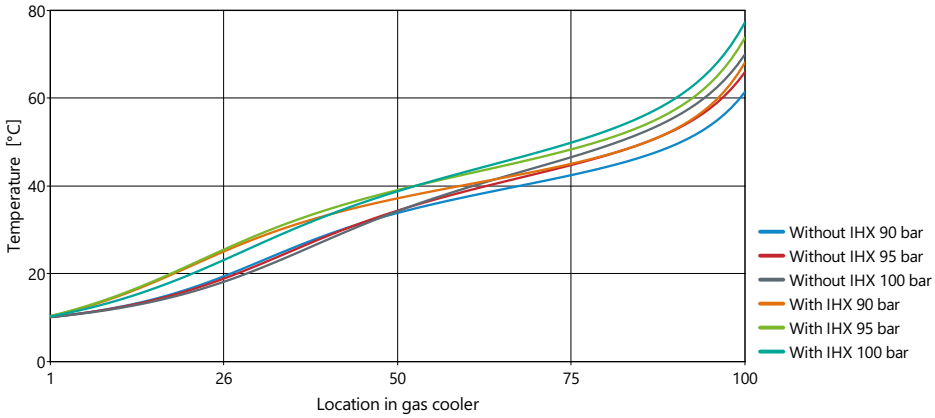

Figure 5.16: The temperature of the water through the gas cooler when using both the model with and without an IHX. The simulations were run at three different high pressures for a better comparison.

5.2 Propane HPWH

Initial simulations with a model of a propane HPWH were conducted. In figure 5.17 the log p-h and T-s diagrams from these simulations are shown. The condensing temperature was set to 60 °C, resulting in heating of water from 10 °C to 60 °C. From the diagrams it is clear that the process has a large degree of subcooling, which is achieved in the condenser.

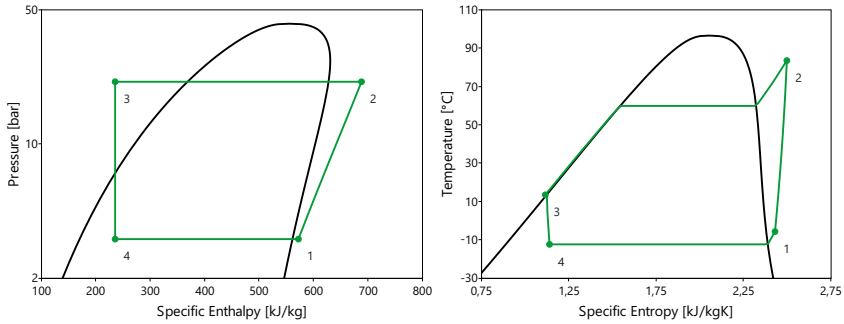

Figure 5.17: Log p-h and T-s diagram for a propane HPWH. The HPWH heats water from 10 °C to 60 °C, and has an evaporation temperature of -12 °C.

The propane HPWH was tested with three different heat sink outlet temperatures, 60 °C, 70 °C and 80 °C. To achieve a higher water outlet temperature the condensation temperature was increased, which can be seen from figure 5.18. The figure also shows how the discharge temperature increases when the water outlet temperature is increased.

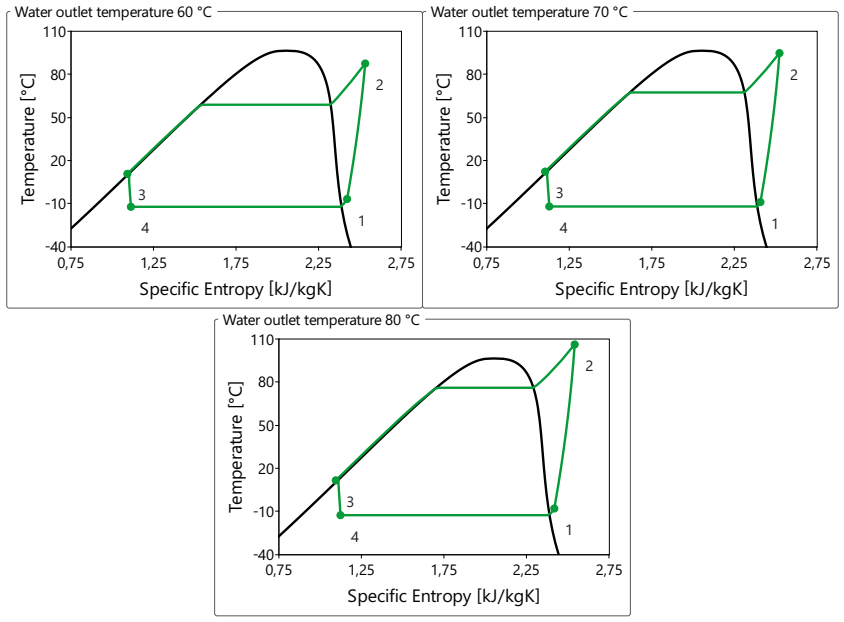

Figure 5.18: T-s diagram for propane HPWH simulated with three different heat sink outlet temperatures, namely 60 °C, 70 °C and 80 °C.

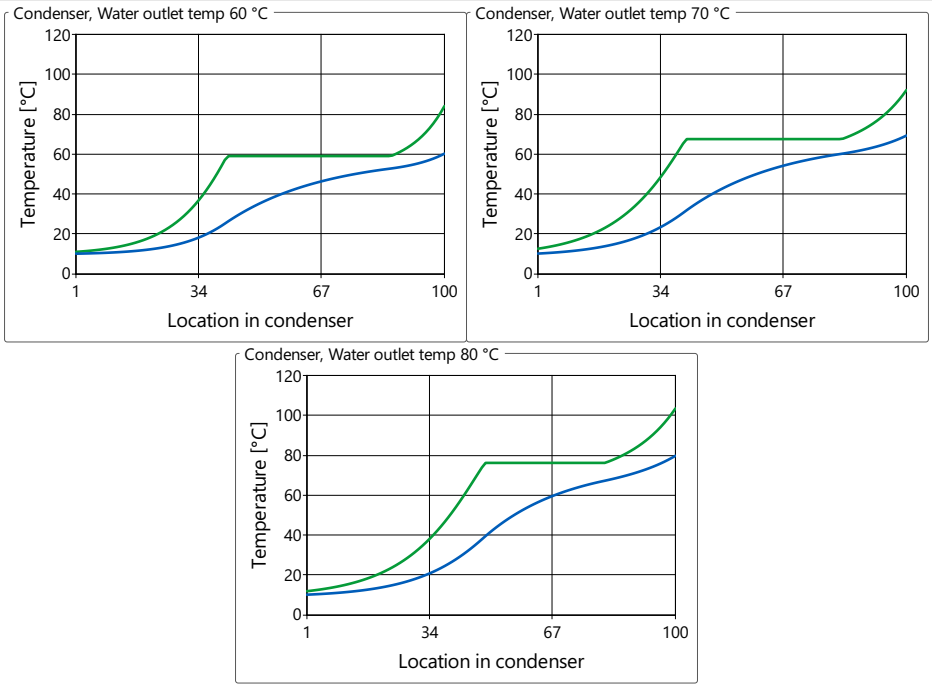

Figure 5.19: Temperature of the propane and the water through the condenser for three different water outlet temperatures, 60 °C, 70 °C and 80 °C. The dark green lines represent the propane in the condenser and the blue lines represent the water.

Figure 5.19 shows the temperature of both the propane and the water through the condenser for all three temperatures tested. The horizontal plateau for the propane illustrates the phase change during condensation. In a propane HPWH the desuperheating process makes it possible to achieve a higher heat sink outlet temperature than the condensing temperature, and this process is shown to the right in the condenser in figure 5.19. To achieve a high performance for a propane HPWH a large degree of subcooling is needed, and this can be seen to the left in the condenser in the same figure.

The propane HPWH model was developed for comparison to the CO_2 HPWH model. Therefore, simulations with three different heat sink temperatures, namely 60 °C, 70 °C and 80 °C, were conducted. Figure 5.20 shows the COP of the CO_2 HPWH model and the propane HPWH for these three water outlet temperatures. In the figure the highest water outlet temperature is 80 °C, however, the results for the CO_2 model were obtained with a heat sink outlet temperature of 78 °C. From

figure 5.20 it is clear that the COP of the propane HPWH model is higher than for the CO_2 HPWH model for all three heat sink outlet temperatures. The largest difference in performance for the two models occurs at the lowest temperature, 60 °C.

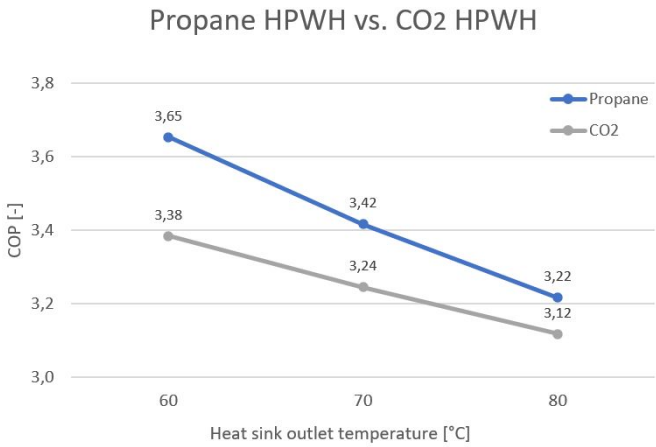

Figure 5.20: Comparison of COP between the propane and the CO_2 models.

5.3 Economic analysis

It has been performed a simplified economic analysis on two different scenarios. Both scenarios use input values obtained from simulations with the developed CO_2 model presented in chapter 4. The results are obtained from simulations with a high pressure set to 95 bar that delivers water at 60 °C, and are summarized in table 5.2. An assumption of 8 700 operating hours for the heat pump during a year has been made (i.e. 99.3 % of the year), resulting in 665 550 kWh delivered heat and an electricity consumption of 196 620 kWh.

Table 5.2: Results from simulations with a CO_2 model having a high pressure of 95 bar delivering water at 60 °C.

High pressure [bar]	Heat delivery rate [kW]	Compressor work [kW]	Delivered heat [kWh]	El. consumption compressor [kWh]
95	76.5	22.6	665 550	196 620

5.3.1 Scenario 1

In this case the electricity cost was set to 0.5 NOK/kWh and the price for delivered heat to 0.4 NOK/kWh. The electricity cost includes all fees additional to the cost of the electricity itself. The lifetime of the heat pump was assumed to be 20 years, and the discount rate was set to 11 %, due to the risk related to the investment. All these parameters are summarized in table 5.3.

Table 5.3: Assumed values for the economic analysis.

Electricity cost [NOK/kWh]	Delivered heat price [NOK/kWh]	Discount rate [%]	Lifetime of heat pump [years]
0.5	0.4	11	20

An assumption for the cost of the heat pump unit itself of 300 000 NOK has been made, and that this cost makes up 1/3 of the total cost, resulting in a total investment cost of the 900 000 NOK. Assuming the maintenance cost make up 10 % of the operating cost, the maintenance cost will be 10 923 NOK. Which means that the total yearly cost of electricity and maintenance is 109 233 NOK. Given the assumed price of delivered heat and assuming all the heat is sold, the total yearly income is 266 220 NOK. Then the net yearly cash flow is 156 987 NOK. The cash flows are summarized in table 5.4.

Table 5.4: Costs and income associated with the heat pump procurement.

Investment cost [NOK]	Yearly income [NOK]	Yearly costs [NOK]	Net yearly income [NOK]
-900 000	266 220	-109 233	156 987

Table 5.5: Results of economic analysis for scenario 1.

PBP [years]	NPV [NOK]	IRR [%]
5.7	350 136	17

Based on all the input parameters the PBP, NPV and IRR were calculated, and the values are given in table 5.5. A positive NPV means the investment will be profitable. The IRR gives the discount rate that will make the NPV equal to zero when calculating for the entire lifetime of the heat pump.

5.3.2 Scenario 2

Scenario 2 is calculated the same way as scenario 1, but with different input parameters. The assumed values for prices, discount rate and lifetime are given in table 5.6. The cash flows related to the heat pump are given in table 5.7.

Table 5.6: Assumed values for the economic analysis.

Electricity cost [NOK/kWh]	Delivered heat price [NOK/kWh]	Discount rate [%]	Lifetime of heat pump [years]
0.60	0.45	9	15

Table 5.7: Costs and income associated with the heat pump procurement.

Investment cost [NOK]	Yearly income [NOK]	Yearly costs [NOK]	Net yearly income [NOK]
-1 200 000	299 498	-131 080	168 418

Table 5.8: Results of economic analysis for scenario 2.

PBP [years]	NPV [NOK]	IRR [%]
7.1	157 561	11

The results of scenario 2 is given in 5.8. As seen from the table the NPV is positive, which means the investment will be profitable, however it will be less profitable than the investment in scenario 1. In addition the PBP for scenario 2 is longer than for scenario 1. However the IRR for scenario 2 is lower than for scenario 1.

Chapter 6

Discussion

In this chapter the results will be discussed, trying to explain why significant findings turned out the way they did. Results that turned out differently than expected will also be addressed, where possible explanations will be given. A discussion on sources of error that may have contributed to less valid results will also be included, in addition to an evaluation of what effect selected assumptions had on the results.

6.1 CO_2 HPWH

From figure 5.1 it is clear that the desired superheat of 5 K has not been achieved in the simulation. Superheat in the suction line protects the compressor from liquid slugging and is therefore common practice. However, the model contains a low pressure receiver, which will prevent liquid from entering the compressor. The receiver will make sure that only saturated gas is allowed to enter the compressor. The figure also shows a low CO_2 outlet temperature from the gas cooler, which may contribute to increased performance for the heat pump.

From the figure showing the temperature profile in the heat exchangers, figure 5.2, it can be seen that the temperature difference in the heat exchanger is lower than 3 K, but it is not significantly lower. From the same figure it can be seen that the evaporation temperature is lower than -12 °C, which potentially could cause problems for the chilling system. However, from the temperature profile in the heat exchanger it can be seen that the outlet temperature of the glycol is approximately

-6 °C, a possible explanation can be that the lower temperature difference in the heat exchanger compensates for the lower evaporation temperature.

6.1.1 Effect of changing the high pressure

An increase in the high pressure will increase the pressure ratio for the compressor. This usually means more work must be done on the working fluid by the compressor to reach the desired end pressure, which can lead to lower performance for the heat pump. From figure 5.4 it can be seen that this is the case for the three highest pressures, but the COP increases from 85 bar to 90 bar. However, a possible explanation to this can be identified by looking at figure 5.3. The figure shows that the outlet temperature of the CO_2 from the gas cooler is significantly higher for a high pressure of 85 bar than for the rest of the pressures tested in the simulations. A high temperature before the expansion valve will lead to large throttling losses during the expansion due to large exergy destruction, and this may be the reason why the performance is lower for 85 bar than for 90 bar.

When the high pressure used in the model was changed the only other modification was changing the displacement volume of the compressor. Thus, the outlet water temperature was not considered, leading to a different outlet water temperature for the four different high pressures. Different outlet water temperatures may affect the performance of the models, making it more uncertain how large the difference in performance really is. However, it is considered to be true that the performance of the heat pump decreases with increasing pressure, but the decrease might be smaller than shown in the results.

The results showing the water temperature in the gas cooler shows a non-linear temperature distribution for the water. This temperature distribution should be linear. A possible explanation is that the resolution used for the gas cooler is too poor. The gas cooler is divided into 100 nodes and the simulations uses 500 intervals. Thus, by increasing the number of nodes and/or intervals the water temperature distribution might become linear.

6.1.2 Optimal high pressure

The results indicated an optimal pressure for the model in the range 85 - 90 bar. However, there may be several uncertainties in this result. First of all the simulations were conducted without strict regulation of the heat sink outlet temperature. This resulted in higher heat sink outlet temperatures as the pressure was increased. Differences in the water outlet temperature may impact the optimal

pressure, making the result less valid as not all pressures were tested with the same temperatures. However, the impact is not considered to be very large as the temperature difference is relatively small, and the conclusion that the pinch point is in the range 85 - 90 bar is evaluated as correct.

Secondly, the pinch points were identified by visual estimation, which may result in a slightly offset pinch point. However, it is assumed that this offset is not big enough to change whether the pinch point is located in the middle or at the outlet of the gas cooler. Therefore, this approximate location of the pinch point is considered as adequate for this master's thesis.

Lastly it must also be mentioned that the previously mentioned non-linear temperature profile for the water may also affect the location of the pinch point. With a linear temperature profile the results may have turned out differently.

6.1.3 Changed heat sink outlet temperature

In the results the discharge temperature of the simulation run with water outlet temperature of 60 °C is the highest, as seen in figure 5.7, which is not as expected. It is expected that when increasing the water outlet temperature the discharge temperature would also increase, as it does from 70 °C to 78 °C. However, a possible explanation can be that the simulation with 60 °C is the only simulation where there is superheat in the suction line. For both the other temperatures the compression seems to start from the saturated gas line. Superheat in the suction line will result in higher discharge temperature and larger losses for the process.

From figure 5.8 it can be seen that the COP of the model decreases with increased heat sink outlet temperature. This is as expected because when the temperature lift increases the performance of a heat pump decreases. However, if looking at table 5.1 it is clear that the simulations don't have the same cooling power, which may affect the result. Anyhow, the trend of decreasing COP with increasing heat sink outlet temperature is considered realistic, but with some uncertainty in the percentage of the reduction.

The results from simulations with the model having a high pressure of 95 bar are given for 60 °C, 70 °C and 78 °C. Originally the plan was to test the model with a water outlet temperature of 80 °C instead of 78 °C. Unfortunately, the model could not give a higher water outlet temperature than 78 °C, and then also changing the area of the gas cooler was tested. An explanation for this could be that 95 bar is too low for CO_2 to heat a water stream from 10 °C to 80 °C. Another explanation

can be that the amount of heat transferred in the heat exchangers is too small, however, table 5.1 shows that the amount of heat transferred increases as the water outlet temperature is increased.

In the theory chapter CO_2 HPWHs were presented, section 2.4.1. In this section a DHW system was presented where the water was heated from 9 °C to 60 °C. This HPWH achieved a COP in the range of 3.0 -4.3 with an evaporation temperature ranging from -20 °C to 0 °C. Assuming a linear increase in performance as the evaporation temperature increases, that means a COP of 3.52 was achieved with an evaporation temperature of -12 °C. From figure 5.8 the COP of heating water from 10 - 60 °C is 3.36, which is a little bit lower than for the heat pump presented in the theory chapter. However, the difference between the COP values are reasonably small, making the simulation result reliable.

6.1.4 Changed CO_2 outlet temperature from gas cooler

From figure 5.10 it can be seen that there is a 5 K difference in the water outlet temperatures between the simulations using a CO_2 outlet temperature of 15 °C and 25 °C. Revealing a trend of slightly increased water outlet temperature as the CO_2 outlet temperature increases. That the water outlet temperature is not equal for the three tested temperatures may affect the performance. As seen from figure 5.11 the performance of the heat pump model decreases as the CO_2 outlet temperature increases, as expected. However, varying water outlet temperature may affect the result, making the reduction in performance too large.

6.1.5 Internal heat exchanger

When inserting an IHX the discharge temperature becomes high, and it increases with increasing pressure. At 100 bar the discharge temperature is 134.7 °C, which is very high, and this may lead to problems regarding oil degradation and compressor cooling. An IHX also makes sure that all the simulations have superheat in the suction line, which as mentioned before will give increased discharge temperature, more losses and lower the performance.

The model with an IHX shows a lower COP than the model without, as seen in figure 2.7. The difference in COP is considerable but becomes smaller as the pressure increases. Nevertheless, the water temperatures the models can deliver may be of importance. From figure 5.16 it can be seen that the model with an IHX delivers water at higher temperature than the model without an IHX at equal pressures. This means that the IHX model delivers higher quality heat but with

a lower COP than the model without an IHX. However, this may also result in a lower COP for the IHX model than what is realistic.

Another thing that can impact the difference in COP between the model with and without an IHX is superheat in the suction line. The IHX model gives superheat in the suction line for all the tested pressures, while for the model without an IHX none of the pressures give superheat in the suction line. As mentioned before, superheat results in both higher discharge temperature and poorer performance. This means that the results for the IHX model might be unfairly poor compared to the ordinary CO_2 model. For a correct comparison there should also have been superheat in the suction line for the model without an IHX.

When using an IHX it is possible to get a lower temperature before the expansion valve than with a model without an IHX. A lower temperature before the expansion valve will lead to lower expansion losses as there is less exergy destruction during the expansion process. Lower losses generally give better performance, however, this is not the case for the results presented in this master's thesis. This may indicate that the effect of superheat losses in the suction line exceeds the effect of the loss reduction due to lower liquid temperature in front of the expansion valve.

In addition, the IHX model have different locations for the pinch points than the ordinary CO_2 model, resulting in a higher optimal pressure. A reason for this can be the superheat in the suction line leading to higher temperatures in the IHX model. Another reason can be the higher water outlet temperature for the IHX model.

6.2 Propane HPWH

The discharge temperature is always higher than the condensing temperature, which in a propane HPWH is exploited by giving a water outlet temperature higher than or equal to the condensing temperature, as can be observed from figure 5.18. This makes it possible to have a lower condensing temperature than the heat sink outlet temperature, which makes the performance of the HPWH model higher due to a lower pressure ratio for the compressor.

Propane has a critical temperature of 96.7 °C which limits the possible outlet water temperature. This also means that the closer to the critical temperature the condensation temperature becomes, the lower the heat of condensation. This means that at higher condensing temperatures it is necessary with more subcooling to achieve the desired heat transfer, which can be seen from figure 5.18. The

propane model was not tested with an outlet water temperature higher than 80 °C. However, by considering the critical point of propane it would be reasonable to assume that this is close to the highest temperature a propane HPWH can deliver in subcritical operation. Thus, for higher temperatures CO_2 is more promising.

In the comparison of performance between the propane model and the CO_2 model, the performance was compared with three different water outlet temperatures. This resulted in a higher COP for the propane model in all the cases. Moreover, it must be mentioned that for a water outlet temperature of 80 °C the results for CO_2 were obtained with an outlet water temperature of 78 °C. Considering the other results obtained in this master's thesis, this means that the actual performance for the CO_2 model would be even lower than given in figure 5.20.

6.3 Economic analysis

The economic analysis is based on a lot of assumptions, which means that it can be errors in every step. First off all it may be errors from the simulation results, which will affect the end result. In addition the prices for heat and electricity have large uncertainties. As the economic analysis methods tries to predict the future, they also represent uncertainty. All of these combined make the results from the economic analysis very unreliable, however, the economic analysis is only included to show how the investments can be profitable. It is very simple replacing the values in the Excel spreadsheet that was used to calculate the results such that the parameters can easily be adjusted to more correct values.

In the economic analysis a CO_2 heat pump without an IHX was used. The results from the IHX model would have given slightly different amounts of heat delivered and the performance would have been lower. In addition, when inserting an IHX the investment cost will be higher due to the need of an extra heat exchanger and most likely additional piping.

If using the propane HPWH in the economic analysis, the operating cost for the heat pump would have been lower than for CO_2 due to higher performance. However, when using propane in heat pump applications strict regulations are imposed, and this may lead to higher investment cost.

6.4 Sources of error

There have been made many simplifications and assumptions in the modeling process. For instance, it is assumed zero pressure drop losses in all the heat exchangers. As there will be pressure drop losses connected to all fluid flows, this will not be a correct assumption. Another simplification is the assumption of no heat transfer to the ambient in any of the components, which would not be the case for a real heat pump. The heat exchangers are also assumed to transfer all the heat between the two fluids without heat transfer losses. All these losses will result in lower performance in reality.

When modeling the heat exchangers, the overall heat transfer coefficients were assumed based on relevant literature. However, these numbers are most likely not correct, and there could be large deviations between the correct values and those used in the model. Additionally, this value is assumed constant throughout the heat exchangers. The heat transfer coefficient depends on the conditions of the working fluid, which means that it for instance will change during the evaporation process as the heat transfer coefficients for gases have smaller values than for liquids. This can give significant errors in the simulations, especially where a phase transition is present. The overall heat transfer coefficients have also been used in calculating the theoretical heat transfer area of the heat exchangers, and wrong U-values will lead to under or oversizing.

As have been mentioned in the methodology, chapter 4, the heat exchangers in the model are oversized compared to the theoretical sizes. This can give errors in the simulation, for instance incorrect temperatures due to low temperature differences. This can also give too large mass flow rates for the heat source and the heat sink. However, that is not considered as an important issue for this master's thesis, as the important aspect is the amount of heat transferred.

In all the models propylene glycol 40 % was used for the heat source stream instead of ethylene glycol 40 % as the latter was not a part of the TIL library. The two types of glycol may have significant differences in relevant properties, which can lead to large errors. It has not been investigated how large/small these differences are, so this can give inaccurate results.

Chapter 7

Conclusion

In this chapter the results and discussion will be summarized, including an evaluation of the impact these results will have on the +CityxChange project.

During this master's thesis, heat recovery by using heat pump technology have been investigated for the +CityxChange project. Sluppenvegen 10 has been the focus, and the proposed solution is a heat pump for heating of hot water. It has been assumed that the heat pump can deliver hot water to customers in the Sluppen area, and the heat pump must be placed close to where the heat is needed. This means the waste heat from the chilling facility must be transported to the heat pump unit, and for this a CO_2 circuit that extracts the heat directly from the glycol stream upstream the chillers have been proposed. For the heat pump configuration two working fluids have been evaluated, CO_2 and propane, as these are environmentally friendly and have suitable properties for hot water heating. Three simplified models of heat pump water heaters have been developed, and simulations with relevant operating conditions have been performed. The three models are a CO_2 HPWH, a CO_2 HPWH containing an internal heat exchanger, and a propane HPWH. All the models have shown good performance, with propane giving the highest COP. The propane model gave a higher COP than the CO_2 model in all cases when simulations were run with three different water outlet temperatures, 60 °C, 70 °C and 80 °C, respectively. When heating the water from 10 °C to 60 °C the propane HPWH model had a COP of 3.65.

The CO_2 model was tested with different high pressures, as well as different water outlet temperatures and CO_2 outlet temperatures from the gas cooler. From these

simulations some conclusions could be drawn. First of all, an increase in the high pressure yields an increase in the discharge temperature and lower COP. Both increasing the outlet water temperature and the CO_2 outlet temperature from the gas cooler results in lower COP. Simulations with the IHX model gave a lower COP than the ordinary CO_2 model at three different high pressures. It has also been performed a simplified economic analysis on two different scenarios using the CO_2 model, and in both scenarios the investment turned out to be profitable.

For Sluppen to become a PED the amount of heat delivered is of importance. Based on the results obtained from the CO_2 model, and assuming 8 700 yearly operating hours, this heat pump can deliver 665 550 kWh heat when delivering water at 60 °C. However, the heat pump will also use electricity, resulting in a net energy delivery of 468 930 kWh. This is a significant contribution to a PED, comparing to today's situation where no heat from the chilling facility is recovered.

Chapter 8

Further Work

In this chapter suggestions for further work will be presented. Some of the points are improvements for the models already developed, while others are suggestions to new models that can be developed. They all have in common that they will explore more possibilities for the +CityxChange to make the end result as good as possible.

Firstly, implementing varying efficiencies for the compressors would be of importance for further work. Varying efficiencies will give a more realistic picture of how the heat pump performs at different operating scenarios. However, it would also be necessary to vary the load for the heat pump, to investigate the performance at part load.

Secondly, to get a better insight in the performance of the heat pump, the model should be as close to the reality as possible, which makes implementing pressure drops and other losses important. It would also be necessary to look closer into the process in the heat exchangers to find the correct heat transfer coefficients. Thereby also deciding the correct size of the heat exchangers.

Another aspect to consider making the model more realistic is to use the right type of glycol for the chilling circuit in the model. As the difference between the glycol type used in the modeling and the glycol in the chilling facility has not been investigated it is uncertain how large error this contributes to. Additionally, in the model only one heat exchanger is used for extracting the heat. As long as there is no heat loss this does not contribute to large errors in the results. However, if heat losses in the heat exchangers are included there may be a larger difference

between using one large heat exchanger and three smaller ones.

The developed model is supposed to be a HPWH, nonetheless, it does only contain the heat pump of the system. Thus, the rest of the hot water production system should be included. This includes, among other things, a hot water tank and an auxiliary heating system for when the heat pump is not sufficient to cover the hot water demand.

An interesting case to look at is simultaneous hot water heating and space heating. This will make the system more flexible as it can deliver hot water, space heating or both simultaneously. The performance of such a system could be compared to a system for only hot water to see which delivers the best performance. In this case it should be considered varying the demand of the two products to get a more correct picture of what will be best economically.

The economic analysis performed in this master's thesis is very simplified. Therefore, before the decision making happens a more detailed economic analysis should be performed. For this analysis more reliable numbers should be gathered from, among others, heat pump suppliers and electricity companies. The economic analysis in this master's thesis includes very many uncertainties that should be eliminated if possible.

Bibliography

C. Arpagaus, F. Bless, M. Uhlmann, J. Schiffmann, and S. S. Bertsch. High temperature heat pumps: Market overview, state of the art, research status, refrigerants, and application potentials. *Energy*, 152:985–1010, 2018.

D. S. Ayou, J. M. Corberán, and A. Coronas. Current status and new developments on high temperature heat pumps. *25th IIR International Congress of Refrigeration, Montreal*, pages 118–129, 2019.

O. Bamigbetan, T. Eikevik, P. Nekså, and M. Bantle. Review of vapour compression heat pumps for high temperature heating using natural working fluids. *International Journal of Refrigeration*, 80:197–211, 2017.

O. Bamigbetan, T. M. Eikevik, P. Nekså, M. Bantle, and C. Schlemminger. Theoretical analysis of suitable fluids for high temperature heat pumps up to 125°C heat delivery. *International Journal of Refrigeration*, 92:185–195, 2018.

O. Bamigbetan, T. Eikevik, P. Nekså, M. Bantle, and C. Schlemminger. The development of a hydrocarbon high temperature heat pump for waste heat recovery. *Energy*, 173:1141–1153, 2019a.

O. Bamigbetan, T. M. Eikevik, P. Nekså, M. Bantle, and C. Schlemminger. Experimental investigation of a prototype r-600 compressor for high temperature heat pump. *Energy*, 169:730–730, 2019b.

Y.-G. Chen. Optimal heat rejection pressure of co2 heat pump water heaters based on pinch point analysis. *International Journal of Thermal Sciences*, 106: 592–603, 2019.

+CityxChange. Trondheim, 2019. URL `https://cityxchange.eu/our-cities/trondheim-norwegian/`.

T. Eikevik. Compendium tep4255. *NTNU*, 2018.

Encyclopædia Britannica. Montreal protocol, 2019. URL https://www.britannica.com/event/Montreal-Protocol.

FN-sambandet. Kyotoprotokollen, 2019. URL https://www.fn.no/Om-FN/Avtaler/Miljoe-og-klima/Kyotoprotokollen.

W. Grassi. *Heat Pumps*. Springer, 1st edition, 2018.

A. Hafner. Integrated CO_2 system for refrigeration, air conditioning and sanitary hot water. *7th IIR Conference: Ammonia and* CO_2 *Refrigeration Technologies, Ohrid*, 2017.

Hagaland Finans. Investeringsanalyse. URL https://haglandfinans.no/tjenester/okonomiske-analyser/investeringsanalyse/.

A. Hesaraki, E. Bourdakis, A. Ploskić, and S. Holmberg. Experimental study of energy performance in low-temperature hydronic heating systems. *Sintef Energiforskning AS*, 109:108–114, 2015.

F. Ju, X. Fan, Y. Chen, T. Wang, X. Tang, A. Kuang, and S. Ma. Experimental investigation on a heat pump water heater using r744/r290 mixture for domestic hot water. *International Journal of Thermal Sciences*, 132:1–13, 2008.

D. H. Kim, H. S. Park, and M. S. Kim. Optimal temperature between high and low stage cycles for r134a/r410a cascade heat pump based water heater system. *Experimental Thermal and Fluid Science*, 47:172–179, 2013.

H. Moisi and R. Rieberer. Refrigerant selection and cycle development for a high temperature vapor compression heat pump. *12th IEA Heat Pump Conference*, pages 1–10, 2017.

A. Mota-Babiloni, C. Mateu-Royo, J. Navarro-Esbrí, F. Molés, M. Amat-Albuixech, and Ángel Barragán-Cervera. Optimisation of high-temperature heat pump cascades with internal heat exchangers using refrigerants with low global warming potential. *Energy*, 165:1248–1258, 2018.

Nasjonal Digital Læringsarena (ndla). Optimalisering av en prosess. URL https://ndla.no/nb/subjects/subject:16/topic:1:194179/topic:1:186406/resource:1:3199.

K. Nawaz, B. Shen, A. Elatar, V. Baxter, and O. Abdelaziz. R290 (propane) and r600a (isobutane) as natural refrigerants for residential heat pump water heaters. *Applied Thermal Engineering*, 127:870–883, 2017.

K. Nawaz, B. Shen, A. Elatar, V. Baxter, and O. Abdelaziz. Performance optimization of co2 heat pump water heater. *International Journal of Refrigeration*, 85:213–228, 2018.

P. Nekså, H. Rekstad, G. R. Zakeri, and P. A. Schiefloe. CO_2 heat pump water heater: characteristics, system design and experimental results. *International Journal of Refrigeration*, 21:172–179, 1998.

Norsk Kjøleteknisk Forening. *Norsk Kulde- og Varmepumpenorm*. Norsk Kjøleteknisk Forening, 1st edition, 2018.

B. Palm. Ammonia in low capacity refrigeration and heat pump systems. *International Journal of Refrigeration*, 31:709–715, 2008a.

B. Palm. Hydrocarbons as refrigerant in small heat pump and refrigeration systems - a review. *International Journal of Refrigeration*, 31:552–563, 2008b.

S. Piscopiello, W. Mazzotti, C. Nota, S. Sawalha, and B. Palm. Performance evaluation of a large capacity water-water heat pump using propane as refrigerant. *Refrigeration Science and Technology*, pages 803–810, 2016.

M. Pitarch, E. Navarro-Peris, J. Gonzálvez-Maciá, and J. M. Corberán. Evaluation of different heat pump systems for sanitary hot water production using natural refrigerants. *Applied Energy*, 190:911–919, 2017.

L. Småland and J. Øverland. *Multiconsults råd om: Kuldemedievalg 2020*. Norsk Kjøleteknisk Forening, 1st edition, 2020.

Standard Norge. NS-EN 378-1:2016 — Kuldeanlegg og varmepumper - Sikkerhets- og miljøkrav, 2016.

Statkraft Varme AS. Tekniske bestemmelser for fjernvarme, kundesentraler og innvendig røranlegg. Gjelder for statkrafts fjernvarmeanlegg i trondheim, 2017. URL `https://www.statkraftvarme.no/globalassets/2-statkraft-varme/statkraft-varme-norge/bedrift/tekniske-bestemmelser-trondheim----rev-aug-2017.pdf`.

Statkraft Varme AS. Om fjernvarme, 2019a. URL `https://www.statkraftvarme.no/om-fjernvarme/`.

Statkraft Varme AS. Trondheim, 2019b. URL `https://www.statkraftvarme.no/om-statkraftvarme/vare-anlegg/norge/trondheim/`.

J. Stene. Residential CO_2 heat pump system for combined space heating and hot

water heating. *NTNU: Fakultet for ingeniørvitenskap og teknologi, Institutt for energi- og prosessteknikk*, 2004.

J. Stene. Residential CO_2 heat pump system for combined space heating and hot water heating. *International Journal of Refrigeration*, 28:1259–1265, 2005.

J. Stene. Iea hpp annex 32 - economical heating and cooling systems for low-energy houses : state-of-the-art report - norway. *Sintef Energiforskning AS*, 2007.

UNIDO. The montreal protocol evolves to fight climate change. URL `https://www.unido.org/our-focus/safeguarding-environment/implementation-multilateral-environmental-agreements/montreal-protocol/montreal-protocol-evolves-fight-climate-change`.

A. Zajacs, A. Lalovs, A. Borodinecs, and R. Bogdanovics. Small ammonia heat pumps for space and hot tap water heating. *Energy Procedia*, 122:74–79, 2017.

Appendix

8.1 Appendix I - Economic analysis

Med VP

Levert kjøling kW	Levert effekt kW	Komp. Arbeid kW
54	77	23

Driftstimer h	Mengde kjøl kWh	Levert varme kWh	Brukt el kWh	El kost VP NOK	Inntekt på VP NOK	Vedlikehold/år NOK	Investerings kostnad	Netto utgift NOK
8 700	468 930	665 550	196 620	98 310	266 220	10 923	900 000	- 156 987

Eksisterende

Kostnad kjøling NOK	COP -	El forbruk 19 kWh	El kostnad 19 NOK	Driftskost NOK
250 000	2	451 272	225 636	24 364

Generelt

Strømpris NOK/kWh	Pris på varme NOK/kWh	Rente	Tidsperiode t år
0,5	0,4	11 %	20

Analyse

PV NOK	NPV NOK	PBP år	IRR %
kr 1 250 136,34	kr 350 136,34	5,7	17 %

8.2 Appendix II - Bitzer software

BITZER Software v6.15.0 rev2454

Semi-hermetic Reciprocating Compressors

Mode	Refrigeration and Air c
Refrigerant	R744 (CO2)
Reference temperature	Dew point temp.
Compressor type	Transcritical
Series	Standard
Operating mode	Transcritical
Motor version	all

Compressor selection

- ○ Cooling capacity: 60
- ◉ Compressor model: 4GTE-20K
- ☐ Incl. former types

Operating point

- Evaporating SST: -12 °C
- ☐ discharge pressure: Auto

Operating conditions

- Gas cooling outlet: 15 °C
- Suct. gas superheat: 5 K
- ☐ Useful superheat: 100 %

Capacity control

- ○ without
- ◉ External FI: 65 Hz

Power supply

- Power frequency: 50Hz
- Power voltage: Standard (400V)

07.06.2020 11:27:54

☑ Show Overview

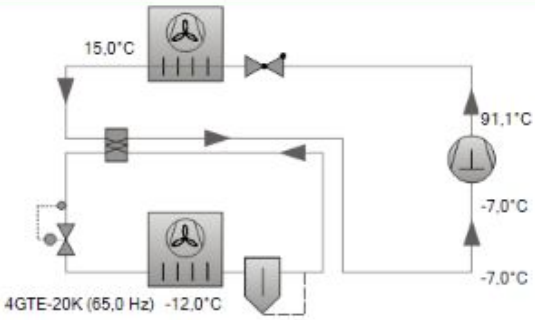

Result | Limits | Technical Data | Dimensions | Information | Documentation | Trainings

Tentative Data.
Power consumption at compressor inlet.

Compressor	4GTE-20K-40P
Frequency compressor	65,0 Hz
Cooling capacity	60,0 kW
Evaporator capacity	60,0 kW
Power input	19,88 kW
Current (400V)	32,5 A
Gas cooler capacity	79,8 kW
COP/EER	3,02
Mass flow	1033 kg/h
min. cooling capacity	20,0 kW (25 Hz)
max. cooling capacity	83,1 kW (68 Hz)
Discharge gas temp. w/o cooling	91,1 °C
optimal high pressure	75,0 bar(a)

8.3 Appendix III - Sluppen

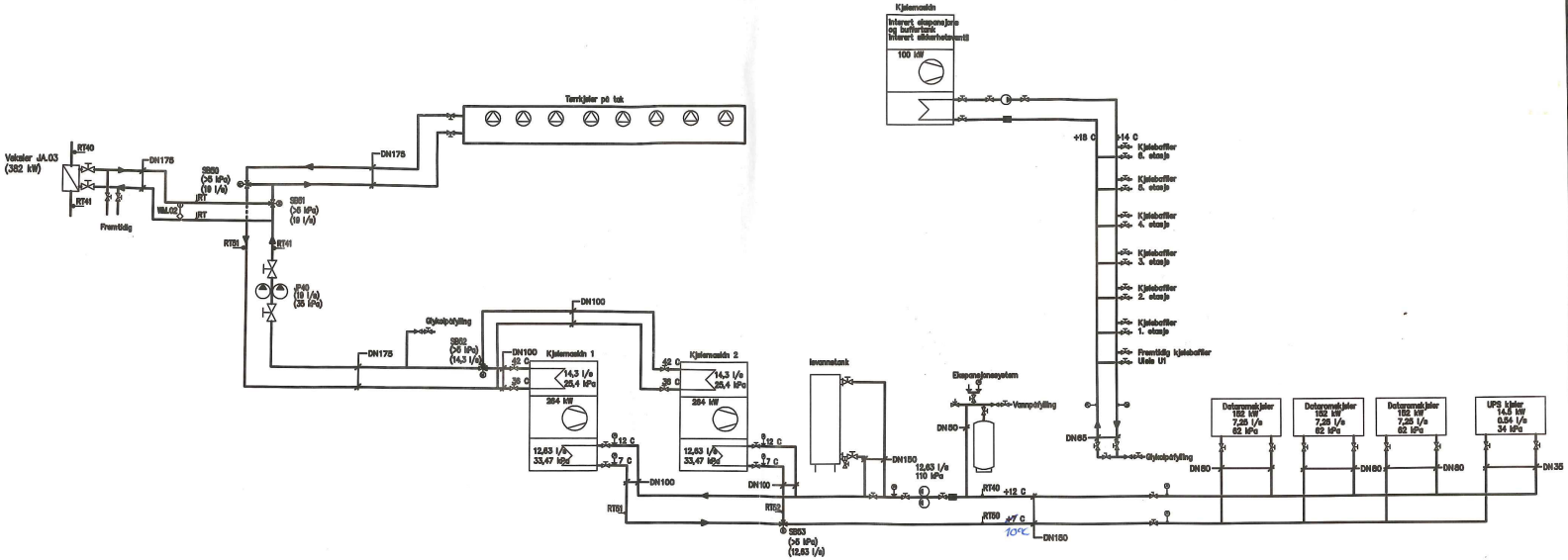

REV	DATO	TEKST	SIGN.
E	04.01.11	AS-BUILT	JNH

Sluppenveien 17a

Systemskjema 3701
Kjøleanlegg

MÅLESTOKK

Dato: 14.06.10
Tegnet av: JNH
Kontrollert av:

Rådgivende Ingeniør MRIF Brann - Energi - VVS
Teknoconsult AS
Hoeggveien 66 - 7036 Trondheim
Tlf. 73 96 65 20, Fax. 73 96 65 21, Mob. 930 45 037

Tegningsnummer:
V3701 E

PLOTTET: ARKIV:

Trondheim Kulde a.s.

norpe partner
Servicekjeden for cool quality

Anleggsorientering:

Generelt
Kjølemaskinen er plassert på fastighetens baksida, utomhus på støpt betongplatta.
Eltavle før kjøleanlæggningen ær plassert i lagerkontoret. Kjølemaskinen har eget påbyggd eltavle.
Anleggene besørger kjøling før samtliga kjølerom.
Utstyret er koblet opp mot lokal IWMAC pc for sentral driftskontroll.

Kjølesystem
Til kjølerom er det levert 1 stk DAIKIN EWAD-480D-SL Luftkyld isvannaggregat med 2 st kapacitetsreglerade skruvkompressorer. Kuldemedium R134a. Isvannaggregatet har en egen Siemensregulator som reglerar kjølemaskinen att leverera isvann efter instællt børværde ca: -6°C.
I kjøleaggregatet finns inbyggd tvillingpump før att cirkulera 40% Etylenglykol mot luftkjølere placerade takhængda i dom rum som skall kylas.

Temperaturen i kjølerom styres av en elektronisk temperaturregulator som reglerar 2 & 3-vægsventiler nær kjølning kallar. Blir rummen før kalla finns elværmare som startas av samma regulator.

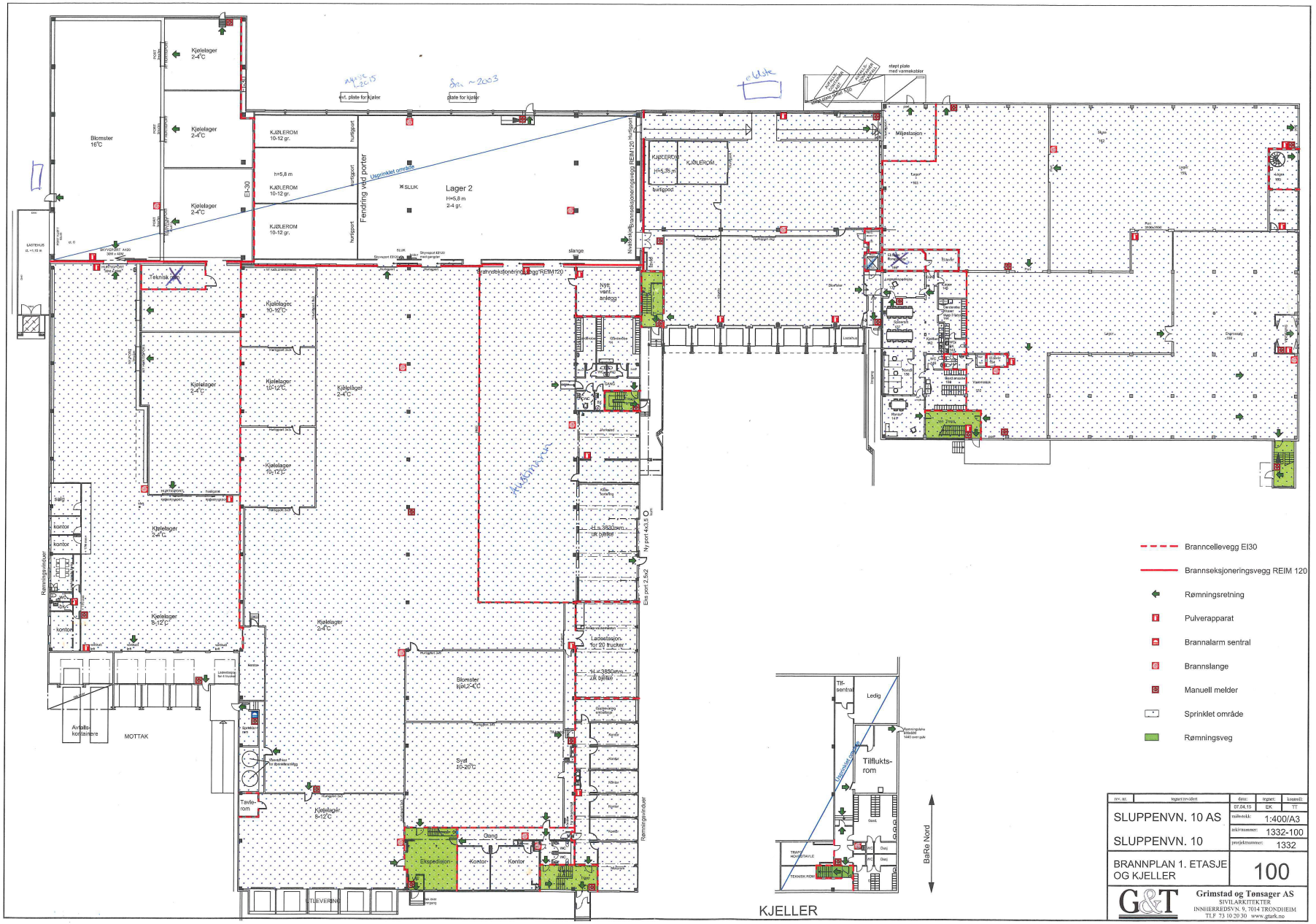

- Brannceilevegg EI30
- Brannseksjoneringsvegg REIM 120
- Rømningsretning
- Pulverapparat
- Brannalarm sentral
- Brannslange
- Manuell melder
- Sprinklet område
- Rømningsveg

rev. nr.	tegningsnivået	dato:	tegnet:	kontroll:
		07.04.15	EK	TT
SLUPPENVN. 10 AS		målestokk:	1:400/A3
SLUPPENVN. 10		arkivnummer:	1332-100
		prosjektnummer:	1332
BRANNPLAN 1. ETASJE OG KJELLER		100	

G&T Grimstad og Tønsager AS
SIVILARKITEKTER
INNHERREDSVN. 9, 7014 TRONDHEIM
TLF 73 10 20 30 www.gtark.no

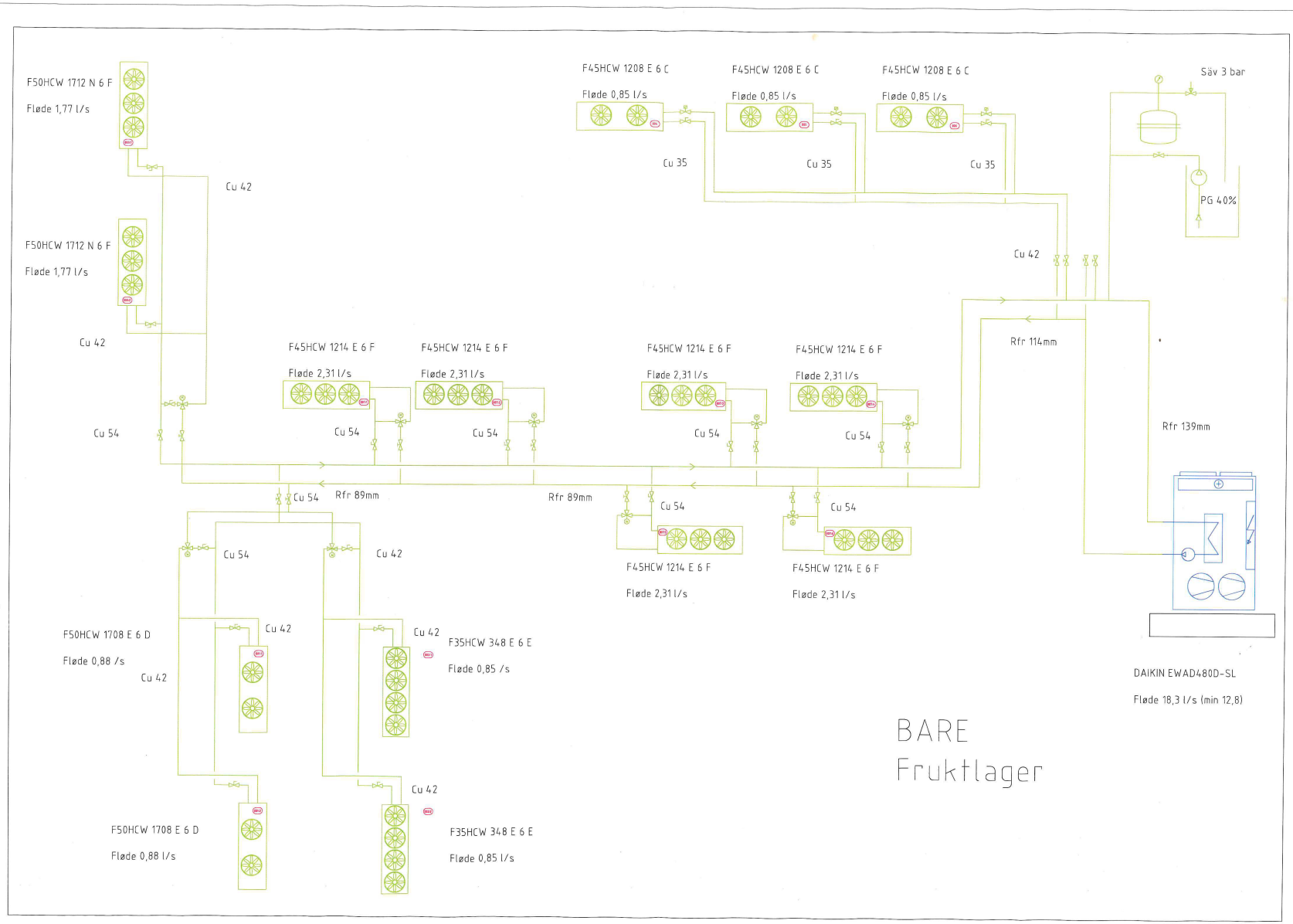
F50HCW 1712 N 6 F
Fløde 1,77 l/s
Cu 42
F50HCW 1712 N 6 F
Fløde 1,77 l/s
Cu 42
Cu 54
F45HCW 1208 E 6 C
Fløde 0,85 l/s
Cu 35
F45HCW 1208 E 6 C
Fløde 0,85 l/s
Cu 35
F45HCW 1208 E 6 C
Fløde 0,85 l/s
Cu 35
Säv 3 bar
PG 40%
Cu 42
Rfr 114mm
F45HCW 1214 E 6 F
Fløde 2,31 l/s
Cu 54
F45HCW 1214 E 6 F
Fløde 2,31 l/s
Cu 54
F45HCW 1214 E 6 F
Fløde 2,31 l/s
Cu 54
F45HCW 1214 E 6 F
Fløde 2,31 l/s
Cu 54
Rfr 139mm
Cu 54
Rfr 89mm
Rfr 89mm
Cu 54
Cu 54
F45HCW 1214 E 6 F
Fløde 2,31 l/s
F45HCW 1214 E 6 F
Fløde 2,31 l/s
Cu 54
Cu 42
F50HCW 1708 E 6 D
Fløde 0,88 /s
Cu 42
Cu 42
F35HCW 348 E 6 E
Fløde 0,85 /s
Cu 42
F50HCW 1708 E 6 D
Fløde 0,88 l/s
Cu 42
F35HCW 348 E 6 E
Fløde 0,85 l/s
DAIKIN EWAD480D-SL
Fløde 18,3 l/s (min 12,8)
BARE
Fruktlager

8.4 Appendix IV - Draft of scientific paper

Development of local energy recovery and distribution

Susanne VESTGREN[(a)], Armin HAFNER[(a)]

[(a)] Norwegian University of Science and Technology (NTNU),
Department of Energy and Process Engineering, Trondheim, 7491, Norway.

ABSTRACT

This paper investigates different heat distribution alternatives for heat recovery at Sluppenvegen 10 in Trondheim. By using a carbon dioxide (CO_2) circuit, the waste heat from the chilling facility is extracted and can be transferred to a heat pump. The waste heat will be used for heating of water with a CO_2 heat pump water heater (HPWH). A model of a CO_2 HPWH was developed using Dymola, and different operating scenarios were tested. The model was tested with different high pressures, water outlet temperatures and CO_2 temperatures out of the gas cooler. These simulations showed that when increasing the high pressure, the discharge temperature also increases and the coefficient of performance (COP) decreases. In addition, both increasing the outlet water temperature and the CO_2 outlet temperature from the gas cooler results in decreased COP. The CO_2 model had lower COP when including an internal heat exchanger (IHX) in the configuration. A model of a propane HPWH was also developed. When compared to the CO_2 model the propane model had a higher COP with three different water outlet temperatures.

Keywords: Heat pumps, Water heaters, Carbon Dioxide, COP, Simulations, Propane.

1. INTRODUCTION

Climate change is gaining importance, and due to large emissions of greenhouse gases and the greenhouse effect, global policy focuses on actions to reduce the harmful impact on the environment and more energy efficient solutions. +CityxChange is a smart city project which focuses on finding solutions for cities to optimize the use of their resources by implementing new technologies (+CityxChange, n.d.). A part of the project is located at Sluppen, Trondheim. The goal is for Sluppen to become a positive energy district (PED). In this context PED is seen as a district with annual net zero energy import and net zero CO_2 emissions, working towards an annual surplus production of renewable energy (+CityxChange, n.d.).

For Sluppen to become a PED waste heat must be recovered in the district, and for this purpose Sluppenvegen 10 and 17A was chosen as they were assumed to have large amounts of waste heat. This paper will focus on Sluppenvegen 10, where the waste heat originates from a chilling facility for fruits, vegetables, and flowers. By using heat pump technology, the waste heat can be recovered and upgraded, i.e. increasing the temperature, to make it more applicable. This paper investigates the performance of a HPWH by developing models representing real life heat pump configurations. These models will be used for running simulations at relevant operating conditions to investigate how the performance is affected by changes in the operating conditions.

2. HEAT PUMP WATER HEATER AND SIMULATION MODELS

2.1. Tools

To conduct an evaluation of HPWHs, models have been built in the simulation software Dymola used in combination with working fluid and component libraries from TLK-Thermo GmbH. The libraries are based on the Modelica language and provides pre-modelled components and working fluids common for heat pumps.

Refrigerant properties used as initialization input in the Dymola models were obtained from the Refrigerant Calculator in CoolPack.

2.2. The models

For extracting the heat from the chilling system at Sluppenvegen 10, a CO_2 circuit was proposed. The CO_2 will absorb the waste heat directly from the glycol circuits in the chilling system upstream the chillers. This way, if the heat cannot be extracted it will be rejected through the air-cooled condensers in today's system. CO_2 is proposed instead of for instance glycol as the pipes can have smaller diameters. The lower part of Figure 1 shows the CO_2 circuit. The outlet temperature for the glycol circuit should be -6 °C.

Three models were developed, two CO_2 models, one with and one without an IHX, as well as a propane model. All the models were initially designed to heat water from 10 °C to 60 °C, and have an evaporation temperature of -12 °C. The models were also designed with a cooling capacity of 60 kW. Further an isentropic efficiency of 0.7 and a volumetric efficiency of 0.8 were assumed for the compressors. It was desired to have a superheat of 5 K in the suction line. The model configuration was simple and contained an evaporator, a liquid receiver, a compressor, a gas cooler and an expansion valve, as seen from Figure 1. For the propane model the gas cooler was replaced by a condenser. The theoretical cooling load, heating load, compressor work and COP for the models are given in Table 1.

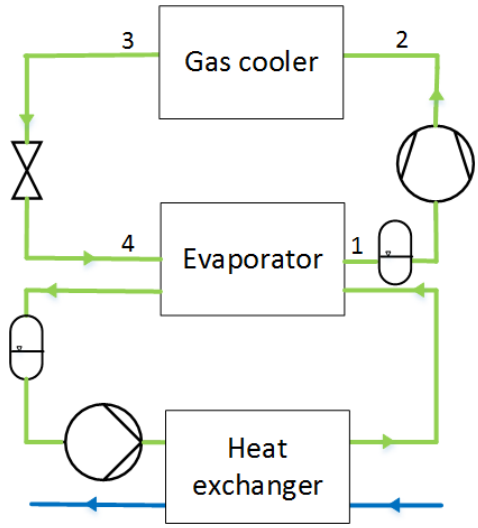

Figure 1: Simple CO_2 model used as a starting point for the modelling.

Table 1: Design cooling load, compressor work, heating load and COP for the models.

Model	$\dot{Q}_0$ (kW)	$\dot{W}_{comp}$ (kW)	$\dot{Q}_c$ (kW)	COP
CO_2 model	60.0	26.4	86.4	3.27
CO_2 with IHX	60.0	26.4	86.4	3.27
Propane model	60.0	23.4	83.4	3.57

Where $\dot{Q}_0$ is the cooling capacity, $\dot{W}_{comp}$ is the compressor power and $\dot{Q}_c$ is the heating capacity of the models.

The CO_2 model was tested with four different high pressures, 85 bar, 90 bar, 95 bar and 100 bar. In addition, three different water outlet temperatures were tested with the model, namely 60 °C, 70 °C and 78 °C. The CO_2 model was also tested with three CO_2 outlet temperatures from the gas cooler, 15 °C, 20 °C and 25 °C. The model was modified by inserting an IHX, and this model was tested with three different high pressures, 90 bar, 95 bar and 100 bar, and the performance was compared to the model without an IHX. For the propane HPWH model three different outlet water temperatures were tested, 60 °C, 70 °C and 80 °C. These results were compared to the results from the CO_2 model.

2.3. Results and discussion

The CO_2 model was tested with four different high pressures, and in Figure 2 the T-s diagram resulting from each of the simulations are shown. From the figure it is clear that the discharge temperature (point 2) increases as the high pressure increases. Additionally, the CO_2 outlet temperature from the gas cooler at the three highest pressures is approximately equal. However, for the simulation with a high pressure of 85 bar, the CO_2 outlet temperature from the gas cooler is significantly higher, which may lead to decreased performance. The figure also shows that none of the simulations resulted in superheat in the suction line, as was desired. Nevertheless, as the model contains a low-pressure receiver, the compressor is protected from liquid slugging.

The CO_2 model was also tested at three different water outlet temperatures and CO_2 outlet temperatures from the gas cooler. Increasing the water outlet temperature resulted in a lower COP for the model, which can be seen from Figure 4. An increased CO_2 outlet temperature also leads to lower COP as seen from Figure 3. This is as expected, as lower temperature before the expansion valve leads to less expansion losses as there is a lower exergy destruction.

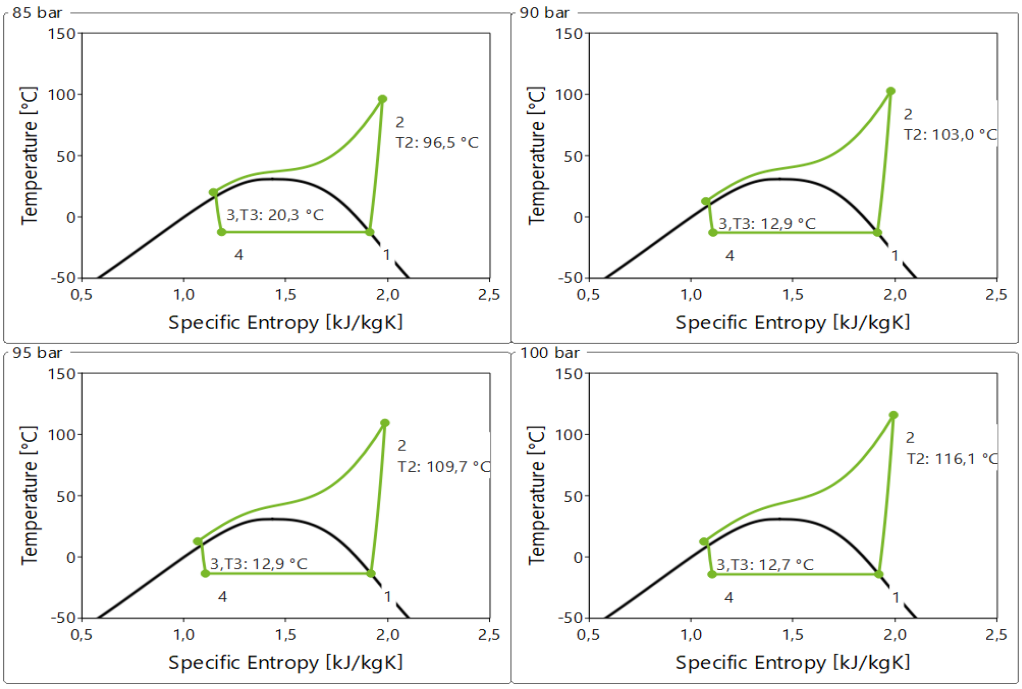

Figure 2: T-s diagrams for simulations with the CO_2 model at four different high pressures.

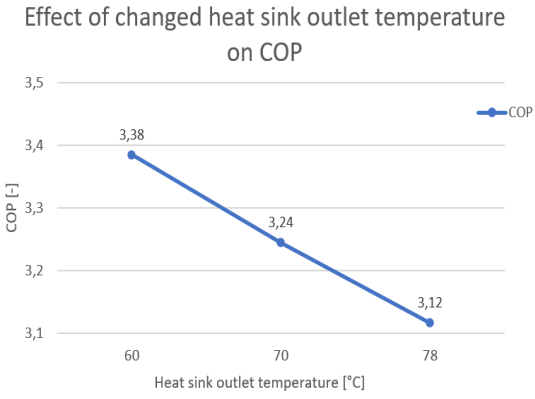

Figure 4: COP of the CO_2 model with three different water outlet temperatures.

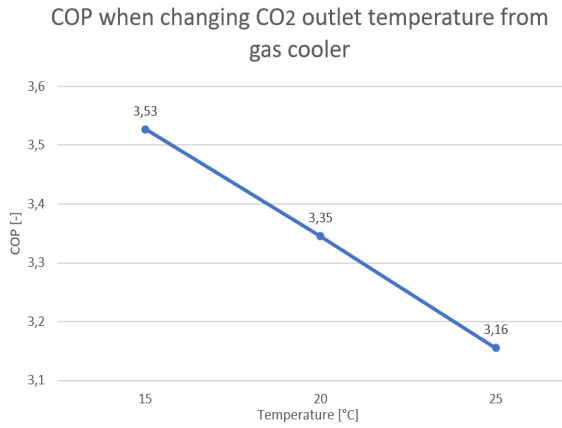

Figure 3: COP of the model with three different CO_2 outlet temperatures from the gas cooler.

Table 2: Cooling, heating and compressor power for the CO_2 model with three different water outlet temperatures.

Water outlet temp.	Cooling power	Compressor power	Heating power	COP
60 °C	53.9 kW	22.6 kW	76.5 kW	3.38
70 °C	62.9 kW	28.0 kW	90.9 kW	3.24
78 °C	69.9 kW	33.1 kW	103.0 kW	3.12

As the water outlet temperature increases the amount of heat transferred in the evaporator and gas cooler also increases, as can be seen from Table 2. The highest water outlet temperature is 78 °C as this was the highest the CO_2 model could deliver with a high pressure of 95 bar. It was even made attempts to increase the outlet water temperature by changing the size of the gas cooler, and when delivering 78 °C the gas cooler is slightly larger than for the other temperatures. This can also affect the amount of heat transferred.

In the article by Nekså et. al (1998) a CO_2 HPWH was presented, where the water was heated from 9 °C to 60 °C. This HPWH achieved a COP in the range of 3.0-4.3 with an evaporation temperature ranging from -20 °C to 0 °C. Assuming a linear increase in performance as the evaporation temperature increases, that means a COP of 3.52 was achieved with an evaporation temperature of -12 °C. From Table 2 the COP of heating water from 10-60 °C is 3.38 for the CO_2 model without an IHX, which is lower than for the heat pump presented by Nekså et. al. However, the difference between the COP values are reasonably small, making the results reliable. Assuming nearly continuous operation of the heat pump and a yearly number of operating hours of 8 700 (99.3 % of the year), the amount of heat the CO_2 model heating water to 60 °C can deliver is 665 500 kWh. However, as the heat pump also uses electricity, the net energy contribution to a PED from the heat recovery at Sluppenvegen 10 is 468 930 kWh.

The IHX CO_2 model was tested with three high pressures, and the resulting T-s diagrams can be seen in Figure 5. The figure shows the discharge temperatures, which supports the results seen from the CO_2 model without an IHX, namely that the discharge temperature increases with increasing high pressure. In addition, the figure shows that the superheat in the suction line is achieved.

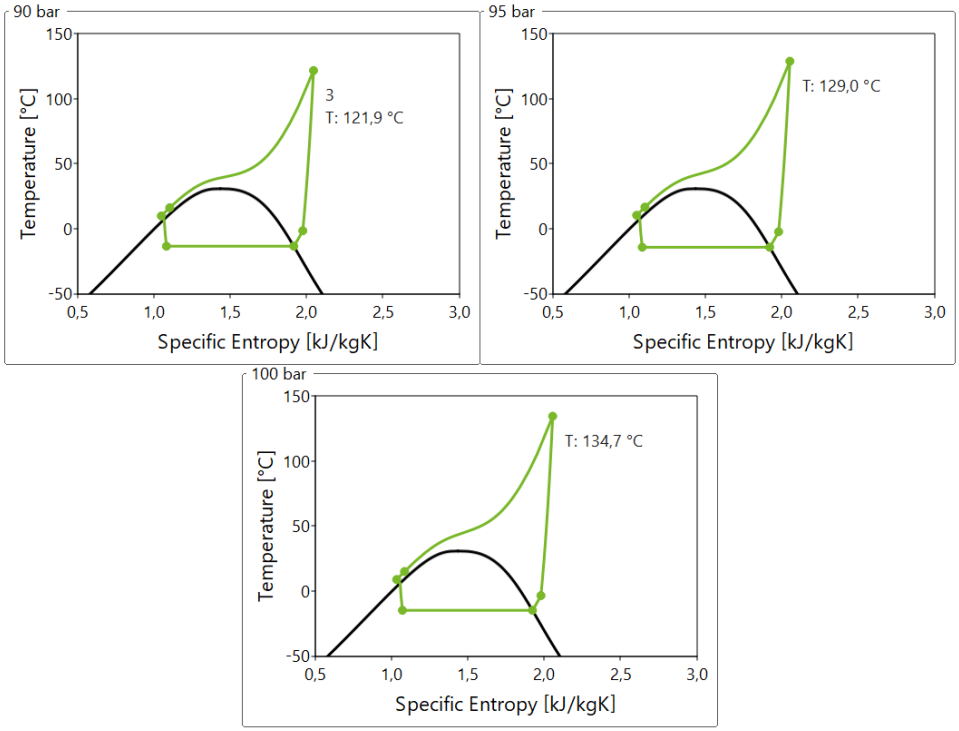

Figure 5: T-s diagram from simulations with CO_2 IHX model at three different high pressures.

Table 3: Water outlet temperatures for simulations at different high pressures for the CO_2 model with and without an IHX.

Model/high pressure	85 bar	90 bar	95 bar	100 bar
Without IHX	60 °C	61 °C	66 °C	70 °C
With IHX	-	68 °C	74 °C	77 °C

When the high pressure of both CO_2 models was changed the only additional modification was changing the compressor's displacement volumes. As the water outlet temperatures were not strictly regulated this resulted in varied water outlet temperatures. Table 3 shows the water outlet temperature for both CO_2 models at different high pressures. The table shows that the water outlet temperature increases as the high pressure increases. Additionally, the water outlet temperatures for the model with an IHX is significantly higher than those for the model without an IHX.

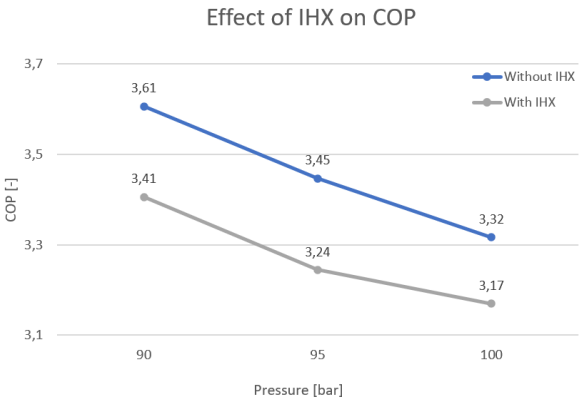

Figure 6: COP for both the CO_2 model with and without an IHX.

Figure 6 gives the COP of the CO_2 model both with and without an IHX. The figure shows that the COP decreases with increasing high pressure. However, in these results the water outlet temperature is not constant and increases with increasing pressure. In addition, the water outlet temperature is higher for the model with an IHX. Thus, this may have an impact on the result, making the difference in COP larger than it should have been. Another factor affecting the COP is that for the CO_2 model without an IHX none of the simulations resulted in superheat in the suction line. Superheat in the suction line will lead to both increased discharge temperature and lower COP, resulting in a comparison based on two models with different operating conditions.

The propane model was tested at three different heat sink outlet temperatures. To achieve a higher water outlet temperature the condensing temperature was slightly increased in each of the cases. In addition the displacement volume of the compressor was adjusted, but the rest of the model was equal in all three cases. The COP of the simulations run with the propane model was compared to the COP of the CO_2 model with the same outlet temperatures, and this comparison can be seen in Figure 7. The figure shows that the propane HPWH model achieved a higher COP than the CO_2 model with all three water outlet temperatures tested. For a water outlet temperature of 60 °C the propane model achieved a COP of 3.65, while the CO_2 model had a COP of 3.38.

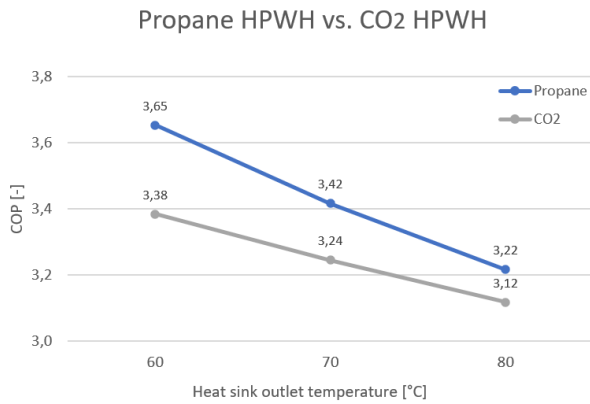

Figure 7: COP of CO_2 model and propane model with three different water outlet temperatures.

3. CONCLUSIONS

Three simplified models of heat pump water heaters have been developed, and simulations at relevant operating conditions have been performed. The three models are a CO_2 HPWH, a CO_2 HPWH containing an internal heat exchanger, and a propane HPWH. All the models showed good performance, with the propane HPWH giving the highest COP. The propane model showed better performance than the CO_2 model for all the simulations conducted for this paper. When heating the water from 10 °C to 60 °C the propane HPWH model had a COP of 3.65. The CO_2 model was tested with different high pressures, as well as different water outlet temperatures and CO_2 outlet temperatures from the gas cooler. From these simulations some conclusions could be drawn. First, as the high pressure increases the discharge temperature also increases and the COP decreases. Both increasing the outlet water temperature and the CO_2 outlet temperature from the gas cooler result in decreased COP. Simulations with the IHX model showed a lower performance than the ordinary CO_2 model at three different high pressures.

For Sluppen to become a PED the amount of heat delivered is of importance. Based on the results obtained from the CO_2 model without an IHX, and assuming 8 700 yearly operating hours (99.3 % of the year), this heat pump can deliver 665 550 kWh heat when delivering water at 60 °C. However, the heat pump will also use electricity, resulting in a net

energy delivery of 468 930 kWh. This is a significant contribution to a PED, comparing to today's situation where no heat from the chilling facility is recovered.

NOMENCLATURE

CO_2	Carbon dioxide	HPWH	Heat pump water heater
COP	Coefficient of performance	IHX	Internal heat exchanger
PED	Positive energy district	$\dot{Q}_0$	Cooling capacity (kW)
$\dot{W}_{comp}$	Compressor power (kW)	$\dot{Q}_c$	Heating capacity (kW)

REFERENCES

+CityxChange, n.d. Trondheim. *https://cityxchange.eu/our-cities/trondheim-norwegian/*.
Nekså, R. Z. S., 1998. CO2 heat pump water heater: characteristics, system design and experimental results.. *International Journal of Refrigeration*, pp. 172-179.

Susanne Vestgren

Development of local energy recovery and distribution

NTNU
Norwegian University of
Science and Technology